Quaternary Science Reviews xxx (2008) 1–38

Contents lists available at ScienceDirect

Quaternary Science Reviews

journal homepage: www.elsevier.com/locate/quascirev

Mid- to Late Holocene climate change: an overview

Heinz Wanner [a,*], Jürg Beer [b], Jonathan Bütikofer [a], Thomas J. Crowley [c], Ulrich Cubasch [d], Jacqueline Flückiger [e], Hugues Goosse [f], Martin Grosjean [a], Fortunat Joos [g,1], Jed O. Kaplan [h], Marcel Küttel [a], Simon A. Müller [g], I. Colin Prentice [i], Olga Solomina [j], Thomas F. Stocker [g], Pavel Tarasov [k], Mayke Wagner [l], Martin Widmann [m]

[a] Institute of Geography and Oeschger Centre for Climate Change Research, University of Bern, Bern, Switzerland
[b] Swiss Federal Institute of Environmental Science and Technology (EAWAG), Dübendorf, Switzerland
[c] Earth Science Institute, School of GeoSciences, The University of Edinburgh, Edinburgh, UK
[d] Institute of Meteorology, Free University of Berlin, Berlin, Germany
[e] Institute of Biogeochemistry and Pollutant Dynamics, Swiss Federal Institute of Technology, Zürich, Switzerland
[f] Institut d'Astronomie et de Géophysique G. Lemaître, Université Catholique de Louvain, Louvain, Belgium
[g] Climate and Environmental Physics and Oeschger Centre for Climate Change Research, University of Bern, Bern, Switzerland
[h] Ecological Systems Laboratory, Ecole Polytechnique Fédérale, Lausanne, Switzerland
[i] QUEST, Department of Earth Sciences, University of Bristol, Bristol, UK
[j] Institute of Geography, Russian Academy of Sciences, Moscow, Russia
[k] Institute of Geological Sciences, Branch Palaeontology, Free University of Berlin, Berlin, Germany
[l] German Archeological Institute, Eurasia Department, Berlin, Germany
[m] School of Geography, Earth and Environmental Sciences, University of Birmingham, Birmingham, UK

ARTICLE INFO

Article history:
Received 26 March 2008
Received in revised form 20 June 2008
Accepted 23 June 2008
Available online xxx

ABSTRACT

The last 6000 years are of particular interest to the understanding of the Earth System because the boundary conditions of the climate system did not change dramatically (in comparison to larger glacial–interglacial changes), and because abundant, detailed regional palaeoclimatic proxy records cover this period. We use selected proxy-based reconstructions of different climate variables, together with state-of-the-art time series of natural forcings (orbital variations, solar activity variations, large tropical volcanic eruptions, land cover and greenhouse gases), underpinned by results from General Circulation Models (GCMs) and Earth System Models of Intermediate Complexity (EMICs), to establish a comprehensive explanatory framework for climate changes from the Mid-Holocene (MH) to pre-industrial time. The redistribution of solar energy, due to orbital forcing on a millennial timescale, was the cause of a progressive southward shift of the Northern Hemisphere (NH) summer position of the Intertropical Convergence Zone (ITCZ). This was accompanied by a pronounced weakening of the monsoon systems in Africa and Asia and increasing dryness and desertification on both continents. The associated summertime cooling of the NH, combined with changing temperature gradients in the world oceans, likely led to an increasing amplitude of the El Niño Southern Oscillation (ENSO) and, possibly, increasingly negative North Atlantic Oscillation (NAO) indices up to the beginning of the last millennium. On decadal to multi-century timescales, a worldwide coincidence between solar irradiance minima, tropical volcanic eruptions and decadal to multi-century scale cooling events was not found. However, reconstructions show that widespread decadal to multi-century scale cooling events, accompanied by advances of mountain glaciers, occurred in the NH (e.g., in Scandinavia and the European Alps). This occurred namely during the Little Ice Age (LIA) between AD ~1350 and 1850, when the lower summer insolation in the NH, due to orbital forcing, coincided with solar activity minima and several strong tropical volcanic eruptions. The role of orbital forcing in the NH cooling, the southward ITCZ shift and the desertification of the Sahara are supported by numerous model simulations. Other simulations have suggested that the fingerprint of solar activity variations should be strongest in the tropics, but there is also evidence that changes in the ocean heat transport took place during the LIA at high northern latitudes, with possible additional implications for climates of the Southern Hemisphere (SH).

* Corresponding author. Tel.: +41 31 631 8885; fax: +41 31 631 8511.
E-mail address: wanner@giub.unibe.ch (H. Wanner).
[1] Present address: Department of Earth and Environmental Sciences, The Open University, Milton Keynes, UK.

0277-3791/$ – see front matter © 2008 Elsevier Ltd. All rights reserved.
doi:10.1016/j.quascirev.2008.06.013

1. Introduction

Since 1990, global mean temperatures have probably been higher than at any previous time during the last 1000 years (Mann et al., 1999; Crowley, 2000; Esper et al., 2002; Jones and Mann, 2004; Moberg et al., 2005; Osborn and Briffa, 2006). In the current discussion about past climatic variability and climatic change, an often-asked question is whether (and if so, why) comparably warm periods occurred earlier, in particular during the present interglacial (the Holocene), i.e. the past ~11,600 years. For example, several multi-century periods of substantial glacier advances and retreats were reconstructed from the North American Cordillera (Porter and Denton, 1967). Denton and Karlén (1973) concluded that the Holocene experienced alternating intervals of glacier advances (600–900 years in duration) and retreats (lasting up to 1750 years), with strongest advances around 200–350, 2800 and 5300 cal years BP. Other studies, based mainly on pollen and macrofossil reconstructions of plant species distributions, have provided long-standing evidence for a general, longer-term cooling of northern high-latitude regions during the Holocene. This cooling is a consequence of orbital variations that produced declining summer insolation in the NH (see the list of abbreviations in Appendix A) (Wright et al., 1993). The nature and causes of multi-century climate variations has been more controversial. Denton and Karlén (1973) invoked solar variability, and Bryson and Goodman (1980) invoked volcanic activity, as possible forcing factors. Both have been implicated in the interpretation of temperature changes during the instrumental temperature record (e.g. Hegerl et al., 2007). Yet most analyses of Holocene climate change have focused either on the millennial scale, or on the decadal to multi-century scale of variability, in part due to the tendency of some proxies (e.g. low-resolution ocean sediment cores) to resolve only the former, while others (e.g. tree rings) resolve mainly the latter. A comprehensive understanding of Holocene climate changes, however, requires consideration of processes operating on both timescales, their causes, and their interactions.

Although various chronostratigraphic terms have been used to subdivide the Holocene, these have not been consistently applied and are generally unhelpful because they refer to climatic stratigraphies that are, at best, regional in validity. Very broadly, however, the Holocene can be usefully considered in three phases (e.g. Nesje and Dahl, 1993). The first phase coincides with the "Preboreal" and "Boreal" chronozones, lasting from about 11,600 to about 9000 years BP. The second phase coincides with the "Atlantic" chronozone and covers the period from about 9000 to about 5000–6000 years BP. This second phase is sometimes called "Hypsithermal", referring to warm conditions in northern mid- to high latitudes (other terms for this phase include "Altithermal" and "climatic optimum", the last being an anomalous survival from the origins of Quaternary science in Scandinavia, where warmer was presumably equated with better!). The third phase coincides with the "Subboreal" and "Subatlantic" chronozones and covers the period from about 5000–6000 years BP to pre-industrial time. This third phase is sometimes called "Neoglacial", referring to the aforementioned periods of glacier advances. These phases can be understood in terms of the time course of climate forcing. Orbital forcing (high summer insolation in the NH) was maximal at around 11,000 years BP, due to a coincidence of the precession and obliquity cycles, however, until about 9000 years BP a large remnant ice sheet persisted in North America (with downstream cooling effects on the climate of the North Atlantic and Eurasia, although not on all Arctic regions; Heikkilä and Seppä, 2003; Kaufman et al., 2004). The second phase corresponds to a period of continuing high summer insolation in the NH, with the North American ice sheet no longer large enough to influence climate at a hemispheric scale. The third phase corresponds to declining summer insolation in the NH.

The greatest progress in understanding Holocene climate change and variability has consistently been made by comparison of large-scale analyses of proxy data with simulations using global climate models. This approach, requiring cooperation between palaeoclimate data specialists and climate modellers, has a history dating over 30 years. Thus the original goal of the Climate Mapping, Analysis and Prediction (CLIMAP) project was to use stratigraphic analyses of ocean cores to provide boundary conditions for modelling the Last Glacial Maximum (LGM) climate using the atmospheric general circulation models (AGCMs) available at that time (CLIMAP Project Members 1976 and 1981). The Cooperative Holocene Mapping Project (COHMAP) subsequently assembled a global array of paleoclimatic observations (especially terrestrial pollen, lake level and plant macrofossil data) to characterise millennial-scale climate changes at 3000-year intervals since the LGM, and used AGCM simulations to assess possible causes of the patterns (Kutzbach and Guetter, 1986; COHMAP Members, 1988; Wright et al., 1993). A key finding was that for the northern tropics, particularly Africa and Asia, high NH summer insolation in the early and Mid-Holocene enhanced the thermal contrast between land and sea producing strong summer monsoons. This accounts for evidence of widespread high lake levels in regions that are arid today (Kutzbach, 1981; Street-Perrott and Harrison, 1984, 1985; Kutzbach and Street-Perrott, 1985; Gasse and van Campo, 1994; see also Gasse, 2000, and references therein). The climatic response to both the insolation changes and the retreating ice sheets produced widespread readjustments in the vegetation of both hemispheres (e.g. Prentice et al., 1991; Harrison and Dodson, 1993; Wright et al., 1993; Williams et al., 2000). Much recent work has centred on developing a more quantitative understanding of changes between the 6000 years BP "timeslice" and the pre-industrial period; including consideration of ocean–atmosphere interactions (as coupled atmosphere–ocean GCMs (AOGCMs) became available) and feedbacks involving the land surface. Since the early 1990s, the Palaeoclimate Modelling Intercomparison Project (PMIP) has organised systematic model intercomparisons and model–data comparisons using AGCMs and later AOGCMs (e.g. Joussaume et al., 1999; Braconnot et al., 2007a, b). The Palaeovegetation Mapping Project (BIOME 6000) of IGBP (Prentice and Webb, 1998; Prentice et al., 2000) was designed to provide a global data set derived from pollen and plant macrofossils for use as a benchmark to test increasingly sophisticated models of past climate, vegetation and their interactions. Additionally, an update of the BIOME 6000 data set for northern high latitudes was used to evaluate PMIP simulation of Arctic climates (Bigelow et al., 2003; Kaplan et al., 2003).

In addition to observational studies based on proxies in ocean and terrestrial sediments, a variety of more recently-developed data sources have shaped current knowledge of Holocene climate change, including tree rings, ice core records, corals, and speleothems (all of these typically having high time resolution) and geophysical techniques, such as borehole temperature measurements, which can be deconvoluted to yield independent palaeotemperature records. Examples of these "new" proxy types are used alongside traditional approaches in this article. In particular, Fig. 2 illustrates climate changes since 6000 years BP for different regions using significant high-resolution archives that depict temporal patterns on both multi-century and millennial timescales.

A recently revived debate concerns the question whether climate variations have been cyclic, not only during the last glacial period, but also during the Holocene (Bond and Lotti, 1995; Bond et al., 1997, 2001; Oppo, 1997; Broecker and Hemming, 2001; Crowley, 2002; Burroughs, 2003). This debate has gained impetus from discussions about the transition from the Medieval Warm Period (MWP; Hughes and Diaz, 1994; Crowley and Lowery, 2000; Broecker, 2001; Bradley et al., 2003), otherwise called the Medieval Warm Epoch (MWE; Lamb, 1965, 1969) or the Medieval Climate

Please cite this article in press as: Wanner, H., et al., Mid- to Late Holocene climate change: an overview, Quaternary Science Reviews (2008), doi:10.1016/j.quascirev.2008.06.013

Anomaly (MCA; Graham et al., 2007), to the Little Ice Age (LIA; Wanner et al., 2000; Grove, 2004; Holzhauser et al., 2005; Matthews and Briffa, 2005), which is the most recent and the most prominent of the periods of glacier advance during the Late Holocene. Motivated by the findings of O'Brien et al. (1995), Bond et al. (1997, 2001) postulated a Holocene "1500-year" cycle based on petrologic tracers of drift ice in the North Atlantic and suggested that this cycle represents the Holocene continuation of the Dansgaard–Oeschger cycles, which are a prominent feature of high-resolution palaeoclimatic records during the last glacial period in the North Atlantic region. On the other hand, it has been argued that there is little evidence of cyclic behaviour in Holocene vegetation and lake-level records from the surrounding continents (e.g. Shuman et al., 2005). One specific goal of this article is to examine whether "Bond cycles" are indeed pervasive in climate records of the past 6000 years.

Recent improvements in computer power, and the development of highly efficient models (fast GCMs and EMICs), have combined to greatly facilitate the simulation of Holocene climates. In addition to quasi-equilibrium experiments for key time slices, transient simulations have covered part or all of the Holocene (e.g. Claussen et al., 1999, 2002; Crowley, 2000; Cole, 2001; Renssen and Osborn, 2003; Goosse et al., 2004; Schmidt et al., 2004; Otto-Bliesner et al., 2006; Braconnot et al., 2007a, b). With the inclusion of more-or-less realistic representations of multiple forcings (including the spatial structure of, e.g. volcanic aerosols) and of natural variability modes of the coupled ocean–atmosphere system (e.g. Bengtsson et al., 2006; Goosse et al., 2006), it has also become possible to use models to analyse a wider spectrum of climate change mechanisms, including those operating on timescales of decades.

The Holocene defines the period during which civilisation developed. Published sources provide multiple examples of societal collapses that occurred during the last 6000 years, on local and regional scales, synchronous with abrupt shifts to drier and/or colder climate regimes (McGhee, 1981; Weiss et al., 1993; Hodell et al., 1995; Dalfes et al., 1996; Weiss and Bradley, 2001; deMenocal, 2001). The frequency of wars has also been closely tied to climate variations during the past millennium (Zhang et al., 2001), testifying to the central importance of climate changes to human well-being.

In this article we expound a general framework for understanding climate changes during the last 6000 years. We intentionally do not include the first millennia of the Holocene because we want to exclude the climatic influence of large continental ice sheets or large mass reorganisations, such as those resulting from extensive outflows of freshwater from the melting ice sheets. Fig. 1 shows that major sea level changes ceased after 6000 years BP (Behre, 2003). In order to aid the interpretation of high-frequency changes, we also present new data sets encompassing the known natural forcings, based on the most accurate timescales with the highest possible temporal resolution. In the final section we attempt to answer the following questions:

1. What was the spatial structure of Mid- to Late Holocene climate changes?
2. Are multi-century scale changes, between colder and warmer (or humid and dry) periods, cyclic, with a quasi-regular period, or not?
3. Can we identify periods with rapid large-scale climate shifts or transitions?
4. Do climate variations coincide with known variations of natural forcing factors, such as orbital parameters, solar irradiance, explosive tropical volcanic eruptions and greenhouse gases?
5. What was the involvement of natural variability modes, such as the El Niño Southern Oscillation (ENSO) and the North Atlantic Oscillation (NAO), in climate change during the Holocene?

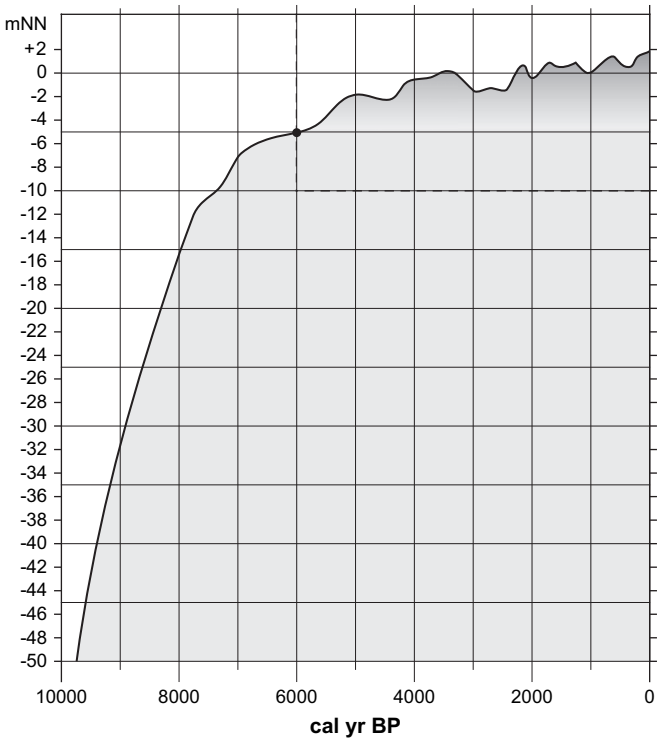

Fig. 1. Sea level changes in the area of the southern North Sea (modified after Behre, 2003). The dashed line with the point marks the period investigated in this paper. NN means "Normalnull". It is the classical German reference level, defined by the average at the Amsterdam North Sea gauge.

6. Are models able to simulate climate variability at different timescales, and to what extent can they diagnose the underlying processes?

2. Observations

We first attempt an overview of observed climate changes during the last 6000 years. For this purpose, a global array of accurately dated palaeoclimatic timeseries is required (Rind and Overpeck, 1993). Three types of information are summarised:

(a) a selection of key timeseries (mainly from single points on the Earth's surface, but including a few multi-site composites) representing proxy-based reconstructions for either annual/warm-season temperature or effective moisture/precipitation (Fig. 2);
(b) global maps of lake status at 6000 ^{14}C years BP (6800 cal years BP) and present, as an indicator for changes in water balance; this map provides spatially extensive information based on a variety of records of low to high resolution (Kohfeld and Harrison, 2000; Braconnot et al., 2004; Fig. 3);
(c) eight timeseries showing glacier advances and retreats during the last 6000 years, covering important glacial regions (Fig. 4).

We split the paper into the two fundamental timescales, "millennial" and "decadal to multi-centennial".

2.1. Changes on millennial timescales

2.1.1. Proxy timeseries

Fig. 2 shows selected timeseries representing climate variations during the last 6000 years (see Table 1, and Bütikofer, 2007, for

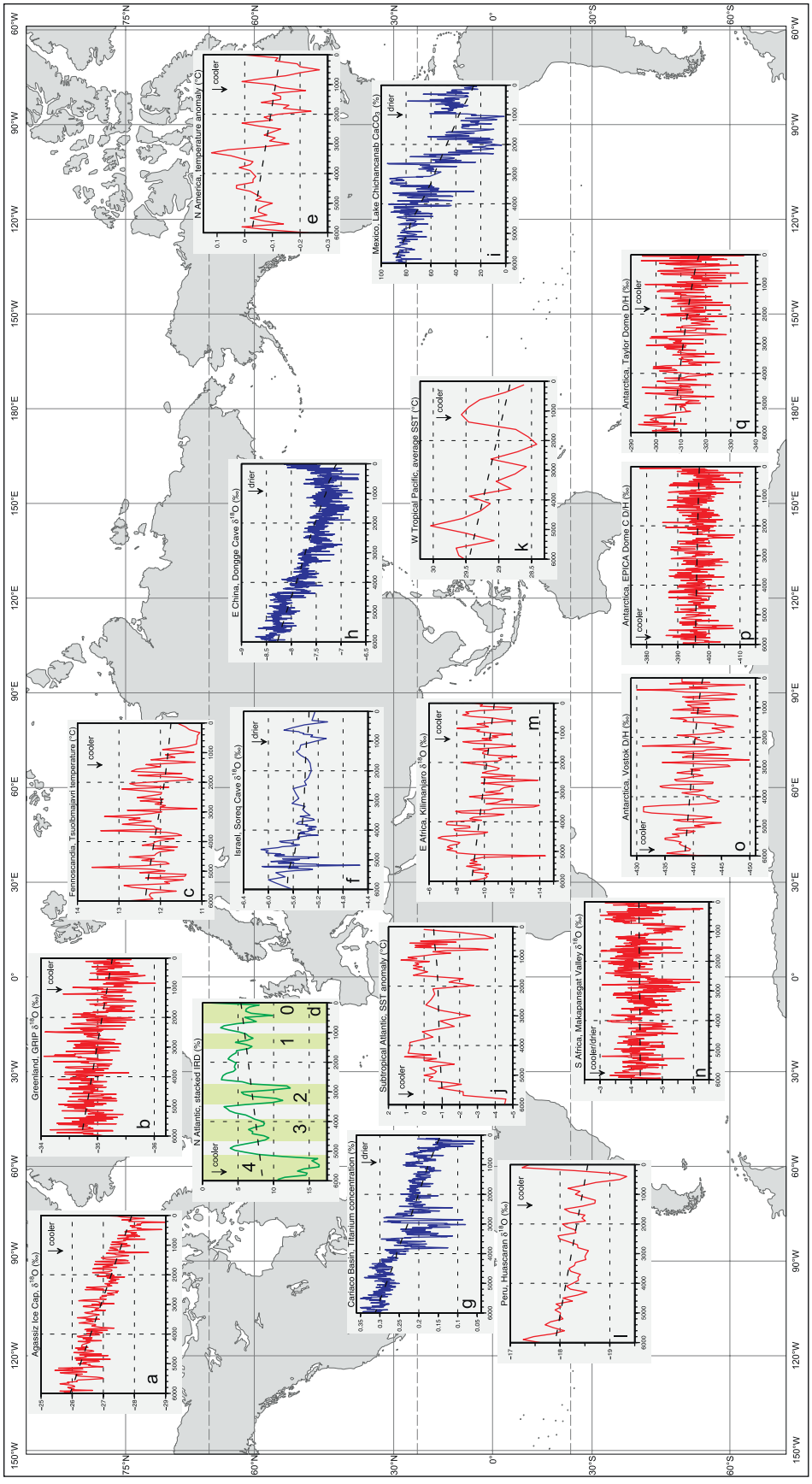

Fig. 2. Global overview based on 17 selected timeseries listed in Table 1. Proxies which likely represent temperature are depicted in red, those indicating humidity/precipitation in blue. The green line shows the IRD curve by Bond et al. (2001). The "Bond events" 0–4 are highlighted as green shaded areas. The dashed line shows the 6 kyr long linear trend (a slightly bent line indicates unequal intervals between the single data points).

Please cite this article in press as: Wanner, H., et al., Mid- to Late Holocene climate change: an overview, Quaternary Science Reviews (2008), doi:10.1016/j.quascirev.2008.06.013

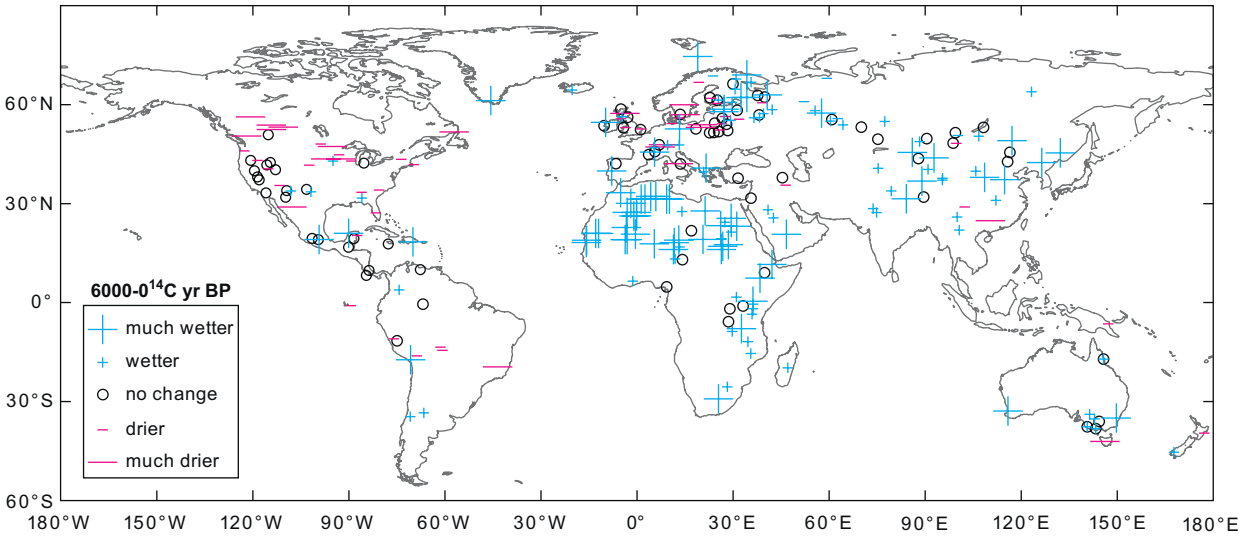

Fig. 3. Change in the global difference in lake status at 6000 ^{14}C years BP (6800 cal years BP) compared to present. The data are derived from the Global Lake Status Data Base (modified after Braconnot et al., 2004).

details), with millennial-scale trends indicated by dashed lines. We consider these timeseries broadly by latitude bands (high latitudes >60°, mid-latitudes 30–60°, subtropics and tropics <30°), supplementing our summaries with information from Fig. 3 and other published literature.

2.1.1.1. Northern high latitudes. The two δ^{18}O records in ice cores from the Agassiz Ice Cap on Ellesmere Island (Fisher et al., 1994; Fig. 2a) and Greenland (GRIP; Vinther et al., 2006; Fig. 2b) show proxy-reconstructed temperature in the high latitudes of the North Atlantic region decreasing almost linearly until the LIA. A similar temperature decline is observed in sea surface temperature (SST) records from the North Atlantic (Marchal et al., 2002), the North Icelandic Shelf (Bendle and Rosell-Melé, 2007), and the Norwegian Sea (Calvo et al., 2002). This temperature decrease is additionally confirmed by a pollen-based July temperature reconstruction from the Fennoscandian tree-line near the North Atlantic seabord by Seppä and Birks (2001; Fig. 2c). Records from the Greenland, Iceland and Norwegian Sea show a decline in SST until 4 kyr BP (Koç et al., 1996). Pollen and plant macrofossil records document a widespread southward retreat of the Arctic treeline implying declining summer temperatures and/or growing-season length (e.g. Prentice et al., 1996; Tarasov et al., 1998; Williams et al., 2000; MacDonald et al., 2000). This response was asymmetrical around the pole, being maximal in central Siberia and minimal in Beringia (TEMPO Members, 1996; Texier et al., 1997; Edwards et al., 2000). Based on the analysis of δ^{18}O of calcite sediments from the Jellybean Lake in Alaska Anderson et al. (2001, 2005) reconstructed mean annual precipitation which is related to the location and strength of the Aleutian low. Their curve shows no millennial trend but depicts remarkable multi-centennial fluctuations with a strong minimum around 2000 years BP.

2.1.1.2. Northern mid-latitudes. The timeseries of ice rafted debris (IRD) (in the form of hematite-stained grains deposited in the North Atlantic by southerly drifting icebergs during cooler periods) by Bond et al. (1997, 2001; Fig. 2d) is represented in Section 2.2 in the discussions about climate cycles. Higher IRD numbers indicate cooler time periods, often called "Bond Cycles" (the cycles from 0 to 4 are marked with a green beam in Fig. 2d). In general, the IRD curve in Fig. 2d suggests a slight warming trend, however this is untypical: a long-term SST decline has been found generally in the North Atlantic between MH and LH(see Marchal et al., 2002; Kim et al., 2004; Rimbu et al., 2004). A mean continental summer temperature anomaly curve from North America was reconstructed by Viau et al. (2006) using >750 dated fossil pollen records (Fig. 2e). A decreasing millennial summer temperature trend is clearly visible, although the amplitude of cooling is less than that seen in the Arctic. A progressive decline in summer temperature since the MH is also well established from pollen and plant macrofossil data in northern and central Europe (see e.g., recent quantitative reconstructions based on >500 dated fossil pollen records by Davis et al. (2003) and Brewer et al. (2007)). Interior N America and the Pacific Northwest in the MH were generally drier than present, as shown by palaeovegetation (Wright et al., 1993; Williams et al., 2000; Thompson and Anderson, 2000) and lake status (Fig. 3) records, becoming wetter towards the present, while monsoonally influenced regions in the American southwest became drier towards the present (Wright et al., 1993; Thompson and Anderson, 2000; Harrison et al., 2003). The Mediterranean region has also become drier from the MH to the present (Wright et al., 1993; Davis et al., 2003). Fig. 2f illustrates this millennial-scale drying trend from a speleothem record, Soreq cave in Israel (Bar-Matthews et al., 2003). A drying trend is also seen in lake (Fig. 3) and pollen (Yu et al., 1998 and 2000) records from China. Wet MH conditions in some mid-latitude regions of N America and E Asia likely reflect enhanced monsoonal activity "spilling over" from the subtropics and tropics, dynamically linked to the dryness shown by areas beyond monsoonal influence (Harrison et al., 2003). An important mid-latitude proxy for the NH is also shown in form of the glacier curve for the European Alps in Fig. 4.

2.1.1.3. Northern subtropics and tropics. A pronounced Holocene drying trend is shown by lake and vegetation records in regions of Central America, Africa and SW, S and E Asia, which receive precipitation from NH monsoon systems today (e.g. Fig. 3, Jolly et al., 1998a; Hoelzmann et al., 1998; Gasse et al., 2000; Fleitmann et al., 2003). This trend from expanded to contracted monsoon rainfall belts can be interpreted as a progressive southward shift of the Intertropical Converge Zone (ITCZ). This millennial-scale trend is consistently shown by high-resolution records from the northern subtropics and tropics: the sedimentary record from the Cariaco Basin (Haug et al., 2001; Fig. 2g), the δ^{18}O record from the Dongge Cave speleothem (Wang Y. et al., 2005; Fig. 2h), and the δ^{18}O record

Please cite this article in press as: Wanner, H., et al., Mid- to Late Holocene climate change: an overview, Quaternary Science Reviews (2008), doi:10.1016/j.quascirev.2008.06.013

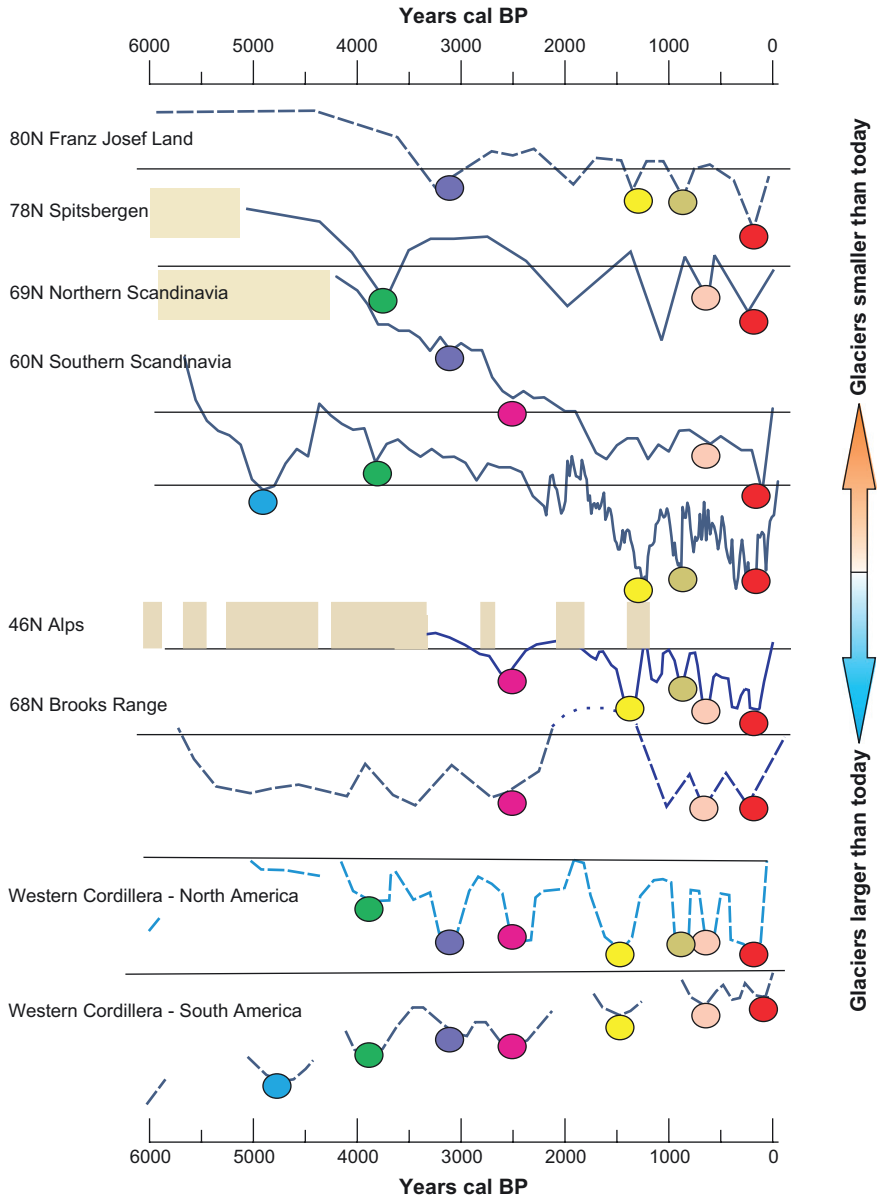

Fig. 4. Timing and relative scale of eight timeseries of glacier advances and retreats during the last 6000 years, covering important glacial regions of the globe. Most series, except for the two Scandinavian curves, are discontinuous because they are at based on geomorphic evidence. For easier interregional comparison all series are presented as curves. The curve for the Alps is the best constrained by documentary and tree-ring data, especially for the last 3500 years (Holzhauser et al., 2005). Except for the Alps and Scandinavia, the precise periods of the glacier retreats are not known and are shown on the picture arbitrarily. The coloured dots mark possible simultaneous Neoglacial advances. The brown shaded areas indicate indirect evidence (wood above the modern tree limit, buried soils etc.). Franz Josef Land: Lubinsky et al., 1999, calibrated. Spitsbergen: curve from Svendsen and Mangerud (1997), corrected with Humlum et al. (2005). Northern Scandinavia: Nesje et al. (2005), Bakke et al. (2005), IPCC (2007). Southern Scandinavia: Matthews et al. (2000, 2005), Lie et al. (2004), IPCC (2007). Alps: Holzhauser et al. (2005, Jörin et al. (2006). Brooks Range: Ellis and Calkin (1984), calibrated. Western Cordillera–North America: Koch and Clague (2006). Western Cordillera–South America: Koch and Clague (2006).

from Lake Chichancanab, Mexico (Hodell et al., 1995; Fig. 2i). The extremely arid period with low lake levels, which started in Mexico around 2000 cal years BP, lasted for approximately one millennium corresponding to the collapse of the Classic Maya civilisation (Hodell et al., 1995; Fritz et al., 2001; Harrison et al., 2003; Haug et al., 2003). The analysis of the SST trends in the northern subtropics and tropics becomes more difficult than those previously discussed, because of the restricted number of data sets. In the subtropical to tropical North Atlantic a slight warming trend is visible (Kim et al., 2004). Based on foraminiferal assemblages off West Africa, DeMenocal et al. (2000) pointed to the strong multicentennial to millennial scale temperature variability (Fig. 2j) which resulted from increased southward advection of cooler temperate or subpolar waters, or from enhanced regional upwelling. The situation is even more complicated in the Indo-Pacific area. The record of foraminiferal Mg/Ca ratios from the western tropical Pacific by Stott et al. (2004) (Fig. 2k) shows a cooling trend since the MH, opposite to signals from further north (Kim et al., 2004). Gagan et al. (2004) demonstrated that no noteworthy SST changes occurred within the Indo Pacific Warm Pool (IPWP) between the Mid- and Late Holocene. Shulmeister (1999) emphasised that the west–east SST contrast in the tropical Pacific drives the Walker Circulation. This contrast was greatly weakened in the Early Holocene (EH) but was enhanced after about 5000 cal years BP. The SSTs in the western Pacific warm pool were probably at, or close to, modern values. SSTs in the eastern Pacific,

Please cite this article in press as: Wanner, H., et al., Mid- to Late Holocene climate change: an overview, Quaternary Science Reviews (2008), doi:10.1016/j.quascirev.2008.06.013

Table 1
Site descriptions, resolutions and references of the 18 timeseries in Fig. 2 (Bütikofer 2007)

	Region	Latitude	Longitude	Resolution (years)	Reference
(a)	Agassiz Ice Cap	80°49′N	72°56′W	25	Fisher et al. (1994)
(b)	Greenland, GRIP	72°35′N	37°38′W	20	Vinther et al. (2006)
(c)	Northern Fennoscandia, Tsuolbmajavri	68°42′N	22°05′E	60	Seppä and Birks (2001)
(d)	N Atlantic	54°15′N	16°47′W	70	Bond et al. (2001)
(e)	North America	25–70°N	55–170°W	100	Viau et al. (2006)
(f)	Israel, Soreq Cave	31°45′N	35°03′E	~50	Bar-Matthews et al. (2003)
(g)	Cariaco Basin	10°42′N	65°01′W	~6	Haug et al. (2001)
(h)	E China, Dongge Cave	25°17′N	108°05′E	~4	Wang Y. et al. (2005)
(i)	Mexico, Lake Chichancanab	19°05′N	88°45′W	~19	Hodell et al. (1995)
(j)	Subtropical Atlantic, off Cap Blanc	20°45′N	18°35′W	~92	deMenocal et al. (2000)
(k)	W Tropical Pacific	6°N-10°S	125–134°E	250	Stott et al. (2004)
(l)	Peru, Huascarán	09°00′S	77°03′W	100	Thompson et al. (1995)
(m)	E Africa, Kilimanjaro	03°04′S	37°21′E	50	Thompson et al. (2002)
(n)	S Africa, Makapansgat Valley	24°01′S	29°11′E	~9	Holmgren et al. (2003)
(o)	Antarctica, EPICA Dome C	75°06′S	123°21′E	~17	Jouzel et al. (2001)
(p)	Antarctica, Taylor Dome	77°47′S	158°43′E	~24	Steig et al. (1998)
(q)	Antarctica, Vostok	78°28′S	106°48′E	~38	Petit et al. (1999)

particularly in the coastal upwelling zone, would have been higher during the EH because wind speeds were lower (Shulmeister, 1999).

2.1.1.4. Southern subtropics and tropics. Lakes in the Altiplano of South America experienced multi-millennial low levels during the MH, to ca 4500 cal years BP. Since then the lake levels have increased stepwise to reach modern levels by ca 3500 cal years BP (Nuñez et al., 2002; Grosjean et al., 2003). Pollen data from SE Brazil also indicate dryness in the MH and increasing rainfall towards the present, opposite to the widespread trend shown in the NH subtropics (e.g., Behling, 1995; Behling and Pillar, 2007). Fritz et al. (2001) noted that MH conditions drier than today were found extensively in mid-latitude regions of both North and South America. However, the causes were likely quite different. Long-term temperature records from the southern tropics and subtropics are very sparse. Fig. 3l and m shows two $\delta^{18}O$ timeseries from glaciers in the high north-central Andes (Huascarán in Peru; Thompson et al., 1995; Fig. 2l) and Eastern equatorial Africa (top of Kilimanjaro; Thompson et al., 2002; Fig. 2m). There is still debate as to whether these curves carry a temperature signal (Pierrehumbert, 1999). Thompson et al. (2002, 2003) assumed that the two curves represent a temperature signal, and that therefore a negative millennial temperature trend was present on both continents. If so, it remains unclear whether this trend is a reaction to the decreasing insolation in the Southern Hemisphere (SH) winter, or the result of a complex reaction to the NH cooling. Data from the Pacific tropics and subtropics are sparse. Abram et al. (2007) show that the MH in the eastern Indian Ocean was characterised by a longer duration of surface ocean cooling. They also point to the strong coupling between the weakening Asian monsoon and the enhanced El Niño activity during the LH.

2.1.1.5. Southern mid-latitudes. Arid or less humid conditions prevailed in the western mid-latitudes of South America between 7700 and ca 5300 cal years BP (Lamy et al., 2001). Thereafter a stepwise precipitation increase has been interpreted as reflecting an intensification of northward moving winter westerlies (Markgraf et al., 1992). This interpretation is consistent with enhanced upwelling along the South American west coast and a strengthening of the Walker Circulation, as well as an increased ENSO activity after ca 5000 cal years BP as recorded in paleodata from the eastern and western Pacific (Shulmeister, 1999; Shulmeister et al., 2004, 2006; see also Section 4.1). No clear trend is visible in the $\delta^{18}O$ curve of a stalagmite from the Cold Air Cave in the Makapansgat Valley in South Africa (Fig. 2n). According to Holmgren et al. (2003) these data reflect fluctuations between warmer (drier) and cooler (wetter) conditions. Pollen data from Australia and Pacific islands (Pickett et al., 2004) indicate little climate change during the Holocene. Shulmeister (1999) showed that northern Australia had a precipitation maximum after 5000 cal years BP. Significantly this occurred at least 1000 years later than in southern Australia because the climate of tropical Australia had become decoupled from that of temperate Australia at that time. This change marked the onset of an enhanced Walker Circulation, as seen today. A concomitant strengthening of the westerlies has also been inferred for New Zealand (Shulmeister, 1999).

2.1.1.6. Southern high latitudes. Three out of 11 Holocene timeseries of water isotope measurements at different sites in Antarctica (Masson et al., 2000) are represented in Fig. 2o–q. The isotopic ratios reveal the long-term temperature trends arising from local ice sheet dynamics, such as elevation fluctuations, superimposed on common temperature changes. The trends shown are small and not uniform (Masson et al., 2000). Vostok (Petit et al., 1999) and Taylor Dome (Steig et al., 1998) show negative trends while EPICA Dome C (Jouzel et al., 2001) shows almost no long-term trend.

2.1.2. Glacier dynamics

Historical descriptions of glacier variations, dates of moraines and lake sediment properties from glacial areas provide important records of former glacier fluctuations. The historical descriptions are limited in space and time, while geological reconstructions generally suffer from the low dating accuracy. One of the most serious limitations in the dating of moraines is the uncertainty in the relationship between the timing of moraine deposition and that of the organic material providing the actual date of advance, which in most cases allows the estimation of the maximum or minimum date of advance only. The accuracy of the methods used for moraine dating ranges from several decades to centuries and is, therefore, inadequate for high-resolution reconstructions. The cross-dating of trees damaged or killed by glacier advances allows improvement in the accuracy, up to annual resolution. However, such data are limited to regions where the upper tree limit reaches the Holocene moraines, such as in the Alps and Patagonia. Glacio-fluvial sediment properties, calibrated against other measures of glacier activity and extent, provide continuous records of past variability and individual advances or retreats of glaciers (Dahl et al., 2003). This method is intensively used in Scandinavia and has provided detailed reconstructions of equilibrium-line altitude variations over the whole Holocene, for both glacier advances and retreats. Until very recently, little was known about the retreat of glaciers

Please cite this article in press as: Wanner, H., et al., Mid- to Late Holocene climate change: an overview, Quaternary Science Reviews (2008), doi:10.1016/j.quascirev.2008.06.013

during the warmer climatic phases between the EH and the MH. The uncertainty of the glacier sizes during the contracted stages still remains. However, due to modern glacial shrinkage, new reconstructions of past variability, based on the analysis of tree rings and organic material buried by the former glacier advances and released in the glacier forefield, recently became possible (Hormes et al., 2001; Koch et al., 2004; Holzhauser et al., 2005; Nesje et al., 2005, 2008; Jörin et al., 2006; Grosjean et al., 2007). Several aspects of glacier dynamics should be kept in mind when using this data for climatic reconstructions. The response time of an advancing or retreating glacier front to a climatic signal differs for different glaciers depending on type, size and morphology of the glacier. For typical alpine valley glaciers the response time is estimated to be 10–50 years (Oerlemans et al., 1998). The best climatic indicators are non-surging mountain glaciers of moderate size and simple shape, which are located on land (without floating tongue), and have a regular accumulation rate (rather than provided by avalanches or snow re-distributed by wind).

Glacial response depends on both temperature and precipitation, so the problem often arises to distinguish between these two parameters (Nesje and Dahl, 2003; Bjune et al., 2005). In most cases in the high and mid-latitudes, summer temperature controls mass balance and, hence, glacier size variations (Oerlemans, 2005; Steiner et al., 2008). In western Scandinavia, the tropics and arid subtropics however, the glaciers are strongly dependent on precipitation (Grosjean et al., 1998; Kaser and Osmaston, 2002; Nesje et al., 2005). In several cases, recent improvement in glacial chronologies, coupled with high-resolution multi-proxy comparisons and climatic reconstructions, have enabled identification of the climatic signal and even in temperate regions attribute several advances to precipitation (Dahl and Nesje, 1996; Luckman, 2000; Wanner et al., 2000; Luckman and Villalba, 2001; Nesje et al., 2001; Nesje and Dahl, 2003). Despite many challenges in the dating and interpretation of glacier variations, glaciers have been successfully used as indicators of past millennial to decadal-scale climate changes (Denton and Karlén, 1973 Mayewski et al., 2004; Oerlemans, 2005). However, due to the wide range of advance and retreat dates, such data can also be misleading and should be interpreted with caution. Fig. 4 shows several well-constrained glacier histories based on both continuous (lake sediments) and discontinuous (moraine based) chronologies.

The glaciers from the mid- to high latitudes in the NH, namely found in the Alps (Jörin et al., 2006), Scandinavia (Bakke et al., 2008; Nesje et al., 2008) and the Canadian Cordillera (Luckman, 2000; Koch and Clague, submitted), were reduced in extent in the EH to MH period, but experienced numerous advances after ca 6000 years BP, reaching their maximum extent in the LIA (Fig. 4). This major trend in the Holocene glacier variations in the NH seems to be related to the gradually decreasing summer insolation driven by orbital forcing. Koch and Clague (2006) suggested that a gradual reduction of the glacier sizes through the Holocene in the SH is in agreement with the increase of the austral summer insolation, opposite to the NH. However, there is evidence that in several regions of the SH many glaciers were of a smaller size during the EH to MH, including those in Patagonia (Glasser et al., 2004; Kilian et al., 2007), Antarctica (see Grove, 2004, and references therein) and the tropical Andes (Abbott et al., 2003). To explain the long-term trend of glacier variations in the tropical Andes (small or absent glaciers in the EH to MH and large in the LH) Abbott et al. (2000, 2003) suggested the following climatic mechanism. The lower summer insolation (January), driven by orbital forcing in the EH to MH, resulted in decreased summer precipitation and the development of an arid climate. The high insolation in winter contributed to more intense melting of glaciers. As a result, the glaciers were non-existent in catchments lower than 5500 m until the LH (ca 2400 cal years BP; Abbott et al., 1997). The gradual re-appearance of the glaciers from north to south can be explained by the onset of wetter conditions related to orbitally-driven summer insolation increase during the LH, which resulted in a progressive southward shift of the location and strengthening of wet-season convection.

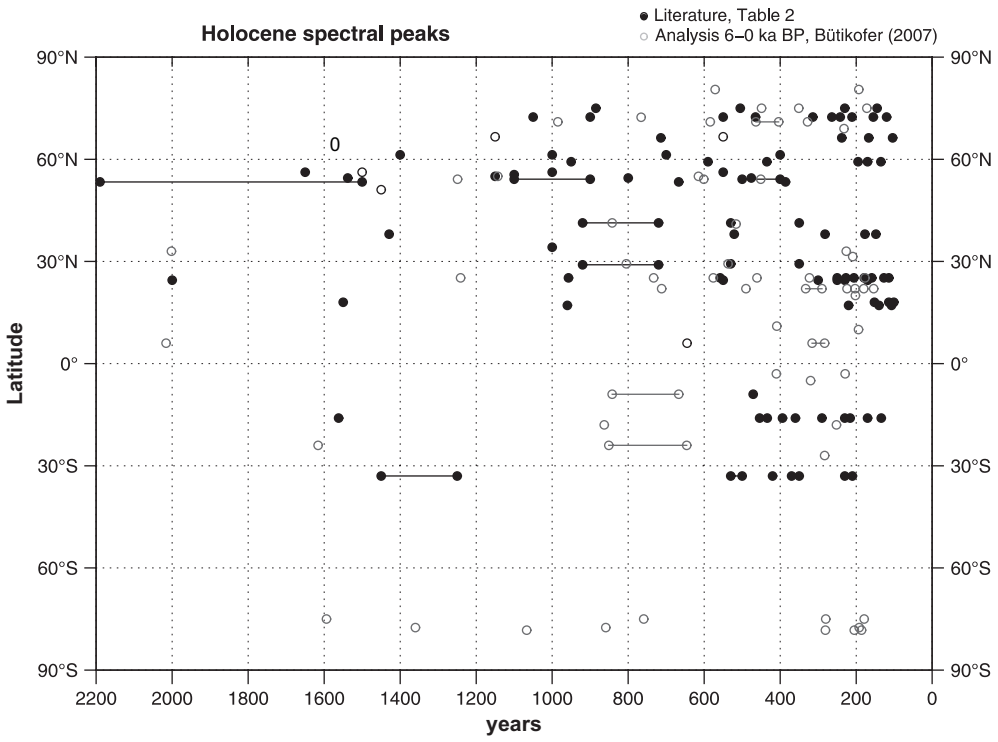

Fig. 5. Overview of the spectral behaviour of the timeseries analysed in Bütikofer (2007) (open circles, see Table 1) or in the references listed in Table 2 (black dots). Each circle or dot marks a spectral peak. Horizontal lines represent broad peaks.

Please cite this article in press as: Wanner, H., et al., Mid- to Late Holocene climate change: an overview, Quaternary Science Reviews (2008), doi:10.1016/j.quascirev.2008.06.013

Shulmeister (1999) explained the lack of moraines between 8 and 5000 years BP in New Zealand and their appearance afterwards, by variations in westerly circulation due to changes in seasonality, as predicted by the precessional cycle. Markgraf (1993) suggested the same mechanism in the subtropics of South America between 30 and 34°S. However, recent modelling does not support the assumption of a strong link between mean SH westerlies and precipitation over southeastern Patagonia (Wagner et al., 2007).

Several authors have emphasised that glaciers in different regions expanded during the Mid- to Late Holocene. They gave this time period, which followed the so-called warmer Hypsithermal between about 9000 and 5700 years BP, the name "Neoglacial" (Porter 2000). Porter (2000), analysing the dates of Holocene moraines in the Andes, west Antarctica and New Zealand, concluded that the first Neoglacial advances in this area culminated between ca 5400 and 4900 cal years BP, i.e., close to the beginning of several noteworthy glacier advances in the NH (Grove, 2004). However, the austral summer insolation (see Fig. 6b) has the opposite trend to the boreal summer insolation and cannot therefore have caused cooling and subsequent Neoglacial glacier advances during the same period in the whole SH. Hodell et al. (2001) suggested that the rapid cooling between 5400 and 4900 cal years BP recorded in the Taylor Dome Ice Core (Antarctica; Fig. 2q), in North Atlantic marine records (as an increase in IRD; Fig. 2d), and coinciding with the end of the African humid period, can be explained by a non-linear response of the Earth's climatic system to gradual changes in NH insolation. It was suggested that the process may have been initiated in the tropics and subtropics (deMenocal et al., 2000) and then propagated to high latitudes in both hemispheres. However, this superficially attractive explanation conflicts with the evidence that the first Neoglacial moraines in different parts of the World span a broad interval up to several millennia, and the oldest Neoglacial advances are almost 1000 years older than the cooling around 5000 cal years BP. Namely, the advances in the Alps and possibly in the Pyrenees, in Scandinavia, the Cascades and the Canadian west coast ranges occurred shortly after 6000 cal years BP (Grove, 2004). This discrepancy might be partly explained by poor dating accuracy, or a different regional forcing for the earliest Neoglacial advances.

2.2. Changes on decadal to multi-centennial timescales

2.2.1. Proxy timeseries

In addition to long-term trends, the curves in Fig. 2 clearly show pronounced higher-frequency variability. The first question is whether these cycles or swings occur synchronously and within the same frequency band, globally, or whether they are rather restricted to more regional scales. As Table 1 demonstrates the time resolution of the different datasets differs remarkably, complicating the comparison of the time spectra. Nevertheless, we performed spectral analyses of the datasets listed in Table 1, and compared the results with the reported spectra of important Holocene palaeoclimatic archives in the literature. Our analyses were restricted to well-defined, detrended datasets covering the last 6000 years BP (for more details see Bütikofer, 2007). All datasets were processed with the same spectral analysis method (REDFIT; Schulz and Mudelsee, 2002). Table 2 lists the references for the (predominantly continental) studies that were used for comparison (for more

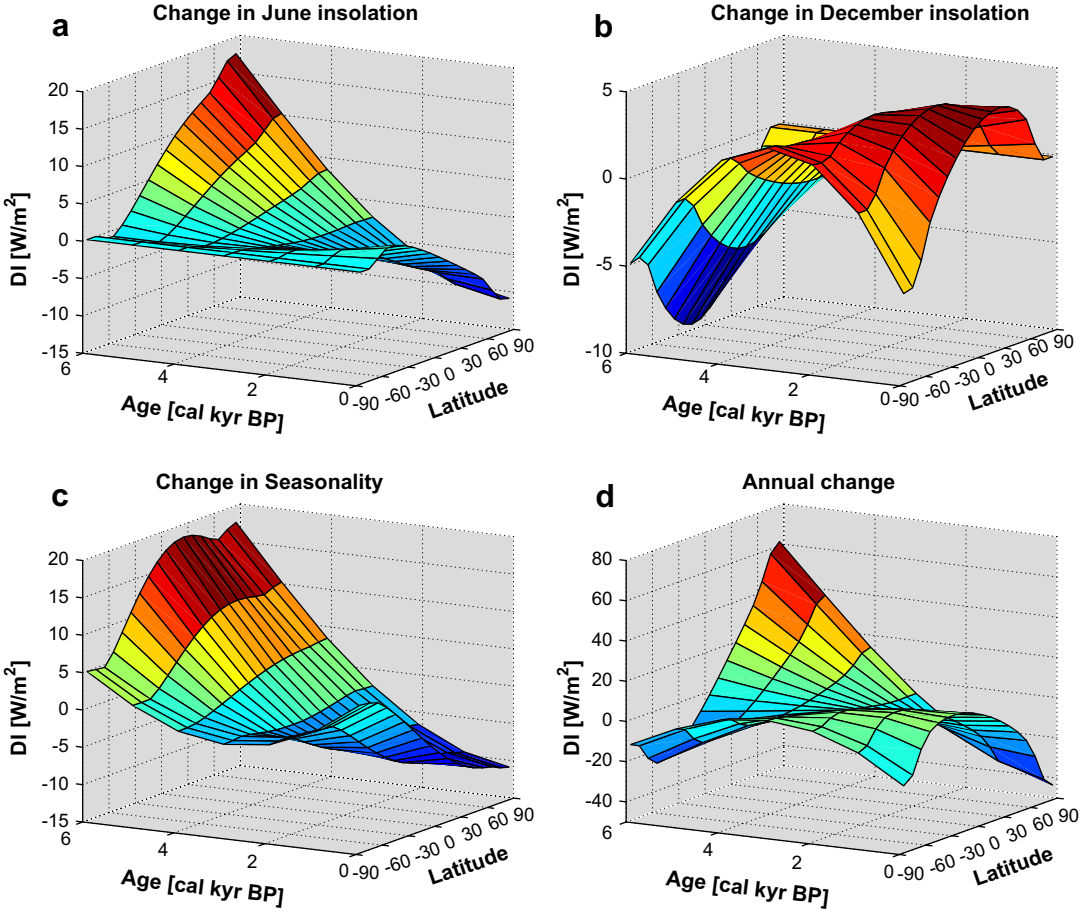

Fig. 6. Calculated deviations of the insolation from the long-term mean values (W/m^2) as a function of latitude for the past 6000 years. (a) June (boreal summer); (b) December (austral summer); (c) seasonality (difference between June and December); (d) annual mean.

Please cite this article in press as: Wanner, H., et al., Mid- to Late Holocene climate change: an overview, Quaternary Science Reviews (2008), doi:10.1016/j.quascirev.2008.06.013

details see Bütikofer, 2007). It should be noted that different authors used different time intervals as well as different methods for their spectral analyses. Fig. 5 presents the significant (90% level) spectral peaks as described in the literature (black dots) and as determined by our analyses (open circles). The dominant peaks found in the different timeseries are plotted against the corresponding latitude of each record. At best, this panel displays weak clustering of spectral peaks, broadly consistent with Wunsch's (2000) contention that a broad band of quasi-periodic variability, rather than any kind of significant spectral peak, is typical for Holocene climate records.

The second question is whether or not the analysed periodicities are stationary. To this end, we calculated wavelet transforms for a set of suitable datasets (we used the interactive software available at http://paos.colorado.edu/research/wavelets/; Torrence and Compo, 1998). Not surprisingly, the results (not shown) confirmed that the climate system is highly intermittent; no specific peaks spanned the whole period of the last 6000 years BP (see Bütikofer, 2007).

As mentioned above, the most discussed postglacial swings or quasi-cyclic patterns are the so-called "Bond Cycles" with periods of approximately 2000–2800 years and, more importantly, ~1500 years. There is still debate as to whether large climate variations, such as the last transition from the MWP/MWE/MCA to the LIA (Bond Cycle 0), were cyclic or not. With the caveat that a 6000 years long time slice is rather short, the analyses in Fig. 5 indicate a small (non-significant) clustering of spectral peaks around 1500 years.

Bütikofer (2007) demonstrated that a millennial-scale cyclicity linked to "Bond Cycles" is postulated in the literature, however, not only for Eurasia, but also for North and South America, and Africa. Various mechanisms have been invoked in explanation. Based on the analysis of GISP2 data, O'Brien et al. (1995) showed that several phases of increased sea salt and terrestrial dust concentrations in Greenland implied either a northward expansion of the polar vortex or an enhanced meridional circulation. Bianchi and McCave (1999), analysing sediment grains from a deep-sea core in the south Iceland basin, suggested that deep-water flow was intensified (reduced) during warm (cold) periods, such as the MWP (LIA). deMenocal et al. (2000), using faunal SST reconstructions from a high-accumulation sediment core off West Africa, found a series of discrete millennial-scale cooling events recurring every ca 1500 ± 500 years. They concluded that this mode was roughly synchronous across the NA basin. In their analysis of a stalagmite $\delta^{18}O$ record from Southern Oman, Fleitmann et al. (2003) argued that variations in NA drift ice may have influenced the IOM indirectly, by way of a monsoon-Eurasian snow-cover link during the EH, a process that became negligible after the NH ice sheets had disappeared. In their monsoon record Gupta et al. (2003) also postulated a link between a weak Asian southwest monsoon with cold events in the NA including the classical transition from the MWP to the LIA. In their analysis of a sediment core from Arolik Lake in southwestern Alaska, Hu et al. (2003) demonstrated that increases in temperature and moisture corresponded to intervals of elevated solar output and reduced NA ice-bearing waters and vice versa. Niggemann et al. (2003) also found a strong coincidence between the drift ice record of Bond et al. (2001) and their $\delta^{18}O$ data from a calcitic stalagmite in Sauerland, northwestern Germany. Yu et al. (2003) analysed a fen peat record from the northern Great Plains and depicted dry and wet cycles with significant periodicities in a broad band between 1500 and 2190 years, as well as around 386 and 667 years. In their pollen data from high-resolution sediment cores taken in Chesapeake Bay in eastern North America, Willard et al. (2005) found periods of ca 3–5 century-long pine minima occurring roughly every 1400 years. Wang Y. et al. (2005) reported on a precisely dated stalagmite oxygen isotope record from Dongge Cave in southern China, which shows that, apart from the large decrease of the monsoon strength and frequency after the EH, weak events occurred in phase with the ice-rafting events in the NA (Bond et al., 2001). A multi-proxy reconstruction from a lake sediment core from the Yanchi playa in arid northwestern China (Yu et al., 2006) revealed persistent millennial-scale climate fluctuations with cold (dry) episodes corresponding approximately to cooling phases in the NA region. Finally, Baker et al. (2005) speculated that the "Bond Cycles" are even visible in their $\delta^{13}C$ data from the SH, namely sedimentary organic matter of Lake Titicaca. They postulated that these events, which were characterised by large negative values of the N–S tropical-Atlantic meridional SST gradient, may have led to increased precipitation on the Altiplano and were thus anti-phased with respect to precipitation variability in the NH monsoon region. Recently, Debret et al. (2007) re-visited well-known series in the North Atlantic Ocean, and found that the Holocene multi-centennial to millennial variability is composed of three periodicities (cycles of 1000, 1600 and 2500 years).

Table 2
Reference, coordinate and record length of the additional Holocene archives whose spectra are represented in Fig. 5 (Bütikofer 2007)

Reference	Latitude	Longitude	Record length (ka)
Sarnthein et al. (2003)	75°N	14°E	4.00
Schulz and Paul (2002)	72°36′N	38°30′W	10.00
Stuiver et al. (1995)	72°36′N	38°30′W	10.00
Risebrobakken et al. (2003)	66°58′N	07°38′E	11.50
Rousse et al. (2006)	66°33′N	17°42′W	10.00
Hall et al. (2004)	61°30′N	24°10′W	10.00
Hu et al. (2003)	59°28′N	161°07′W	10.30
Bianchi and McCave (1999)	56°22′N	27°49′W	10.00
Chapman and Shackleton (2000)	56°22′N	27°49′W	10.60
Langdon et al. (2003)	55°50′N	03°20′W	7.50
Viau et al. (2006)	25–70°N	45–165°W	14.00
Turney et al. (2005)	54–55°N	6°W	7.47
Bond et al. (2001)	54°15′N	16°47′W	12.00
Yu et al. (2003)	53°35′N	118°01′W	8.07
Niggemann et al. (2003)	51°07′N	07°54′E	6.00
Lamy et al. (2006)	41°32′N	31°10′E	7.50
Willard et al. (2005)	38°N	76°W	4.59
Nederbragt and Thurow (2005)	34°18′N	120°05′W	10.00
Lamy et al. (2006)	29°30′N	34°57′E	7.50
Dykoski et al. (2005)	25°17′N	108°05′E	11.00
Wang Y. et al. (2005)	25°17′N	108°05′E	8.85
Poore et al. (2003)	23–26°N	91.9–95.5°W	4.60
Gupta et al. (2005)	18°03′N	57°37′E	11.00
Fleitmann et al. (2003)	17°10′N	54°18′E	5.30
Baker et al. (2005)	16°S	69°W	13.00
Skilbeck et al. (2005)	33°20′S	151°30′E	10.00

2.2.2. Glacier dynamics

Comparable variability (or periodicity?) has also been detected in glacier fluctuations. In Fig. 4 we roughly identify eight periods of Neoglacial glacier advances. Each is marked with a coloured dot. Four events occurred more or less simultaneously in several regions around 5400–4800, 3800, 3100 and 2500 cal years BP. Their determination is not as precise as for the striking events of the last two millennia, which occurred around AD 600, 1050–1150, and between 1300 and 1850 (two to three major advances are reported in the latter LIA period depending on the region).

2.2.2.1. 5400–4800 cal years BP. The advances in this time period occurred in several parts of the world, including the Alps, Alaska, New Zealand and Patagonia (Grove, 2004). Thompson et al. (2006) reported an abrupt cooling and a related expansion of the Quelccaya ice cap at about 5200 cal years BP. These glacier advances broadly coincide with one of the major IRD events taking place at ca 5530 cal

Please cite this article in press as: Wanner, H., et al., Mid- to Late Holocene climate change: an overview, Quaternary Science Reviews (2008), doi:10.1016/j.quascirev.2008.06.013

years BP (Bond et al., 2001; see also Porter and Weijian, 2006). The suggested potential forcing is the orbitally induced change in insolation enhanced by a non-linear reaction of the climate system.

2.2.2.2. 3800 and 3100 cal years BP. Grove (2004) identified this period of glacier advances in the Alps, Scandinavia, the Himalaya, in the Canadian West and the Rockies, Alaska, Mount Kenya, tropical South America, and New Zealand. More detailed records obtained recently in different parts of the World show two separate advances clustering around 3800 and 3100 (Fig. 4). No specific process has been suggested so far to explain these advances.

2.2.2.3. Around 2500 cal years BP. Grove (2004) identified the advances occurring worldwide between 3000 and 2300 cal years BP. In the Swiss Alps these are dated between 3000–2600 cal years BP (Holzhauser et al., 2005), in Norway they culminated at 2750 cal years BP (Matthews et al., 2005), in the Western North American Cordillera (Koch and Clague, 2006) between 2900 and 2300 cal years BP, and in northern Chile (29°S) after 2800 cal years BP (Grosjean et al., 1998). In Patagonia, the advances took place between 2900 and 1950 cal years BP (Mercer, 1982). However, due to the limited accuracy of the dates, it is difficult to assess whether or not these advances were synchronous. The time period from 2800 to 2500 cal years BP broadly coincides with the Subboreal–Subatlantic boundary with a prominent cooling and increase of humidity in Northern Europe. Van Geel et al. (2000) claimed that the cooling and the glacier advances in the third millennium BP can be related to the abrupt decrease of solar activity around 2800–2900 cal years BP (see Fig. 7a). These authors considered this period to be an analogue of the LIA, peaking during the Maunder Minimum (AD 1630–1715). A reduction of the solar activity of ca 1 W/m^2 was attributed to an increase in cosmic rays stimulating cloud formation and reducing solar UV intensity, a decline of ozone formation, and a related decrease of absorption of sunlight in the stratosphere. Van Geel et al. (2000) also suggested that the related weakening of the monsoon and the onset of dry conditions in tropical Africa have the same origin. The uncertainty of the chronologies of records from the Asian monsoon regions (Zhou et al., 1991, Grove 2004) is still too large to support or reject this hypothesis.

2.2.2.4. First millennium AD. Besides the above mentioned advances at about AD 600, the best constrained chronologies in the Alps (Holzhauser et al., 2005), Alaska (Wiles et al., 1995) and Southern Tibet (Yang et al., 2008) confirm synchronous glacier advances in these regions around AD 200, 400, and 800–900. The most prominent advance around the 6th century AD (yellow marker in Fig. 4) is also identified in the North (Reyes and Clague, 2004) and South American Cordillera (Koch and Clague, 2006), Scandinavia (Lie et al., 2004; Matthews et al., 2000, 2005; Nesje et al., 2008), and Franz Josef Land (Lubinsky et al., 1999). The simultaneity of these advances suggests a common forcing, most probably solar or volcanic (Figs. 7 and 9), although the plausibility of these mechanisms has yet to be tested by modelling studies.

2.2.2.5. 2nd millennium AD. Evidence of generally warm climate (reconstructed from wood macrofossils, upper tree limits, pollen, diatoms, ice-cores, and other proxy data) and reduced glacier activity (derived from soils and trees in the moraines, proglacial lake sediments) between AD 900 and 1240 is found in various parts of the world (Roethlisberger, 1986; Bradley et al., 2003; Grove, 2004). Conversely, some glacier advances were recorded during this period. Advances occurred between AD 1050 and 1150 (Grove and Switsur, 1994), namely in the Alps (Holzhauser et al., 2005), Alaska (Ellis and Calkin, 1984; Wiles et al., 1995), North and South Patagonia, British Columbia (Luckman and Villalba, 2001), New Zealand (Gellatly et al., 1988), Greenland (Geirsdottir et al., 2000), Franz Josef Land (Lubinsky et al., 1999), and southeast Tibet (Zheng et al., 1994). Some of these advances were of small extent, but others, for instance those in the Alps, Franz Josef Land, northern Patagonia and southeast Tibet, were very prominent. However, the precise extent of the maximum glacier advances during the MWP is unknown in most places. Despite the low accuracy of some of these dates, the period of advances between AD 1050 and 1150 seems to be of global extent and roughly coincides with the so-called Oort minimum of solar activity (see Fig. 7). Based on the common pattern in glacier behaviour, Grove (2004) identified the LIA as a time interval from AD 1300 to 1850 composed of several periods, each lasting several decades, when glacial extents were larger. So far, the LIA is the only period during the Holocene for which glacial advances have been identified in all parts of the globe (see Fig. 4). In the Alps the LIA consisted of three major periods of glacial advance with moderate retreat in-between (Wanner et al., 2000; Holzhauser et al., 2005). The largest Alpine glacier, the Great Aletsch Glacier, peaked around AD 1350, 1670 and 1850. In most parts of the world the mountain glaciers reached their maximum between the 17th and the 19th century. Even though the peaks of glacier activity, centred at AD 1300, 1450, 1650, 1850 in the Alps, Alaska and Rockies Mountains, roughly correspond to the Wolf, Spoerer, Maunder, and Dalton minima (Wiles et al., 2004; Holzhauser et al., 2005; Luckman and Wilson, 2005), clear mechanistic principles explaining how low solar activity caused glacier advances do not exist. Interestingly, Luckman and Villalba (2001), comparing the well-dated records

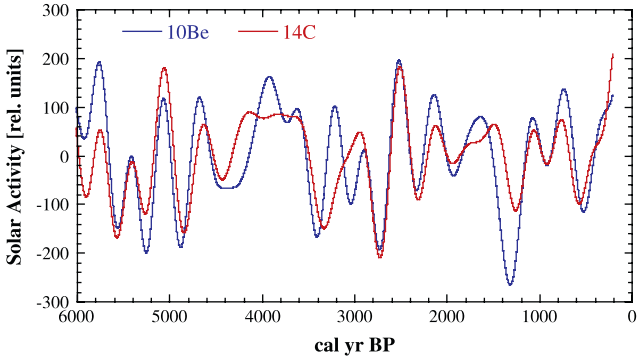

Fig. 7. Reconstructions of the solar activity based on ^{10}Be and ^{14}C. The ^{10}Be production rate was derived from ^{10}Be concentrations measured in the GRIP ice core (Vonmoos et al., 2006). The radiocarbon production rate was calculated with the Bern3D dynamic ocean carbon cycle model (Müller et al., 2006) by prescribing the tree-ring records of both hemispheres (Reimer et al., 2004; McCormack et al., 2004). Both curves were band-pass filtered with a window from 300–3000 years.

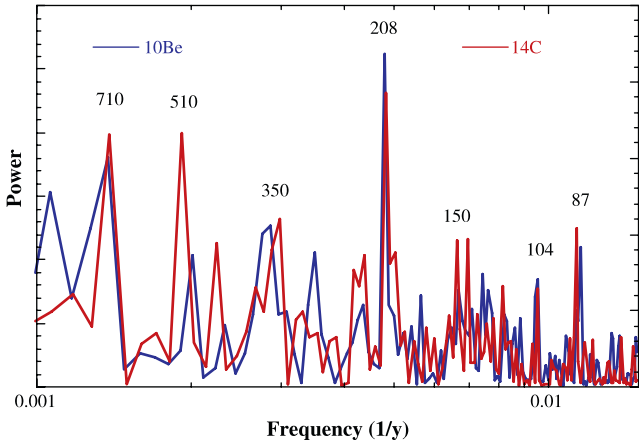

Fig. 8. Power spectra of the two solar activity records of Fig. 7, spanning the last 10,000 years.

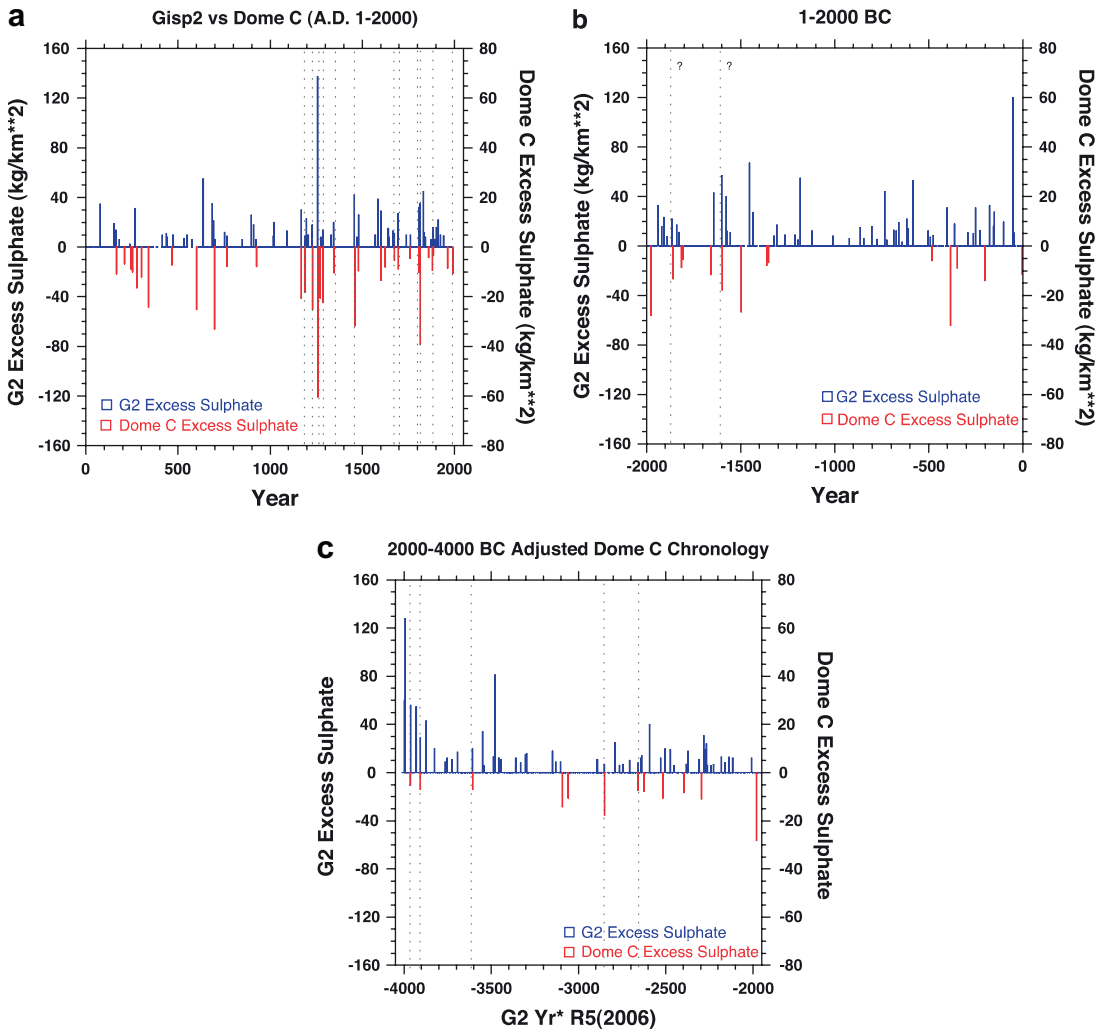

Fig. 9. Excess sulphate loadings for Dome C (Antarctica; red bars) and GISP2 ice cores (Greenland, blue bars) in kg/km^2 for the last 6000 years. The records are shown on synchronised timescales (see text for details). Vertical dashed lines indicate times of large eruptions with global influence (Crowley and Vinther, 2008).

from Alaska, British Columbia, the Canadian Rockies and Patagonia, demonstrated a broad simultaneity in the initiation (13th through 14th century) and timing of main glacier advances over the last millennium in North and South America. They explain a broad similarity of glacier fluctuations during the last millennium in the Cordillera of North and South America by the dominating role of the tropical Ocean in the organisation of the climatic system across the American Cordillera.

2.2.2.6. Last 150 years. After the mid-19th century, glaciers began to retreat, both in the Northern and Southern hemisphere (Oerlemans, 2005). Glacial retreats after the LIA maximum coincide with the increase in global atmospheric temperature since the middle of the 19th century. The rate of retreat increased in the 1950s in response to a sustained atmospheric warming trend. Since about the year 2000, glacier retreat has accelerated in many regions (Grove, 2004; Solomina et al., 2008). The current rate of glacial retreat is in coherence with the global temperature rise of the last 150 years, which is largely attributed to the anthropogenic greenhouse effect (Hegerl et al., 2007).

3. Forcings

In addition to accurately dated timeseries of the basic climatic state variables, we also need reliable timeseries of the important forcing factors (Rind and Overpeck, 1993). Even though the following section is called "forcings", we are fully aware that several forcing factors, such as greenhouse gases (GHGs), vegetation or stratospheric ozone, are also reactors and are involved in complex feedback mechanisms. During most of the Holocene, variations in predominantly three natural forcings (orbital, solar and volcanic) can be invoked as influences on global climate. Only during the last millennium, or possibly centuries, has forcing induced by human activities (such as rapid land cover change, increase of greenhouse gases and aerosols, and stratospheric ozone depletion) started to play an increasing role. The "cocktail" of all these forcing factors has been constantly changing during the last 6000 years and has not shown the same composition at any time. A rough summary of the state of knowledge on the regional influence of the important forcing factors is discussed in more detail in Sections 3.1–3.5.

3.1. Orbital forcing

The amount of solar radiation arriving at the top of the atmosphere is related not only to the energy output from the Sun but also to the position and the orientation of the Earth relative to the Sun. As a consequence of the gravitational forces of the other planets (mainly Jupiter and Saturn) acting on the Earth, the orbital

parameters of the Earth change with main periodicities around 400,000 and 100,000 years (due to changes in orbital eccentricity), 40,000 years (due to changes in the Earth's axial tilt) and 20,000 years (due to the precession of the Earth's axis). The theory of orbital forcing (often called Milankovitch theory) is unique in the sense that the orbital forcing is the only forcing that can be calculated precisely, not only for the past several million years, but also for the future (Berger, 1978; Laskar et al., 2004).

Fig. 6 depicts the calculated changes in insolation for the last 6000 years in W/m^2 as a function of latitude. The changes were calculated for each latitudinal band of 10 degrees relative to its mean insolation for the last 6000 years (Laskar et al., 2004). In June (Fig. 6a), there is a steadily decreasing trend in the north of up to 30 W/m^2. Moving south the slope becomes less steep and reaches a minimum around 1500 years BP, followed by a slight increase. In December (Fig. 6b), the changes are generally smaller (<20 W/m^2). Moving from north to south, there is little change observed at the beginning of the series. Then slowly a parabolic curve develops with a maximum between 1000 and 3000 years BP. To illustrate the changes in seasonality, the difference between June and December is also plotted (Fig. 6c). 6000 years ago the seasonality was dominant in the NH by an amplitude of 20–30 W/m^2 and then steadily decreased. Around 3000 years ago the situation reversed and the seasonality of the SH became larger. Fig. 6d shows how the mean annual insolation is changing at different latitudes. At high northern latitudes it decreases steadily by about 100 W/m^2 in total. Moving south the slope disappears slowly and at the equator the curve is flat. At high southern latitudes the mean annual insolation increases by about 20 W/m^2 and reached a maximum at 3 kyr BP, before decreasing again.

3.2. Solar forcing

Reconstructing the solar forcing caused by changes in the radiation emitted from the Sun is a much greater challenge than calculating the forcings related to orbital parameters. Based on the standard stellar model there is general agreement that the energy production in the core of the Sun does not change by a measurable quantity within a few thousand years. On the other hand, satellite-based radiometers reveal changes in total and spectral irradiance, which are correlated with solar activity. However, the change of the total solar irradiance (TSI) over an 11-year cycle is approximately 0.1%, which corresponds to a mean global forcing of 0.24 W/m^2. As a result of two competing effects – darkening by sunspots and brightening by faculae – larger activity leads to a brighter sun (Lean et al., 1995). A crucial question is whether the fluctuations of 0.1% in TSI, as observed during the past 30 years, reflect the full range of variability? Or if, on longer timescales, more significant changes are to be expected. Although there is no final answer yet, there is some evidence for larger changes:

(1) From the solar physics point of view there is no reason why the Sun should not show larger variability, as many other stars do, which, however, are not always exactly comparable with our Sun.
(2) The present period is characterised by a high, but not unusually high, solar activity (Solanki et al., 2004; Muscheler et al., 2005; Vonmoos et al., 2006). From the sunspot record we know that solar activity increased steadily from the Maunder Minimum (AD 1645–1715), when almost no sunspots were observed, until 1960. It is therefore not unreasonable to assume that the TSI and possibly also the solar spectral irradiance (SSI) show a similar trend. The difficulty is in quantifying how much TSI and SSI changed. Consequently, it is not surprising that estimates by different authors show a relatively large scatter ranging from 0.1% to 1% (Fröhlich and Lean, 2004), with recent studies pointing to rather small changes over the past few centuries (e.g. Solanki and Krivova, 2003; Wang Y.M. et al., 2005b). Recent climate model studies suggest that even low amplitude solar variations can affect climate on multi-decadal to centennial timescales (Ammann et al., 2007).

A number of paleoclimatic records provide some evidence for a link between climate changes and solar activity changes (Bond et al., 2001; Neff et al., 2001). We note that measured total solar irradiance averaged over the 11-year Schwabe cycle does not show a clear trend since the beginning of the satellite measurements in 1978. Solar irradiance changes can therefore not explain the concurrent global warming.

A clear link between solar activity and solar forcing based on physical processes is still missing. Direct observations of solar activity are restricted to the period since the invention of the telescope (AD 1610). To extend this period over the past 6000 years we have to rely on indirect proxies of solar activity. Such a proxy exists in the form of cosmogenic radionuclides, which are produced by cosmic rays in the atmosphere. The Sun modulates the cosmic ray intensity and, therefore, also the production rate of cosmogenic radionuclides by emitting solar wind with frozen-in magnetic fields. The more active the Sun, the larger is the shielding effect and the lower the production rate. After production, cosmogenic radionuclides are stored in natural archives, such as polar ice (^{10}Be) and tree rings (^{14}C). Analysing these independently dated archives provides a means to reconstruct the solar variability over at least the past 10,000 years (Vonmoos et al., 2006). However, both records are a combination of changes in the production and in the behaviour of the global system. While the production processes are very similar for the two nuclides, their geochemical systems are completely different. After production, ^{10}Be becomes attached to aerosols and is removed from the atmosphere within about 1–2 years, mainly by wet precipitation. ^{14}C on the other hand, forms $^{14}CO_2$ and enters the carbon cycle where it is exchanged between the atmosphere, biosphere and the ocean.

Fig. 7 shows recent reconstructions of the solar activity based on ^{10}Be and ^{14}C. The ^{10}Be production rate was derived from the ^{10}Be concentrations measured in the GRIP ice core, Greenland (Vonmoos et al., 2006). The radiocarbon production rate was calculated with the Bern3D dynamic ocean carbon cycle model (Müller et al., 2006, 2008), complemented by a land-biosphere module (Siegenthaler and Oeschger, 1987), by prescribing the atmospheric ^{14}C history as recorded in tree-ring records from both hemispheres (Reimer et al., 2004; McCormack et al., 2004). The choice of the ^{14}C data guarantees precise timing because its timescale is based on tree ring counting and is, therefore, very accurate (Muscheler et al., 2007). Since the still-unknown relationship between solar modulation and solar irradiance is not necessarily linear, we use relative units. The data have been band-pass filtered with a window from 300 to 3000 years. A characteristic feature of this solar forcing record is the occurrence of century-scale minima, corresponding to the so-called grand solar minima, such as the Spoerer minimum 500 cal years BP. The good agreement between the solar variability derived from ^{10}Be and ^{14}C on centennial timescales indicates that disturbances induced by the transport from the atmosphere into the respective archive are relatively small for these timescales and for the Holocene.

Power spectra of the solar activity are displayed in Fig. 8, based on the two records used for Fig. 7 band-pass filtered (25–3000 years) and spanning the last ca 10,000 years. In general, the spectral peaks displayed in Fig. 8 agree well with previous spectral estimates of centennial-scale solar variability (e.g. Clemens, 2005, and references therein). This holds especially true for the distinct peaks at 208 and 87 years, corresponding to the well-known Suess (or de Vries) and Gleissberg cycles. The good agreement between

Please cite this article in press as: Wanner, H., et al., Mid- to Late Holocene climate change: an overview, Quaternary Science Reviews (2008), doi:10.1016/j.quascirev.2008.06.013

the two spectra supports the assumption that both ^{10}Be and ^{14}C records are mainly reflections of solar variability.

3.3. Volcanic forcing

In large volcanic eruptions, a few to over a hundred Tg of insoluble silicate matter (tephra) and gases are emitted to the troposphere and stratosphere to an altitude of 20–25 km (Zielinski, 2000; Ammann and Naveau, 2003). The silicate matter quickly settles out of the atmosphere. The contribution of CO_2 is minor. The acids formed from the sulphur gases produced (SO_2, H_2S) however remain aloft for longer periods of time, and form the source for climatic perturbation. About 14% of the global sulphur emissions in the troposphere are of volcanic origin (Graf et al., 1997). Precise measurements of the radiative effects of volcanic eruptions are only available for the last 25–30 years. Because of their efficient absorption of solar radiation, volcanic aerosols heat the layer between 20 and 25 km and cause cooling at the Earth's surface. This is mainly the case during summer, when radiative processes dominate. The negative radiative forcing amounts to a few W/m^2, normally less than five (Crowley, 2000). According to analyses by Robock (2000) the global average cooling at the surface following a volcanic eruption can reach values of 0.1–0.2 °C. The NH reacts more quickly because of the larger land surface area. In winter, the radiative effect is outweighed by dynamical processes, namely an increase of the meridional temperature gradients, which induce stronger mid-latitude westerlies. Above all, this strengthening of the westerlies leads to positive NAO/AO indices and, therefore, a winter warming of the western part of the NH continents (Graf et al., 1993; Shindell et al., 2004; Fischer et al., 2006). This process can be strengthened by aerosol-induced ozone depletion in the polar regions (Solomon, 1999). In general, the following regions are subject to a major cooling: Alaska, Greenland, North Africa, Middle East and China (Robock, 2000; Shindell et al., 2004).

Although Ammann and Naveau (2003) suggested that the tropical explosive volcanic eruptions during the last 600 years followed a 76-year cycle, there is no known mechanism for a cyclic behaviour of large volcanic eruptions. Polar ice sheets are extensive sources of information on past volcanic activity. Initial analyses of paleo-volcanism concentrated on the analysis of single ice cores from Greenland (Zielinski et al., 1994, 1996; Zielinski, 2000) or Antarctica (Castellano et al., 2005). Fig. 9 shows a reconstruction of tropical explosive volcanic eruptions perturbing the stratosphere over the last 6000 years based on ice cores from both hemispheres (Crowley and Vinther, in preparation). The reconstruction is based on a comprehensive compilation of sulfate records from the Greenland GISP2 and the Antarctic Dome C ice cores. In a first step, the timeseries were controlled and differences in the chronologies eliminated at both sites by using additional data sources (e.g. from GRIP, Siple Dome and Taylor Dome). Secondly, the two sites were compared and some apparently coincident events were eliminated based on evidence for two simultaneous non-tropical eruptions that took place, for example in Iceland and Antarctica. The dashed lines in Fig. 9 indicate times of possible large "bipolar" tropical eruptions, which were clearly observed in both hemispheres and may represent large tropical eruptions affecting global climate (Crowley and Vinther, in preparation). If we concentrate on these events we can state that their distribution over time is highly inhomogeneous. No less than 12 strong eruptions were observed during the last 850 years, with a large number of events during the LIA. The climatic impact of such an accumulation of volcanic events will be discussed later. The AD 1256 event (Gao and Robock (submitted) allocate it to the year AD 1259) was likely the strongest during the last six millennia. During the whole investigated period before AD 1150 a decline in tropical volcanic activity was observed, although it should be kept in mind that the uncertainty of the Dome C dates is larger prior to 1900 cal years BP. This fact is also discernible in the new reconstruction by Gao and Robock (submitted).

3.4. Forcing through land cover change

Paleo-ecological synthesis of global land-cover change since the MH display broad spatial and temporal variability (Prentice et al., 2000; Takahara et al., 2000; Yu et al., 2000; Marchant et al., 2002; Bigelow et al., 2003; Pickett et al., 2004), but may be summarised into three major trends: (1) desertification in the African and southwest Asian subtropics related to the weakening of the Afro-Asian monsoon system, (2) shifts in NH temperate forest types and modest southward migration of the Arctic treeline related to the gradual reduction in NH summertime solar forcing, and (3) anthropogenic deforestation and draining of wetlands to create cropland and pasture, concentrated mainly in eastern and southern Asia, the Mediterranean, and Europe. While the first two land-cover changes listed above occurred in concert with changes in atmospheric and oceanic conditions, the drivers behind Holocene land-cover changes were not limited to climate fluctuations. Since the end of the Pleistocene the development of peatlands played an important role in Holocene land-cover change. Furthermore, global land cover did not respond passively to climate variability but could have influenced aspects of the evolution of Holocene climate. Land-cover change, through both biophysical and biogeochemical feedbacks to the climate system, may have had a noticeable influence on the evolution of Holocene climate (Diffenbaugh and Sloan, 2002).

Land cover feeds back to the atmosphere chiefly through changes in surface roughness, albedo and latent vs. sensible heat exchange (Charney, 1975). Forests and wetlands have a significantly different surface energy budget than grasslands and deserts. However, these biophysical effects are not the only climate-driving component of land-cover change. The biogeochemical dynamics of the terrestrial biosphere may have had a secondary influence on the climate system through long-term changes in the terrestrial carbon cycle and emissions of GHGs to the atmosphere (see greenhouse gas forcing, Section 3.5).

The terrestrial biosphere at 6000 years BP was characterised by three major differences in vegetation distribution compared to the present day: the subtropics of Africa and south Asia were occupied by grassland, xerophytic shrubland and wetlands in areas that are now desert (Hoelzmann et al., 1998), the composition of temperate and boreal forests was different and the Arctic forest limit was shifted up to 150 km north compared to the present (Prentice et al., 2000; Bigelow et al., 2003; Kaplan et al., 2003), and mesic areas of temperate Eurasia and North America were occupied by forests in areas that are now under cultivation (Fig. 10). The most dramatic of these land-cover changes occurred in the hyper-arid regions of the Sahara, Arabian Peninsula and south Asia, but this desertification of the "Green Sahara" likely caused only small carbon emission (Indermühle et al., 1999).

Over the past decade, a great deal of research has attempted to explain the massive land-cover change in the MH subtropics, particularly focusing on the mechanisms that supported and eventually led to the decline of the optimistically termed "Green Sahara" (Claussen and Gayler, 1997; Brostrom et al., 1998; Brovkin et al., 1998; Ganopolski et al., 1998; Harrison et al., 1995, 1998; Hoelzmann et al., 1998; de Noblet-Ducoudré et al., 2000; Doherty et al., 2000; Texier et al., 2000; Carrington et al., 2001; Irizarry-Ortiz et al., 2003; Renssen et al., 2003, 2006b). It is generally accepted that the increased NH solar forcing in the EH and MH was the major external driver of the intensified Afro-Asian summer monsoon system (Kutzbach, 1981; Kutzbach and Otto-Bliesner, 1982; Kutzbach et al., 1996; Rossignol-Strick, 1983). However, a major challenge for climate modellers has been to reproduce the climate

Please cite this article in press as: Wanner, H., et al., Mid- to Late Holocene climate change: an overview, Quaternary Science Reviews (2008), doi:10.1016/j.quascirev.2008.06.013

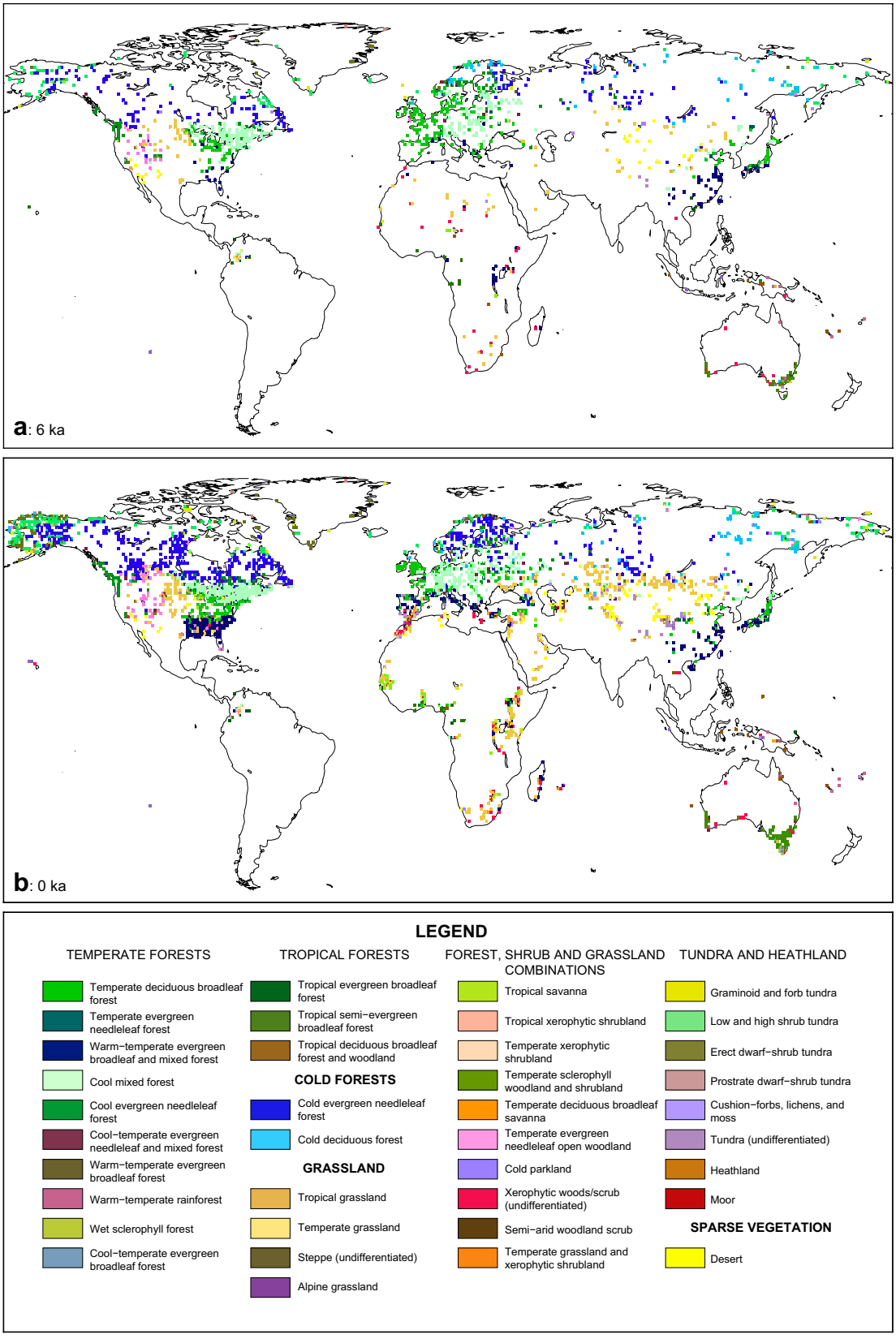

Fig. 10. Biomes at the Mid-Holocene (6000 ± 500 years BP) and present day inferred from pollen assemblages using the method of biomisation. For references on data and methods see: Prentice et al. (2000), Harrison et al. (2001), Bigelow et al. (2003), Pickett et al. (2004) and Marchant et al. (2001, 2002).

Please cite this article in press as: Wanner, H., et al., Mid- to Late Holocene climate change: an overview, Quaternary Science Reviews (2008), doi:10.1016/j.quascirev.2008.06.013

conditions suitable to sustain the type of vegetation observed in the paleo-ecological record (Hoelzmann et al., 1998; Jolly et al., 1998a, b; Prentice et al., 2000). Generally, a combination of feedbacks between the land surface, ocean and atmosphere must be invoked to increase precipitation significantly northward into the Sahara (Braconnot et al., 1999). However, even fully coupled atmosphere–ocean–vegetation model simulations often fail to reproduce inferred land cover conditions (Joussaume et al., 1999; Doherty et al., 2000). Most recent modelling studies indicate that soil development, which is usually not included in coupled models, and re-parameterisation of soil albedo in climate models to account for very bright desert soils, may be processes critical for successfully reproducing MH land cover conditions in the Sahara (Bonfils et al., 2001; Levis et al., 2004; Knorr and Schnitzler, 2006). Whatever the combination of external forcing and internal feedbacks that created the vegetated Sahara may have been, model studies, suggesting a positive biogeophysical feedback between rainfall and vegetation (Claussen et al., 1999) indicate a rapid transition from a "green Sahara" to the desert state. In a new study, based on a 6000-year reconstruction of paleoenvironmental proxies, Kröpelin et al. (2008) have shown that no indication for such an abrupt Mid-Holocene climate change is given. In addition, Marchant and Hooghiemstra (2004) have shown that the change in land cover was synchronous with a shift to more mesic vegetation types in equatorial Africa and in South America. From the perspective of the climate system, the climate effect of the change in Saharan land cover from steppe and shrublands to bright, sandy desert would have been more important than the increased forest density and canopy closure in equatorial regions. Contrary to the tropical and subtropical situation, changes in forest composition, rather than increasing or decreasing vegetation cover, were the major climate-relevant land-cover change in the high latitudes of the NH (Edwards et al., 2000; Bigelow et al., 2003).

Increased summertime insolation in the EH and MH had an effect on circumarctic land cover compared to the present. Synthesis of paleo-ecological data illustrates a northward shift of forest biomes, compared to the present, in the European Arctic and in western and central Siberia (MacDonald et al., 2000; Bigelow et al., 2003). However, landmasses on both sides of the Bering Strait showed little change in vegetation cover, and in Quebec and Labrador the forest limit was probably further south at 6000 years BP than at present, owing to the presence of the remnants of the Laurentide ice sheet. The asymmetric pattern of changes in the forest limit may be related to the downwind forcing of sea ice on surface temperatures, and to changes in the northward transport of heat to the Arctic Ocean. Because of sea ice and cold SSTs, in continental areas of the Arctic, growing season temperatures become sharply colder as one approaches the coast (Simpson et al., 2005). Despite generally warmer summer temperatures during the MH, this steep temperature gradient inhibited substantial northward displacement of the polar treeline relative to the present (Kaplan et al., 2003).

Data and model simulations agree that the geographic shifts in forest biomes southward of the polar treeline were larger than the changes in treeline itself. Changes in northern-temperate forest composition from cold temperate mixed forests to temperate deciduous forests implied an additional wintertime warming, in contrast to the orbital forcing. Vegetation model experiments indicate that a modest winter warming (Kaplan et al., 2003), which may have been amplified by the extension of forests of the high latitudes (Ganopolski et al., 1998; Wohlfahrt et al., 2004; Gallimore et al., 2005), could have effected temperature changes consistent with vegetation patterns observed in the paleorecord. However in light of comprehensive paleodata-model synthesis, the magnitude of vegetation feedbacks inferred by previous modelling studies may have been overestimated (Foley et al., 1994).

Between the MH and the end of the preindustrial period (AD ~1750), substantial anthropogenically driven land-cover changes took place in temperate and subtropical Eurasia. Already in the EH, deforestation is recorded in the Middle East concurrent with the origin of the first Neolithic societies (Bar-Yosef, 1998). By 6000 cal years BP, substantial Neolithic deforestation is recorded in Western Europe, and southern and eastern Asia (Kirch, 2005). Paleobotanical evidence suggests that anthropogenic deforestation, which began in the MH, might have caused irreversible changes to plant communities through soil erosion and the feedback of land-cover change on regional climate (de Beaulieu et al., 2005). However, Joos et al. (2004) and Strassmann et al. (in press) show that anthropogenic land use and other land-cover changes caused only a small carbon release.

Comparisons of global potential natural vegetation simulated by the global vegetation model BIOME4 (Kaplan, 2001; Kaplan et al., 2003) and the HYDE anthropogenic land use dataset (Klein Goldewijk and Ramankutty, 2004) indicate that up to 2.5×10^6 km^2 of temperate and tropical forests had already been converted to cropland and pastures by AD 1700. At this time, areas of Western Europe, China and the Ganges delta region were up to 50% deforested. This deforestation would generally result in regional cooling, due to albedo and latent heat feedbacks (Diffenbaugh and Sloan, 2002), though even this level of anthropogenic land cover change may have affected climate globally (Matthews et al., 2003).

Finally, the slow development of peatlands following deglaciation and gradual rise in atmospheric CO_2 concentrations promoted the accumulation of 50–100 Pg carbon in the terrestrial biosphere since the beginning of the Holocene (Gajewski et al., 2001; Kaplan et al., 2002; Smith et al., 2004; MacDonald et al., 2006). This carbon uptake was balanced by releases of carbon from both vegetation changes, resulting from increased LH aridity, and anthropogenic deforestation. The sum of these fluxes, albeit small, contributed to the variations in atmospheric GHG concentrations during the Holocene.

3.5. Greenhouse gas forcing

Measurements of the greenhouse gases CO_2, CH_4 and N_2O in ice cores from both polar regions exhibit small but consistent variations in concentration over the preindustrial part of the last 6000 years BP (Fig. 11a). CO_2 and CH_4 both show a generally positive trend, though a major increase in CH_4 is observed only after 3000 years BP, while CO_2 increases over the entire period. Superimposed on these long-term trends are weak centennial timescale variations. In the CO_2 record, these variations are smaller than 3 ppmv and thus approach the limits of how well ice core data can represent global atmospheric CO_2 concentration, except for the 5 ppmv increase that begins at about AD 1000 and the following decrease of similar magnitude. In the CH_4 record, conspicuous characteristics on centennial timescales are the accelerated increase in concentration around AD 1000 and the nearly constant concentrations between AD 1150 and 1700. The long-term increase of N_2O is small, and the record is dominated by variations of less than 10 ppbv on the centennial to millennial timescale. However, these variations are at the limit of significance given the analytical uncertainty of the data and, therefore, cannot be meaningfully interpreted. The magnitude and rate of the anthropogenically-induced increase in the combined radiative forcing from CO_2, CH_4 and N_2O after AD 1750 (Fig. 11b) are unprecedented in at least 16,000 years and are much larger than any of the variations in the Holocene (Joos and Spahni, 2008). The general increase in the three GHG's over the preindustrial part of the last 6000 years BP to the onset of the industrial revolution corresponds to an increase in radiative forcing of 0.30, 0.07 and 0.03 W/m^2 for CO_2, CH_4 and N_2O, respectively. Such a small (and slow) change in GHG forcing over

Please cite this article in press as: Wanner, H., et al., Mid- to Late Holocene climate change: an overview, Quaternary Science Reviews (2008), doi:10.1016/j.quascirev.2008.06.013

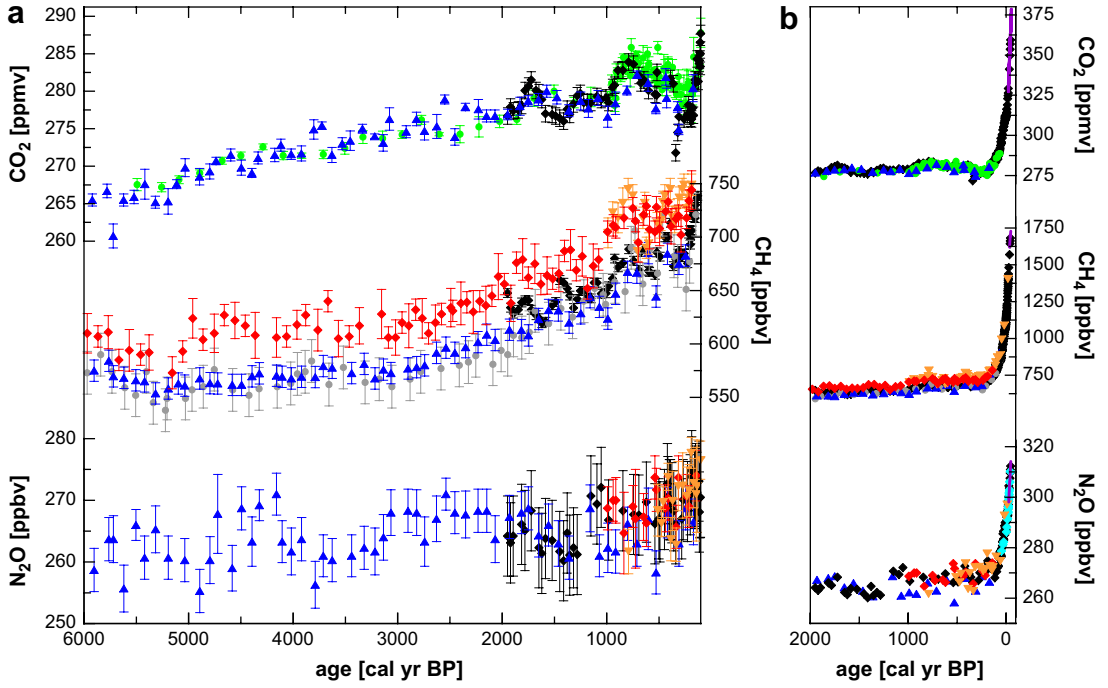

Fig. 11. Preindustrial CO_2, CH_4 and N_2O variations over the last 6 kyr together with their analytical reproducibility (a), and the rapid anthropogenic increase of the three greenhouse gases occurring after 1750 (b). Shown are data measured along the Greenland ice cores GRIP (red diamonds) (Blunier et al., 1995; Chappellaz et al., 1997; Flückiger et al., 1999) and Euro Core (orange triangles) (Blunier et al., 1993; Flückiger et al., 1999; Stauffer et al., 2002), together with data from the Antarctic ice cores EPICA Dome C (blue triangles) (Flückiger et al., 2002; Monnin et al., 2004), EPICA Dronning Maud Land (green circles) (Monnin et al., 2004; Siegenthaler et al., 2005), D47 (grey circles) (Chappellaz et al., 1997), and Law Dome ice and firn air samples (black diamonds) (MacFarling Meure et al., 2006). South Pole firn measurements are shown in cyan diamonds (Battle et al., 1996). Atmospheric CO_2 measurements from Mauna Loa, Hawaii (http://cdiac.esd.ornl.gov/trends/trends.htm) as well as CH_4 and N_2O measurements from Cape Grim, Tasmania (Prinn et al., 2000) are shown as purple line. The offset between Greenland and Antarctic CH_4 measurements manifests the interhemispheric gradient caused by uneven distribution of the sources in the two hemispheres and the short CH_4 life time. All data are plotted on their original time scale.

the last 6000 years is associated with a relatively small change in global mean temperature (0.3 °C for a climate sensitivity of 3 °C for a nominal doubling of CO_2).

Over the past decade, several hypotheses have been put forward to explain the millennial trend in CO_2. Indermühle et al. (1999) suggested that the long-term increase in CO_2 after 8000 years BP was a combination of a progressive release of carbon by the terrestrial biosphere, a weak warming of the ocean's surface until about 6000 years ago, and a minor contribution from changes in the calcite cycle of the ocean. An alternative hypothesis by Broecker et al. (2001) explains the slow increase of atmospheric CO_2 before industrialisation by a slow adjustment of the ocean's carbonate chemistry. The build-up of the terrestrial biosphere after the last ice age has drawn down atmospheric CO_2 and hence increased the ocean's CO_3-content. This caused the saturation horizon of calcium carbonate (lysocline) to deepen, reducing CO_3^{2-} in the surface waters and increasing atmospheric CO_2 correspondingly. Ridgwell et al. (2003) suggested that the build-up of coral reefs, which lead to a higher surface water CO_2 saturation and, therefore, to oceanic outgassing of CO_2, could partly explain the observed rise in atmospheric CO_2. Controversially, Ruddiman (2003) attributed the slow rise in CO_2 concentrations to early anthropogenic activity.

Two of the mechanisms put forward are unlikely to be the main driver of the observed atmospheric CO_2 rise: (1) The early anthropogenic hypothesis has been challenged through modelling studies by Joos et al. (2004) who showed that the modelled land use emissions would have to be revised upward by a factor of 3–4. Additionally, such a scenario would not be compatible with the best-available record of δ^{13}C-CO_2 from ice cores (Indermühle et al., 1999); (2) Recent modelling studies attempting to quantify the change in terrestrial C storage during the Holocene do not agree in the sign of the change (Kaplan et al., 2002; Brovkin et al., 2003; Joos et al., 2004; Schurgers et al., 2006). However, because of the relatively small magnitude of the change in terrestrial C storage modelled in these studies, and the fact that none of the current models considers the development of peatland, which led to additional terrestrial carbon storage (see previous section), all agree that natural changes in the terrestrial biosphere were unlikely to have been the main driver for the observed rise in CO_2 concentrations.

We conclude that a range of mechanisms most likely contributed to the 20 ppmv CO_2 rise between 8000 years BP and the preindustrial, including calcite compensation, SST changes, coral reef build up and, to a minor extent, C uptake and release through changes in the terrestrial biosphere (Joos et al., 2004). Better quantification of the contributions of the different sources will require more highly resolved and precise δ^{13}C measurements on ice-core CO_2, together with improved, fully-coupled models of the land-ocean-atmosphere global carbon cycle.

Calculations of global CH_4 source distributions based on the interhemispheric gradient measured in ice-core CH_4 (Chappellaz et al., 1997; Brook et al., 2000) suggested that the low CH_4 concentrations of the MH were caused by gradual desiccation in parts of the tropics, mainly in the Sahel and Sahara regions. The top-down calculations also suggest that the development of boreal wetlands were at least partly responsible for the CH_4 increase observed after 5000 cal years BP. This is, however disputable, since records of peatland development do not support a high NH origin of the observed CH_4 increase (MacDonald et al., 2006). Recent modelling studies have pointed out that changes in the OH sink of CH_4 influence the atmospheric CH_4 concentration during the Holocene substantially and could be more important than previously thought (Kaplan et al., 2006; Harder et al., 2007). As with CO_2, the gradual increase in CH_4 concentrations after 5 kyr BP has been

attributed to early anthropogenic activity, particularly through the advent of rice cultivation (Ruddiman and Thomson, 2001). This hypothesis is based on the observation that the evolution of CH_4 was unique during the Holocene, compared to earlier interglacials. However, CH_4 data over Marine Isotope Stage 11 display variations in CH_4 concentrations similar to the Holocene (Spahni et al., 2005), supporting explanations based on natural variability. On the other hand, a comprehensive bottom-up modelling study by Kaplan et al. (2006) could not dismiss the role of early anthropogenic activity in the increase of atmospheric CH_4 concentrations since 5 kyr BP.

Because of the heterogeneous nature of CH_4 sources and interaction with other reactive trace gases and aerosols that influence the CH_4 sink in the atmosphere, the problem of understanding the drivers of Holocene CH_4 variability eludes a simple explanation. However, promising new observations (e.g. $\delta^{13}C$-CH_4 in ice cores), and new activities employing state-of-the-art coupled land-atmosphere chemistry-climate modelling should lead to a much greater understanding of the CH_4 record in the near future.

Finally, evaluation of the N_2O variability over the Holocene is in its earliest stage (Flückiger et al., 2002). The range of N_2O sources (oceanic and terrestrial) defies a simple interpretation of the record and a combination of additional measurements and modelling efforts will likely be required to understand the N_2O evolution during the Holocene.

4. Modes of variability

Changes in the dominant modes of climate variability may contribute substantially to climate change at the regional scale. Such changes could be related to internally generated, quasi-random variability (also called "internal forcing") or to changes in the external forcing. We concentrate here on the major high-frequency climate variability modes in the Pacific (El Niño Southern Oscillation, ENSO) and the Atlantic (North Atlantic Oscillation, NAO), with some attention to multi-decadal to century scale climate variability modes, namely the Pacific Decadal Oscillation (PDO) and the Atlantic Multidecadal Oscillation (AMO), which interact with ENSO and NAO respectively. The variability of the Atlantic Meridional Overturning Circulation (AMOC) is also considered.

4.1. El Niño Southern Oscillation (ENSO)

The ENSO phenomenon represents the most important branch of internal variability of the global climate system (Diaz et al., 2001). Its spatial influence encompasses the Pacific Ocean and its surroundings, almost the whole SH, the Pacific tropics, and spreads to southwestern North America and even into the Atlantic area. Several authors tried to reconstruct ENSO variability during the Holocene (e.g. Shulmeister and Lees, 1995; Gagan et al., 1998; Rodbell et al., 1999; Clement et al., 2000; Moy et al., 2002; Rein et al., 2004). Fig. 12 shows two ENSO timeseries, one based on lithic flux in marine sediments off Peru (Rein et al., 2004, 2005), the other on results of a coupled ocean–atmosphere model (Clement et al., 2000). Both the observed lithic flux and the model-based frequencies (events/500 years) show a clear positive trend indicating a shift to higher ENSO activity during the LH compared to the MH. Reduced ENSO activity during the MH is confirmed by dry conditions on the Peruvian coast (Keefer et al., 1998) and arid conditions with high rainfall intensity in central Chile (Jenny et al., 2003). In addition, a warmer and wetter climate prevailed in the Austral-Asian region (Shulmeister and Lees, 1995; Gagan et al., 2004; Rein et al., 2005). Based on the lithic flux curve (Fig. 12), a strong increase of ENSO variability and even frequency took place between 5600 and 3500 cal years BP (Rein et al., 2005), followed by a constant frequency between 3500 and 2000 cal years BP. During this latter time period the model results indicate a lower ENSO activity. Between about 1300 and 700 cal years BP the ENSO activity decreased strongly, after which only the lithic flux curve increased. McGregor and Gagan (2004), based on oxygen isotope ratios in corals from Papua New Guinea, identified large and protracted El Niño events around AD 600 and AD 1600 (1350 and 350 cal years BP). Rein et al. (2004) associated the weak late medieval ENSO activity to dryness in the northern Arabian Sea and the mid-latitudes of both Americas, and wetness in the Cariaco Basin. They show that the recurrence period of very strong El Niño events is 60–80 years, and Moy et al. (2002) attribute the variance between 4- and 15-year periods to El Niño activity. Probably the ENSO variability also influenced the frequency of intense hurricanes over the past 5000 years in the Caribbean and perhaps the entire North Atlantic basin in the sense that La Niña like conditions favoured the development of more intense hurricanes (Donnelly and Woodruff, 2007). Longer La Niña periods with increased hurricane frequencies occurred between 4400 and 3600 years BP, between 2500 and 1000 years BP and from 250 years BP to the present.

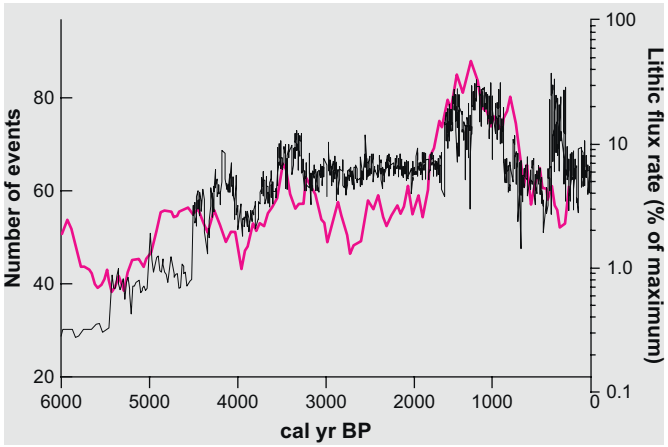

Fig. 12. Two timeseries representing the ENSO activity during the last 6000 years: (a) the black curve is based on lithic flux in marine sediments off Peru (Rein et al., 2004, 2005); (b) the pink curve represents model results by Clement et al. (2000).

4.2. North Atlantic Oscillation (NAO)

The North Atlantic Oscillation (NAO), Arctic Oscillation (AO) and Northern Annular Mode (NAM), represent the major modes of climate variability in the NH. They are a major source of inter-decadal, or even longer-term, climate variability (Wanner et al., 2001; Thompson and Wallace, 2001). Their influence is clearly strongest in winter and the related circulation indices show notable decadal- to century-scale variability (Luterbacher et al., 2001). The NAO dynamics are not as well investigated or understood, as in the case of ENSO (Hurrell et al., 2003), with only a few studies dealing with Holocene NAO/AO reconstruction or modelling (e.g. Keigwin and Pickart, 1999; Noren et al., 2002; Rimbu et al., 2003; Gladstone et al., 2005; Otto-Bliesner et al., 2006). Fig. 13a shows the smoothed timeseries of the expansion coefficient representing the first principal component, which describes 69% of the SST field variance, based on alkenone data from sediment cores from the North Atlantic, the Mediterranean Sea and the northern Red Sea. There is evidence that the NAO played a role in generating millennial-scale SST trends in that the positive (negative) phase was accompanied by relatively mild (cold) winters over northern Europe and a relatively cold (warm) climate in the eastern Mediterranean and the Middle East (Rimbu et al., 2003). The generalised map in Fig. 13a shows the SST trends in different regions between 6000 cal years

Please cite this article in press as: Wanner, H., et al., Mid- to Late Holocene climate change: an overview, Quaternary Science Reviews (2008), doi:10.1016/j.quascirev.2008.06.013

BP and the present. A negative SST trend in the northeast Atlantic and the western Mediterranean Sea, combined with a positive trend in the western subtropical Atlantic and the northern Red Sea, indicates that the NAO index was likely subject to a trend from positive values in the MH to negative ones in the LH. This shift is nicely represented by the almost linear trend from negative to positive values of the expansion coefficient timeseries in Fig. 13a between 6000 and 2000 cal years BP. At about 2000 cal years BP a weak reversal occurred. Fig. 13b shows the difference between simulated NH sea level pressure at 6000 years BP and present day conditions (Rimbu et al., 2003). The simulation was carried out with ECHAM 3 (Lorenz et al., 1996). The strongly negative values in the Iceland area point to positive NAO indices at 6000 years BP as well. Keigwin and Pickart (1999) suggested that the NAO may be a useful analogue for millennial-scale ocean variability during interglacial climate states. A negative NAO regime might be a key feature of cold LIA-type events (LIATE's; Wanner et al., 2000) although the circulation characteristics of the intervening warm periods are less obvious (Bond et al., 1997).

Based on terrigenous inwash layers in cores from 13 lakes in the northeastern United States, Noren et al. (2002) found a quasi-periodic behaviour of the NAO (periodicity of about 3000 years) with increased storminess at around 5800 and 2600 years BP. However Gladstone et al. (2005) warned against jumping to conclusions about the role of NAO in Holocene climate change. Based on their analysis of PMIP2 model simulations, they found only minor differences in NAO characteristics between the MH and pre-industrial climates, with some tendency to a more positive average NAO index during the MH. Otto-Bliesner et al. (2006) indicated that the AO patterns of the MH are similar to those of the preindustrial period.

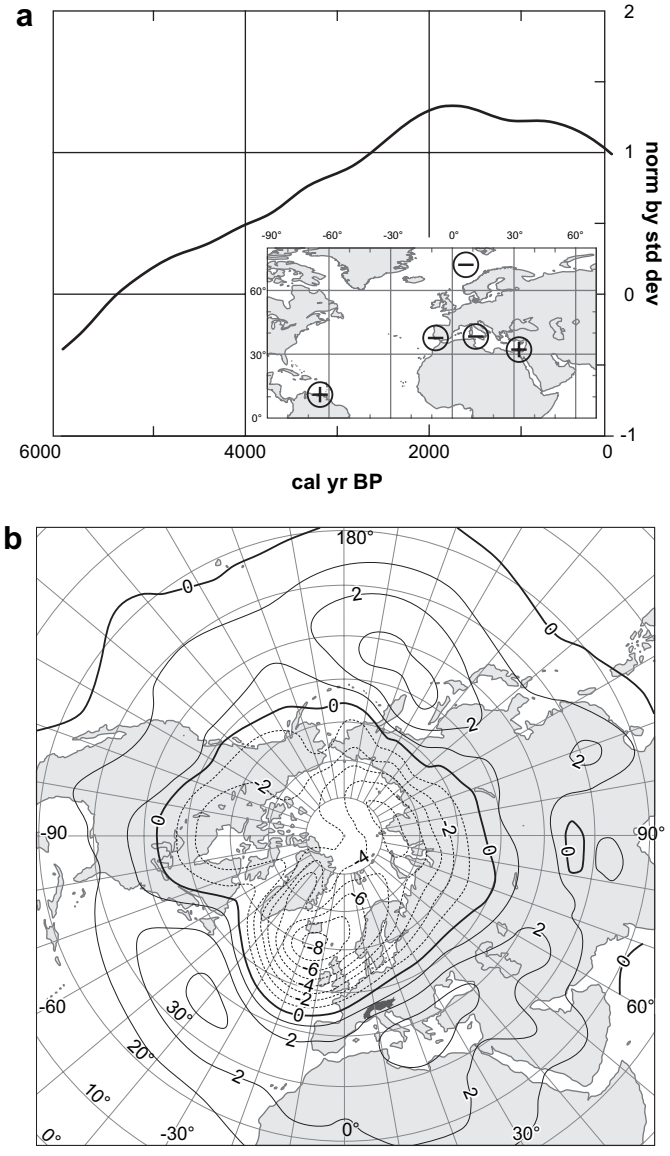

Fig. 13. (a) Curve: smoothed timeseries of the expansion coefficient representing the first principal component which describes 69% of the SST field variance of the studied area on the represented map and which is therefore highly correlated with the NAO (Rimbu et al., 2003). Negative values stand for NAO+ tendency, positive values indicate a NAO− tendency. Map: geographic overview showing the SST trends in the areas where alkenone data are available. (b) Difference between simulated Northern Hemisphere sea level pressure at 6 kyr BP minus present day conditions (modified after Rimbu et al., 2003).

4.3. Multi-decadal to century timescale variability, Pacific Decadal Oscillation (PDO), and Atlantic Multidecadal Oscillation (AMO)

Timescales of decades to centuries deserve a special focus in the discussion of natural climate variability. This is because one needs to disentangle the role of external forcing and internal variability when addressing question about the cause of such phenomena as the MWP, the LIA, or the supposed 1500-year cycle (Bond et al., 1997). Early reviews (Stocker and Mysak, 1992; Stocker, 1996) are outdated now because the past decade has seen a major increase in the number and quality of paleoclimatic reconstructions from many different archives (Delworth and Mann, 2000), more long-term simulations using more complex models, and better theoretical understanding of the mechanisms leading to multi-decadal to century timescale variability.

Analysis of SST anomalies in the North Pacific during the 20th century reveal distinct patterns that persist for several decades (Mantua et al., 1997). The leading mode of an EOF analysis exhibits warm conditions in the central tropical Pacific, which extend northward along the American west coast up to Alaska. Cold conditions spread from the west across the Pacific north of about 20°N. This pattern is associated with positive values of the PDO index, which is defined as the principal component of the leading mode of monthly North Pacific temperature anomalies (with respect to the global mean SST) poleward of 20°N (Mantua and Hare, 2002). Usually, the mean is taken over the months November through March for the PDO index. The PDO index over the 20th century exhibits a persistent positive phase from the 1920s to the 1940s, and then turns negative from about 1947 to 1977. The latter change in sign is also associated with observed shifts in many climate variables in the Pacific region. Analysis of 20th century data suggests that there is not a strictly periodic process underlying the PDO, but rather modes that persist for several decades (Minobe, 1997). Although such persistence offers the possibility of enhanced predictability of the Pacific ocean-atmosphere system, a consistent theory for the PDO is still missing.

In addition to the changes in SST, surface air temperatures and precipitation over the North American continent show distinct patterns (Mantua et al., 1997). Winter air temperature anomalies correlate positively with the PDO, especially in the Alaskan panhandle, while winter precipitation correlates negatively with the PDO, except along the Alaskan coastal range where strong positive correlations occur likely due to warmer SSTs off shore. Furthermore, strong westerly wind anomalies are associated with a positive PDO index around 30°N in the central Pacific Ocean. The PDO is an important climate indicator for the fisheries along the entire North American coastline of the Pacific (Hare et al., 1999).

Tree ring networks along the North American west coast have been used to reconstruct the PDO for the past few centuries

Please cite this article in press as: Wanner, H., et al., Mid- to Late Holocene climate change: an overview, Quaternary Science Reviews (2008), doi:10.1016/j.quascirev.2008.06.013

(D'Arrigo et al., 2001; Gedalof and Smith, 2001). An important finding is that rather rapid regime shifts of Pacific climate variability have occurred frequently in the past. However, the combination of several records into an optimal reconstruction suggests that the PDO is not a persistently dominant feature of Pacific variability (Gedalof et al., 2002). Tree rings can also be utilised to reconstruct the changes in dryness at locations characteristic for the PDO during the last millennium (MacDonald and Case, 2005). Multi-decadal variability of summer rainfall in China can also be linked to the PDO and was used to reconstruct a PDO index back to AD 1470 (Shen et al., 2006).

Another important mode of multi-decadal variability is now commonly referred to as the Atlantic Multidecadal Oscillation (AMO) (Delworth and Mann, 2000; Kerr, 2000; Enfield et al., 2001). This mode is characterised by basin-wide, coherent SST anomalies in the Atlantic Ocean, north of the equator. An AMO index can be derived by averaging, detrending and low-pass filtering (to remove subdecadal variations) the annual mean SST anomalies over the North Atlantic. The signal is quite robust with respect to the choice of the filter (Enfield et al., 2001; Sutton and Hodson, 2005; Knight et al., 2005), and shows five periods with positive SST anomalies in the late 19th century, from AD 1931 to 1960, and negative anomalies from AD 1905 to 1925, and from AD 1965 to 1990. During the last 15 years the AMO index has been positive with an increasing trend. Amplitudes of the AMO-induced temperature variations in the North Atlantic SSTs are in the order of 0.2 °C.

The impact of the AMO for regional to hemispheric climate is significant. Part of the globally observed warming in the 1930s to 1970s is thought to be caused by a positive mode of the AMO. The extreme drought in the US in the 1930s falls into this period, and links to the AMO have been suggested (Schubert et al., 2004). Consistent with this, rainfall and river flows are enhanced in the US during the negative phase of the AMO (Enfield et al., 2001). Changes of SST in the tropical and subtropical Atlantic associated with swings in the AMO may influence hurricane activity (Goldenberg et al., 2001). Multi-decadal signals are also found in timeseries of Arctic sea-ice cover (Venegas and Mysak, 2000).

Delworth and Mann (2000) attempted a reconstruction of the AMO back to AD 1650 based on their multi-proxy reconstruction of hemispheric temperature anomalies (Mann et al., 1998). The AMO was captured in the 5th mode of an EOF analysis and, therefore, explained only little variance of the total signal. Nonetheless, spectral power in a band from 50 to 100 years was reported. Gray et al. (2004) used only tree ring records from sites strongly influenced by Atlantic SST variability and demonstrated good reconstruction skill using a linear combination of the first five eigenvectors. They identified 13 positive and negative AMO phases since AD 1567, with a duration exceeding a decade. However, only six of these phases lasted for several decades, which is typical for the AMO in terms of duration. A spectral analysis revealed non-stationary power over a wide band from 40 to 130 years. Remarkable is the existence of a rather long quiet phase, with respect to AMO, from about AD 1710 to 1760. In summary, these reconstructions suggest that the AMO does not exhibit well-defined periodicity and hence should not be termed an "oscillation". By the same argument, it appears very unlikely that variations in solar activity, such as the Gleissberg cycle (Peristykh and Damon, 2003), play a role in the generation of this internal mode of variability.

Information on the AMO further back in time can be extracted from reconstructions of hydrologic conditions. Booth et al. (2006) present two 2000-year drought records based on pollen assemblages from the Great Lakes region. Several multi-decadal dry phases occurred between AD 950 and 1250, and they hypothesise that this might have been caused by warmer than normal Atlantic SST conditions. This could indicate a series of strongly positive AMO phases during the MWP, themselves contributing to the MWP. Fischer and Mieding (2005) analysed high-resolution sodium records measured on several Greenland ice cores for the last 1000 years. They found persistent variability on a timescale of about 10 years, and mutidecadal variability of about 60 years after AD 1700.

Reconstruction of multi-decadal variability over the entire Holocene may be possible from Greenland ice cores (Yiou et al., 1997), or from high-resolution marine sediments. Risebrobakken et al. (2003) reconstructed SST and water-mass properties from foraminiferal abundance and stable isotope measurements. This was performed on a sediment core from the eastern Norwegian Sea, which covered the entire Holocene and part of the termination of the last ice age. The timeseries contain consistent power around 80 and 110 years.

4.4. Natural variability generated by changes in the Atlantic Meridional Overturning Circulation (AMOC)

Multi-decadal variability is also identified in climate model simulations and there are multiple lines of evidence that this is due to variations in the North Atlantic meridional overturning circulation (AMOC). Models of various degrees of complexity show multi-decadal to centennial variations (e.g. Stocker and Mysak, 1992; Delworth et al., 1993; Timmermann et al., 1998; Latif et al., 2004; Vellinga and Wu, 2004). Delworth et al. (1993) found irregular oscillations on a timescale of about 50 years in their coupled Atmosphere-Ocean General Circulation Model (AOGCM) simulations. These oscillations are driven by surface density anomalies influencing the AMOC, which itself feeds back on the advection of the surface anomalies from lower latitudes. Timmermann et al. (1998) found variability on timescales of 35 years in their multi-century model integration, and show that the cycles are associated with changes in the AMOC. Also, an interaction between the Atlantic and the Pacific was discussed, suggesting teleconnections associated with these changes. The clear link between Atlantic SST anomalies and the AMOC can be used to estimate current and future changes of the AMOC (Latif et al., 2004). Furthermore, increased predictability on the decadal timescale is expected (Sutton and Hodson, 2005).

A 1600-year unforced simulation using a coupled AOGCM exhibited strong interannual to centennial fluctuations of the AMOC (Vellinga and Wu, 2004) with intermittent spectral power in the band of 70–120 years. The study suggests that the tropical atmosphere also plays an important role in these fluctuations. When the AMOC is in a weak phase (negative AMO index), the Atlantic part of the ITCZ and the associated rainfall move southward toward the equator. This causes a surface freshwater deficit of the waters flowing northward along the western boundary of the Atlantic basin producing positive salinity anomalies. These are then advected with the AMOC into the areas of deepwater formation where they accelerate the AMOC. This then induces the strong phase of the oscillation (positive AMO; see also Section 5). This suggests that the positive AMO phase of the last 15 years may have been caused by a stronger AMOC (Knight et al., 2005). An interaction of AMO with the NAO was found in a 1200-year simulation using a coupled AOGCM (Dai et al., 2005). While the fluctuations with a period of about 24 years are caused by variations in the AMOC, the associated changes in SST and sea ice distribution in the Arctic also imprint this periodicity on the NAO. This was previously suggested by Sutton and Hodson (2003) who analysed simulations with an Atmosphere General Circulation Model (AGCM) forced by observed SSTs. An outline of relevant simulation results is given at the end of Section 5.2.

5. Simulations

The most complex tools to simulate and diagnose climate changes during the Holocene are GCMs. They are used to simulate

Please cite this article in press as: Wanner, H., et al., Mid- to Late Holocene climate change: an overview, Quaternary Science Reviews (2008), doi:10.1016/j.quascirev.2008.06.013

synoptic- to global-scale phenomena. However, the explicit calculation of many atmospheric and oceanic processes comes at the expense of high computational costs. Although the horizontal resolution of GCMs used in palaeoclimatology is restricted to a few hundred kilometres and thus important processes at subgrid scale are still only included in an approximate way, the length of the simulated periods with GCMs is presently limited to approximately 500–2500 years for most of the models. However, some GCMs have recently been optimised for speed by further reducing spatial resolution or simplifying some aspects of the model physics and have been successfully run for longer periods, such as the entire Holocene (e.g. Schurgers et al., 2006; Liu et al., 2007).

Models with an even higher reduction of complexity are, therefore, a complementary tool to GCMs, in particular the so-called Earth system Models of Intermediate Complexity (EMICs) (Claussen et al., 2002), which allow a large number of long simulations to be performed, but include some simplified representations of large-scale atmosphere and ocean dynamics. Furthermore, many EMICs include coupled modules for land ice and vegetation dynamics, or for the carbon cycle, which is not yet standard for GCMs used in palaeo-simulations. Although these components have recently been included in many GCMs and simulations from the mid-19th century to the end of the 21st century (e.g. Friedlingstein et al., 2006), the required computation time is still a problem in longer simulations. One consequence of the reduced complexity of atmosphere and ocean dynamics in EMICs is a reduced level of internally generated variability. Thus EMICs are well suited to investigate externally large-scale forced climate change, but are less suited to analysing the role of internally generated variability. In addition, EMICs have limitations with respect to simulating circulation and regional climates.

In the first part of this section simulation results related to millennial timescales are discussed, while the second subsection covers decadal to multi-centennial variability. The major part of each subsection describes changes in the climatological mean conditions, but both subsections end with a discussion of changes in higher frequency variability, such as ENSO and NAO. The relative importance of externally forced vs. internally generated variability is considered in each subsection.

5.1. Changes on millennial timescales

Transient simulations performed with EMICs over the Holocene have generally produced a relatively smooth temperature evolution (Weber, 2001; Crucifix et al., 2002; Brovkin et al., 2002; Renssen et al., 2005a, b; Wang Y.M. et al., 2005a). This evolution can be interpreted as a response of the climate system to changes in insolation (Fig. 6) and to a lesser extent to those in the GHG concentrations (Fig. 11), taking into account the thermal inertia of the ocean and the feedbacks that amplify or damp the response in various regions. One of the main characteristics of those simulations is a general decrease in summer temperature at mid- and high (northern-)latitudes over the last 6000 years associated with the decline of insolation in boreal summer (Weber, 2001; Crucifix et al., 2002; Brovkin et al., 2003; Renssen et al., 2005a; Wang Y.M. et al., 2005a), in agreement with reconstructions (Figs. 2–4). In boreal winter, the temperature decreases north of 60°N, mainly because of a memory effect of the sea ice and the ocean, while at mid-latitudes winter temperatures slightly increase during the Holocene. The behaviour in the Southern Ocean is also very different between the seasons, with a cooling over the last six millennia during the austral summer, spring and winter, and a warming in autumn over the whole Holocene (Renssen et al., 2005b). Those results underline the crucial importance of taking into account the seasonal signal when interpreting proxy records (e.g. Fig. 2) and when performing model-data comparison.

Modelling of palaeoclimate with GCMs was pioneered in the 1970s and 1980s (e.g. Alyea, 1972; Williams et al., 1974; Mitchell, 1977; Manabe and Hahn, 1977; Kutzbach and Otto-Bliesner, 1982). The majority of these early studies focused on the LGM and the EH. Kutzbach and Guetter (1986) presented simulations for the climate during several periods between the LGM and today. A large part of the more recent GCM studies on the MH climate has been undertaken in the framework of the PMIP, which is a coordinated comparison of results from several models with proxy data in order to assess the ability of climate models to simulate climate states that considerably differ from the present climate. PMIP focuses on the LGM and on the MH, with simulations undertaken for 21,000 years BP and 6000 years BP. In the first phase (PMIP1) atmospheric GCMs were driven by SST climatologies or the models were coupled to simple mixed layer ocean models (Joussaume and Taylor, 1995; Hall and Valdes, 1997; Vettoretti et al., 1998; Masson et al., 1999; PMIP, 2000). In the second phase (PMIP2) fully coupled atmosphere–ocean and atmosphere–ocean–vegetation GCMs were used (Masson-Delmotte et al., 2006; Braconnot et al., 2007a, b). PMIP is based on quasi-equilibrium simulations in which the orbital parameters, GHG concentrations, and ice sheets are specified. The models are run with these forcings until they approach an equilibrium state, which is typically after several hundred years. The climate for the period of interest is then estimated from a few hundred simulated years in the quasi-equilibrium state.

An overview of the PMIP2 simulations is given in Braconnot et al. (2007a, b). They are, in general, in better agreement with proxy data than the PMIP1 simulations. Fig. 14 is taken from Braconnot et al. (2007a) and shows the ensemble mean northern summer temperature and precipitation anomalies at 6000 years BP compared to preindustrial. The main features of the simulated MH mean climate are a stronger (weaker) seasonal temperature cycle on the NH (SH) compared to modern conditions (Fig. 14a). Substantially increased temperatures over the NH continents during boreal summer of up to 2 K lead to stronger thermal lows and stronger summer monsoons, which in turn changes temperatures and precipitation over parts of Africa and India. The SH continents show also weak positive temperature and precipitation anomalies during this season, while over the SH oceans there is little change. In boreal NH winter a mainly continental cooling is found, which is associated with a stronger winter monsoon. These anomalies are consistent with those simulated by EMICs. Only some of these changes can be understood as a direct, instantaneous response to the insolation forcing, while others clearly show memory and feedback effects caused by the ocean or sea-ice (Liu et al., 2004; Mikolajewicz et al., 2003; Zhao et al., 2005; Bracconnot et al., 2007b; Ohgaito and Abe-Ouchi, 2007). The role of the vegetation feedback has been found to be smaller in the PMIP2 simulations than in earlier studies, which is partly attributed to the lack of consistent reference simulations in earlier studies (Braconnot et al., 2007b).

Transient GCM simulations that include the MH have mostly been performed using acceleration techniques to reduce computation time. Lorenz and Lohmann (2004) simulated the last 7000 years with an AOGCM by changing the orbital forcing for every simulated year by an increment that is associated with 10 years in reality. Thus the climate response to the orbital forcing for the entire 7000-year long period can be estimated with a simulation that is only 700 years long. In a second simulation the acceleration factor was set to 100 to simulate a much longer period. This approach can be expected to capture the response of the atmosphere and the mixed layer ocean to the orbital forcing, as these components of the climate system quickly reach equilibrium under changed forcings. The response of slow ocean components and the climatic effects of internally generated ocean variability, however, are not fully represented. The simulation of Lorenz and

Please cite this article in press as: Wanner, H., et al., Mid- to Late Holocene climate change: an overview, Quaternary Science Reviews (2008), doi:10.1016/j.quascirev.2008.06.013

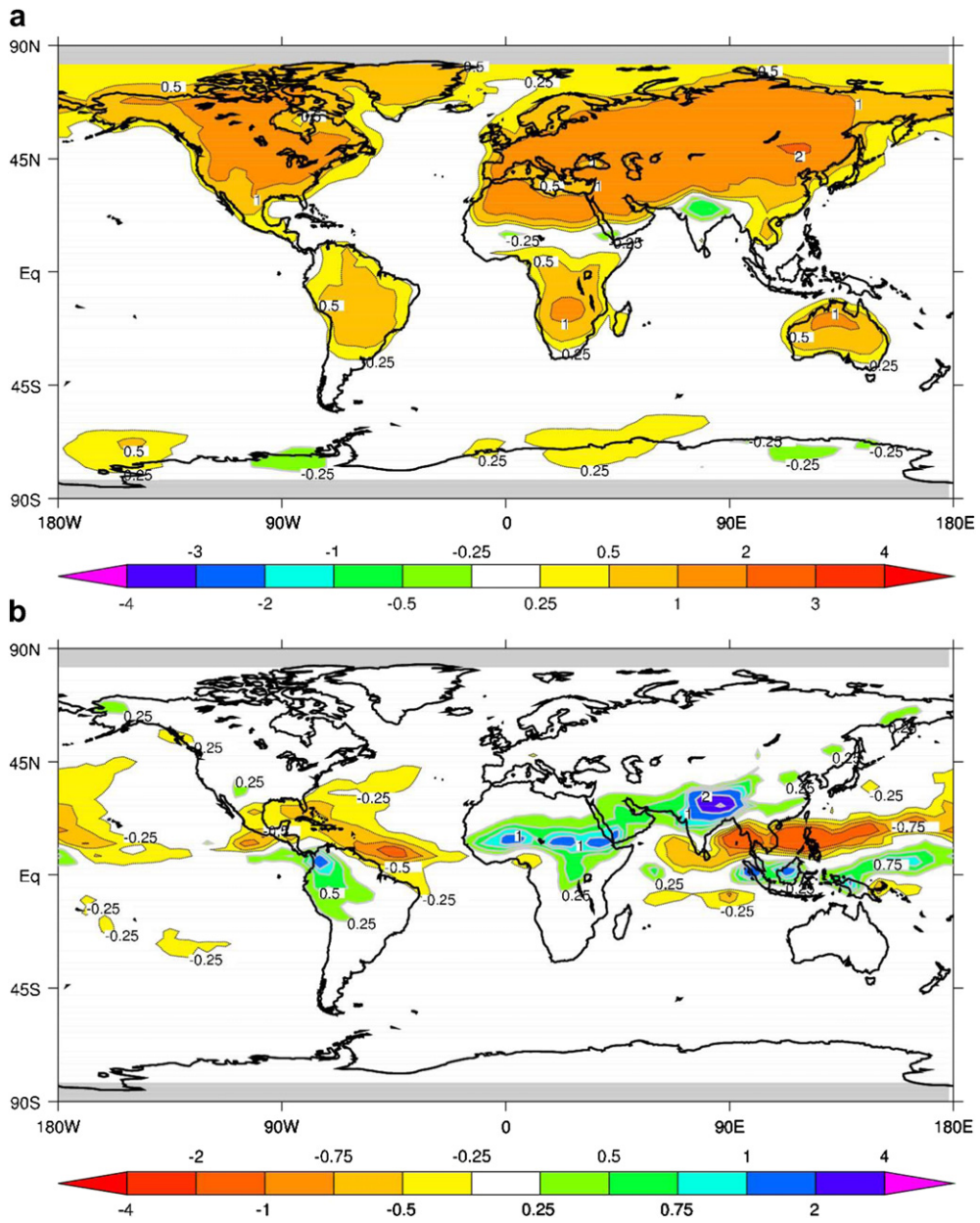

Fig. 14. Ensemble mean of PMIP2 simulations: (a) JJAS mean surface air temperature (°C) differences between Mid-Holocene and preindustrial (0 ka). (b) Same as (a) but for precipitation (mm/day). From Braconnot et al. (2007a).

Lohmann (2004) shows a smooth transition from the MH to the present with opposing temperature trends in the tropics and extratropics. The same acceleration technique was employed by Hall et al. (2005) in a simulation with an AGCM coupled to a simple mixed layer ocean to study the response of atmospheric circulation to orbital forcing.

The period 7000 years BP to 4500 years BP has been simulated by Wagner et al. (2008) with the coupled AOGCM ECHO-G without using acceleration techniques. The simulation was forced by orbital changes and by estimates for solar variability, which were obtained by scaling production rates of cosmogenic ^{14}C (Solanki et al., 2004), such that the difference between present-day and Maunder Minimum solar activity is 0.3% (Crowley, 2000). A second simulation for the same period with only orbital forcing was also performed. The temperature differences between the simulated summer and winter mean temperatures in the orbitally forced simulation for the period 6250–5750 years BP, and the mean temperature in a 300-year long equilibrium simulation for the preindustrial period, are similar in the NH to the PMIP2 MH temperature anomalies. There are some differences in the SH, however, due to a different behaviour of the SH sea ice and an associated cooling in the ECHO-G simulation, the causes of which are being investigated.

Forcing on millennial timescales not only affects the simulated mean climate state. High frequency variability modes such as ENSO and NAO may also change, both in terms of variability patterns and in terms of temporal behaviour. Note that the analysis of high frequency variability is usually based on considering anomalies relative to the climatological mean of the period under investigation, and should not be confused with representing mean anomalies relative to the modern climate through their projection on variability patterns such as the NAO or NAM pattern.

The difference between the mean NH sea level pressure field during the MH and the modern climate in the ECHO-G simulation is

Please cite this article in press as: Wanner, H., et al., Mid- to Late Holocene climate change: an overview, Quaternary Science Reviews (2008), doi:10.1016/j.quascirev.2008.06.013

similar, but not identical, to the NAO pattern (Wagner et al., 2008). A similar circulation response is also found in simulations with the ECHO-G model for the last interglacial (Kaspar et al., 2005), and in some, but not all, MH simulations with other GCMs (Masson et al., 1999; Gladstone et al., 2005). The mean NH SLP anomaly during the MH is thus associated with a positive NAO (or NAM) index, relative to modern conditions, which is in accordance with the response of the NAM index to orbital forcing discussed in Hall et al. (2005). The NH MH temperature anomaly during winter has a strong contribution from this circulation response to the forcing, for instance, increased temperatures over parts of Eurasia during the generally cooler NH winter.

As mentioned above, Otto-Bliesner et al. (2006) state that the NAM patterns of the MH are similar to those of the preindustrial period, which is also the case for the MH ECHO-G simulation. An analysis of ECHO-G simulations for the last interglacial and the last glacial inception (125,000 years BP and 115,000 years BP respectively) has also shown that the NAM pattern is not greatly affected by the orbital forcing. However, because of the mean flow anomaly, the relationships between high frequency circulation and temperature anomalies can change (Groll et al., 2005; Groll and Widmann, 2006).

An overview on the response of the mean climate and the variability of the tropical Pacific to orbital forcing has been given by Timmermann et al. (2007). This topic has been studied using EMICs (Clement et al., 1999, 2001) and GCMs (DeWitt and Schneider, 1998; Codron, 2001; Otto-Bliesner, 1999; Liu et al., 2000; DeWitt and Schneider, 2000; Otto-Bliesner et al., 2003; Clement et al., 2004; Brown et al., 2006). Some of these simulations show an EH to MH ENSO suppression, in accordance with ENSO reconstructions (Tudhope et al., 2001; Moy et al., 2002). However, ENSO is difficult to simulate as it crucially depends on the mean state and the seasonal cycle of the tropical Pacific, which are often not realistically represented in GCMs (for more details see Timmermann et al., 2007).

5.2. Changes on decadal to multi-centennial timescales

Forced variability on timescales shorter than millennia can be either a response to a forcing on these timescales, or a result of slower forcings in combination with feedbacks and thresholds in the climate system. In addition, there is a considerable contribution of internally generated, quasi-random variability.

The most spectacular example of the importance of feedbacks in some model simulations is the relatively fast desertification of the Saharan region between about 6000 and 4000 years BP (e.g. Claussen et al., 1999; Brovkin et al., 2003; Renssen et al., 2003; Wang Y.M. et al., 2005a; Patricola and Cook, 2007). The generally accepted explanation of this vegetation decrease is related to a positive atmosphere-vegetation feedback, triggered by the comparatively slow changes in orbital forcing (Fig. 6). Due to a decrease in the intensity of the African monsoon, related to the decrease in summer insolation, precipitation decreases in the Sahara during the Holocene. This induces a decrease in the vegetation cover, and thus an increase of the surface albedo. As a consequence, there is an additional cooling and reduction of precipitation that amplifies the initial decrease in vegetation cover. The amplification is particularly strong when a threshold is crossed, leading to a rapid desertification and the fast changes noticed in the simulations (e.g. Claussen et al., 1999; Brovkin et al., 2002; Wang Y.M. et al., 2005a). It has also been proposed that during this transition the system could shift several times, in some regions of the Sahara, from a "relatively green state" with a relatively large vegetation cover to desert state, both states being quite stable for a longer period. As a consequence, during this transition period the centennial- to millennial-scale variability of the system may have been enhanced because of this flip-flop between the two states (Renssen et al., 2003).

However, additional analyses are required to assess how important the mechanism described above is in more recent simulations, because the magnitude of the atmosphere-vegetation feedbacks appears smaller in the new results from PMIP2 (Braconnot et al., 2007a, b) than in earlier studies. In particular, Liu et al. (2007) simulated an abrupt transition between green state and desert state around 5 kyr BP in a long transient simulation using a coarse resolution GCM, while changes in precipitation where more gradual. This led them to argue that the simulated abrupt vegetation change was not caused by a climate-vegetation feedback, but rather by the non-linear response of the vegetation to strong internal climate variability when a bioclimatic threshold is crossed (Liu et al., 2006).

As an example of a transient GCM simulation, boreal winter and summer temperatures from the ECHO-G simulation with orbital and solar forcing for three regions (south of Greenland, central and northern Europe, and Mongolia), along with the solar forcing, are shown in Fig. 15. A more comprehensive analysis can be found in Wagner et al. (2008), where increased spectral power on multi-decadal timescales, in accordance with other studies, was found. Although the simulation is too short to allow a meaningful spectral analysis on multi-centennial to millennial timescales, a qualitative visual inspection of the regional temperatures can give some indication whether cyclicities on these timescales are simulated. Boreal summer and winter temperatures south of Greenland show strong centennial variability, which dominates multi-centennial and longer components. In addition to this centennial variability,

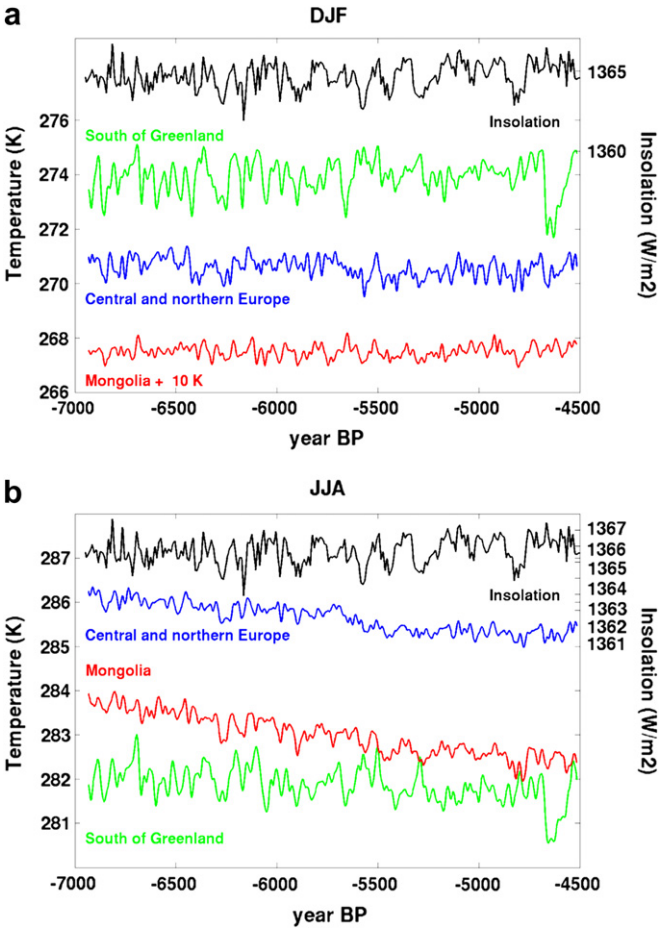

Fig. 15. Transient GCM simulations of boreal winter (a) and summer (b) air temperatures at three Atlantic-European sites (southern Greenland, central and northern Europe, Mongolia), based on orbital and solar forcing, along with the insolation curves that were used to force the model (after Wagner et al., 2007, 2008).

Please cite this article in press as: Wanner, H., et al., Mid- to Late Holocene climate change: an overview, Quaternary Science Reviews (2008), doi:10.1016/j.quascirev.2008.06.013

summer temperatures have a cooling trend, which is consistent with the decreasing NH summer orbital forcing (Fig. 6). The simulated temperature variability over Mongolia is also dominated by centennial-scale variability and a pronounced summer cooling trend. European winter temperatures likely show some millennial-scale variability with amplitudes similar to the centennial-scale variations, but the length of the record makes it impossible to comment on regularity and specific frequencies. European summer temperatures again show the expected cooling trend.

Teleconnections between low-frequency temperature variability in the three areas are low in winter, while summer temperatures over Europe and Mongolia are clearly correlated ($r = 0.65$ for detrended, 101-year filtered values). Temperature teleconnections can be due to the spatial structure of dominant, internally generated circulation patterns (Groll and Widmann, 2006), or to a common response to solar or other forcings. The solar signal during summer is moderate over Europe and strong over Mongolia (with correlations between 101-year filtered solar forcing and temperatures of 0.43 and 0.80, respectively), and it seems likely that the partial synchroneity between low-frequency temperature variability in the two regions is caused by a combination of the structure of internal variability and a common response to the solar forcing.

A noteworthy feature in those simulations is the strong negative summer and winter temperature anomaly south of Greenland around 4700 years BP, which lasts several hundred years and appears to be unrelated to the solar forcing. This is thus likely to be an internally generated fluctuation due to ocean and/or sea ice dynamics and highlight the role of internal variability on regional changes on this timescale (note in this context that such variations might be related to changes in the thermohaline circulation as discussed in Sections 4.3. and 4.4.).

For the more recent past, simulations performed with GCMs, EMICs, and Energy Balance Models (EBMs) include additional natural forcing (changes in solar irradiance and the influence of large volcanic eruptions; see Fig. 16a and b) and anthropogenic forcing (changes in land cover, increase in the GHG concentration and sulfate aerosols; Fig. 16 c). There are several estimates of these forcings as indicated by Fig. 16a–c (Jansen et al., 2007) and as a comparison with the Figs. 7–11 shows. The simulations cover the last 500–1000 years (e.g. Crowley, 2000; Bertrand et al., 2002; González-Rouco et al., 2003; Gerber et al., 2003; Bauer et al., 2003; von Storch et al., 2004; Goosse et al., 2004, 2005b; Zorita et al., 2004; Tett et al., 2007; Ammann et al., 2007; for a comprehensive overview see Jansen et al., 2007), but some forcings have also been used in longer simulations (e.g. Weber et al., 2004; Goosse et al., 2005a; Wagner et al., 2008; Renssen et al., 2005a, b). Compared to the simulations covering the Holocene with orbital and GHG forcings only, higher frequency changes are simulated when those additional forcings are included. There is a large spread between the simulations, caused by the different forcings and the different climate sensitivities of the models. EMICs simulate relatively modest changes during the period AD 1000–1850, with peak to peak variations in the order of 0.5 °C, a range that seems compatible with the results of a carbon cycle model included in one of the simulations (Gerber et al., 2003), while some GCMs simulate slightly larger changes (for discussion of the causes of the differences between the simulations, see for instance Goosse et al., 2005a; Osborn et al., 2006; Jansen et al., 2007). In general, a significant part of last millennium NH temperature variations can be explained by external forcing (Jansen et al., 2007).

Common to all simulations, the calculated climate is relatively mild at the global scale during the early millennium (albeit cooler than during the late 20th century), followed by a gradual cooling until the 19th century (Fig. 16d). This picture is consistent with the general view of a warm MWP followed by the cold LIA. In models, this large-scale climate evolution is mainly due to the applied changes in solar and volcanic forcing, as well as changes in land cover. In particular, the simulated transition at hemispheric-scale, from generally mild conditions to colder conditions, is due to a lower solar irradiance and more frequent volcanic eruptions during roughly the period AD 1450–1850. As a consequence of this forcing and of the long-term cooling trend during the Holocene (see above), the LIA appears as the period with the lowest simulated annual mean temperature averaged over the NH in simulations covering the last 8000 years (Renssen et al., 2006a). However, because of the uncertainties in the timeseries of the forcing and in the reconstructions of temperature changes from proxy-data (see Section 2), the attribution of the observed changes to particular forcings is not an easy task for the period AD 1000–1850 (e.g. Hegerl et al., 2003, 2007). On the other hand, the observed warming during the 20th century is clearly due to anthropogenic forcings and could not be simulated if those forcings are not taken into account (e.g. Crowley, 2000; Bertrand et al., 2002; Hegerl et al., 2003, 2007; Stott et al., 2006). In one study, the different forcings have been applied individually, as well as in combination. These experiments show that the forcings can, to a first approximation, be considered as linearly additive during the Holocene (Cubasch et al., 2006).

At the hemispheric scale, the simulated decadal to millenial climate variations are, to a large extent, dominated by the response to the changes in external forcing. Internal variability plays a larger role at the regional scale then at hemispheric scale, and is sometimes dominant (Goosse et al., 2005b; Tett et al., 2007). Some authors even suggest that changes in the forcing are not required to explain the observed variation at regional scale (e.g. Hunt, 1998; Bengtsson et al., 2006), the changes generated by purely internal dynamics alone provide a good hypothesis.

However, the response to the forcing should also be taken into account, as this response could display a clear spatial pattern leading to changes of much larger amplitude in some regions than at hemispheric scale. In particular, the impact of land-use change has a clear regional signature, the climate response being larger in an area (or close to the area) where the largest land-use changes occurred (e.g. Matthews et al., 2004; Feddema et al., 2005; Brovkin et al., 2006; Jansen et al., 2007). As a consequence, for regions like Europe where large-scale deforestation occurred during the pre-industrial era, land-use change could be a dominant forcing during the period AD 1000–1750 (e.g. Goosse et al., 2006).

Volcanic forcing is also believed to have an influence on atmospheric circulation, which can be responsible for large regional anomalies leading to a warming of the NH continent in the winter following a large tropical volcanic eruption. This is due to a larger warming of the stratosphere in the tropics than at high latitudes, and thus a stronger meridional temperature gradient caused by the volcanic eruption. This is associated with a stronger polar vortex and a more intense advection of warm air to the continents in winter, which overprints the direct radiative cooling (Robock, 2000; Shindell et al., 2004).

The spatial pattern of the temperature response to the solar forcing has been estimated in detection and attribution studies (Cubasch et al., 1997; Hegerl et al., 1997; Cubasch and Voss, 2000; Hegerl et al., 2007). Cubasch et al. (2004) isolated the solar signal on longer timescales by performing an idealised simulation with a periodic solar forcing with the 76 years periodicity of the Gleissberg cycle and the 11 years periodicity of the Schwabe cycle. The correlations between 5-year low-pass filtered temperatures of the latter simulation and the solar forcing are shown in Fig. 17. Both figures show, in general, highest correlations over the tropical Atlantic and Indian Ocean and decreasing correlations towards higher latitudes. As in the case of the orbital forcing signal, the solar signal is a combination of direct responses to changes in the local radiative balance. Additionally, an indirect effect, caused by the

Please cite this article in press as: Wanner, H., et al., Mid- to Late Holocene climate change: an overview, Quaternary Science Reviews (2008), doi:10.1016/j.quascirev.2008.06.013

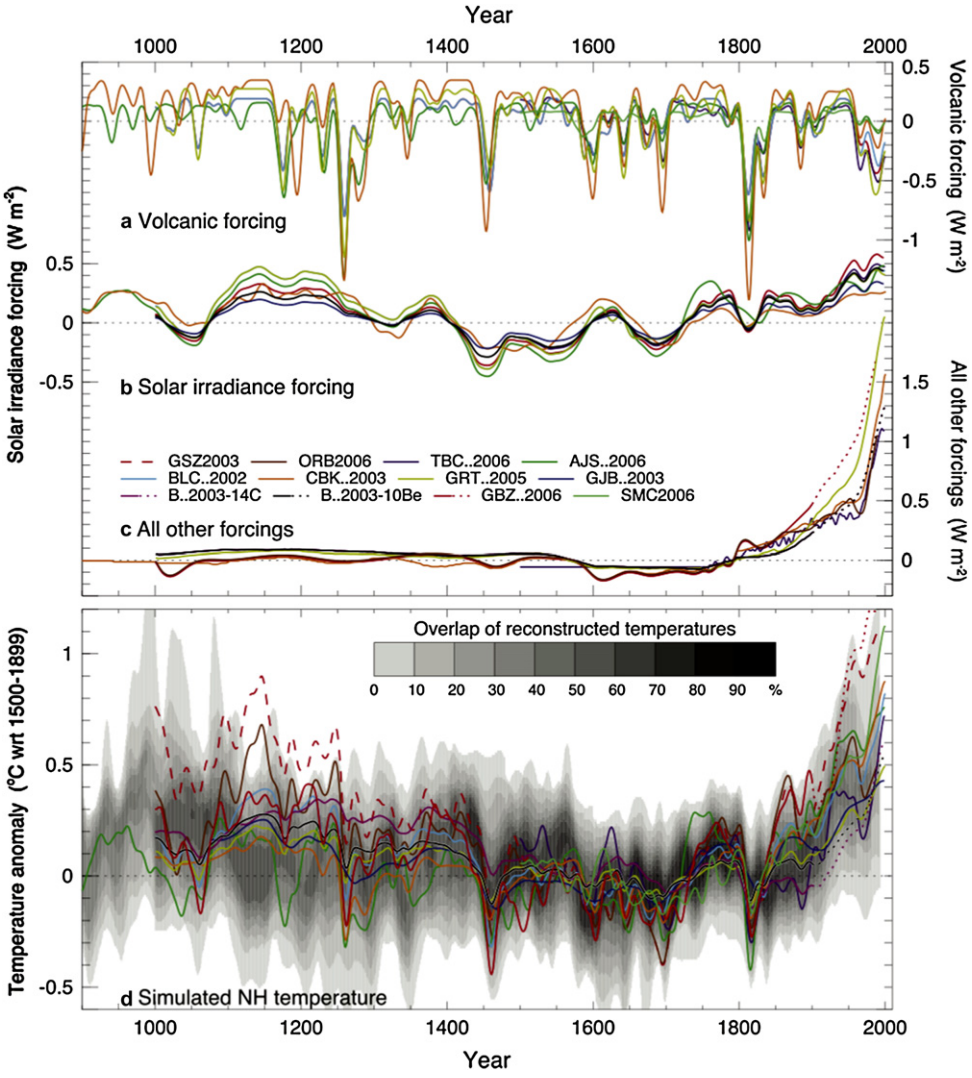

Fig. 16. Radiative forcings and simulated temperatures during the last 1.1 kyr. Radiative forcing (W/m^2) used to drive climate model simulations due to (a) volcanic activity, (b) solar irradiance variations and (c) all other forcings. (d) Annual mean NH temperature (°C) simulated under the range of forcings shown in (a) to (c), compared with the concentration of overlapping NH temperature reconstructions (shown by grey shading). All forcings and temperatures are expressed as anomalies from their 1500 to 1899 means and smoothed with a Gaussian-weighted filter. From Jansen et al. (2007).

radiative heating of the ozone layer in the stratosphere (Kodera and Kuroda, 2002) through increased UV-radiation during a solar maximum, reinforces the response to solar variability. The altered stratification of the higher atmosphere could lead to circulation changes, for instance of the Hadley Cells, the Indian Monsoon, the NAM and the ENSO cycle (e.g. Haigh, 1996; Shindell et al., 2001; White et al., 2003; van Loon et al., 2004, 2007; Kodera, 2005; White, 2006). The mechanisms leading to circulation changes are not yet fully understood and are the topic of intensive ongoing research. To investigate them in detail, fully coupled ocean-troposphere-stratosphere models have to be employed, which have only recently been run for long periods (e.g. Huebener et al., 2007).

Simulations using models including a dynamic ocean have shown that, in response to an increase in solar irradiance, the magnitude of the AMOC tends to decrease by a few percent probably because of a warming and reduced ocean surface density at high latitudes (e.g. Weber et al., 2004). This reduces the northward oceanic heat transport in the Atlantic and thus provides a local negative feedback to the initial warming, due to the increase in solar irradiance. Nevertheless, a positive oceanic feedback has also been described (Goosse and Renssen, 2004). During some years, because of the internal variability of the system, the oceanic heat transport toward the Norwegian Sea is reduced and sea ice covers the sites where deep mixing and intense heat flux from the ocean to the atmosphere occurs during normal years. This leads to very cold conditions in the northern North Atlantic and surrounding areas, and to changes in wind patterns that could reinforce the initial perturbations. The probability of such a cold year depends strongly on the mean state of the system. In particular, the sea ice should be thick enough to survive when transported from the Arctic to the Nordic Seas and to decouple the ocean from the atmosphere in those regions. As a consequence, the probability of those events is nearly zero in simulations covering the EH or the late 20th century because of a too thin ice layer during this period (Renssen et al., 2005a; Goosse and Renssen, 2004). On the other hand, the probability is higher during the second half of the Holocene, in particular during some cold periods like the LIA, providing a potentially strong amplification of the response to the solar forcing during those periods (Goosse and Renssen, 2004). In a recent study covering the last 9000 years, Renssen et al. (2006a) found that these simulated cold events are consistent with proxy evidence for Holocene cold phases in the North Atlantic, and could thus provide a hypothesis to explain the observed anomalies during those periods.

Please cite this article in press as: Wanner, H., et al., Mid- to Late Holocene climate change: an overview, Quaternary Science Reviews (2008), doi:10.1016/j.quascirev.2008.06.013

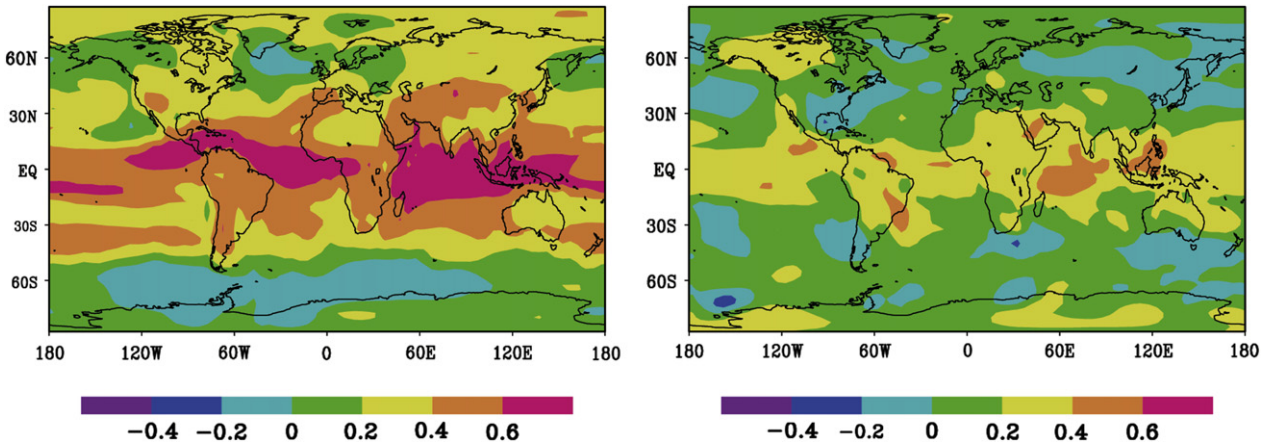

Fig. 17. Left: correlation between a simulated 76-year cycle (corresponding to the Gleissberg-cycle; S76) and the 5 year low-pass filtered response in near surface temperatures. Right: same as left Fig., but for an 11-year solar forcing (corresponding to the Schwabe Cycle; S11).

6. Synthesis and conclusions

Here we focus on the six questions posed in the introduction. For the first three questions, we focus on the observed (reconstructed) climate. Answering questions 4–6 requires consideration of available knowledge from simulation studies.

6.1. Question 1: What was the spatial structure of Mid- to Late Holocene climate changes?

By combining the available information derived from proxy reconstructions, Fig. 18 summarises in cartoon form the difference between the preindustrial period (AD ~1700) and the MH (~6000 cal years BP). Due to the weakened orbital forcing in NH summer (Fig. 6) the ITCZ shifted south and a cooling trend, mainly during summer, occurred over the northern continental land mass (Viau et al., 2006; Seppä and Birks, 2001) and the North Atlantic Ocean (Marchal et al., 2002; Kim et al., 2004). The length of glaciers was smaller during the MH, e.g. in the European Alps and Scandinavia, and many glaciers of the NH reached a maximum extent during the LIA (Fig. 4). Reconstructions of the NAO index (Rimbu et al., 2003), though uncertain, depict positive values for the MH and negative values for the preindustrial period, although the indices increased slightly after 2000 cal years BP (Fig. 13). The North Pacific SST trend was positive, counter to the forcing (Kim et al., 2004), and humidity in the interior mid-latitudes of North America increased (Fig. 3). In the context of the southerly moving ITCZ (Haug et al., 2001) the Afro-Asian summer monsoon weakened greatly, causing aridity in subtropical Africa and Asia and in Central America. As a consequence of a changing SST gradient between the Indo-Pacific warm pool and the eastern Pacific Ocean the Walker Circulation intensified after 5000 cal years BP, and large El Niño events occurred more frequently (Shulmeister, 1999; Gagan et al., 2004; Stott et al., 2004; Abram et al., 2007).Antarctic temperatures remained constant or slightly cooled (Masson et al., 2000, Fig. 2).

6.2. Question 2: Are multi-century scale changes between colder and warmer (or humid and dry) periods cyclic, with a quasi-regular period, or not?

Several authors (e.g. Bray, 1971, 1972; Denton and Karlén, 1973; Bond et al., 1997, 2001) have postulated the existence of postglacial cycles or swings with periods of about 2000–2800 or 1200–1500 years, and recent publications have suggested these to be Holocene equivalents of the Late Pleistocene Dansgaard–Oeschger cycles. Examination of different timeseries of proxies for temperature and humidity in Fig. 2 and glacier dynamics in Fig. 4 suggests that such swings exist; but the number of Neoglacial advances recorded in several parts of the world is highly variable and in many cases they are not synchronous (Bradley and Jones, 1995). Some degree of coincidence is visible when considering the coloured dots marking roughly simultaneous glacier advances in Fig. 4. However, if we detect and list all notable positive or negative peaks in the timeseries in Fig. 2 (not shown here), a clear coincidence cannot be found.

Fig. 19 shows the frequency of all spectral peaks with significant power found in our timeseries analyses as well as in the literature, which are represented in Fig. 5 (see also the refs. in Tables 1 and 2). As expected, the number of spectral peaks grows with decreasing timescale because the number of longer periods is limited due to the length of the time intervals analysed. Small, (and non-significant) clusterings of spectral peaks occur at about 200, 500, 900 and 1500–years (dark bars in Fig. 19). There is thus scant evidence for consistent periodicities and it seems likely that much of the higher-frequency variability observed is due to internal variability or complex feedback processes that would not be expected to show strict spectral coherence (Hunt, 1998; Wunsch, 2000, 2006).

Do "Bond Cycles" (Bond et al., 1997, 2001) constitute an exception? Andrews et al. (2006), Moros et al. (2006) and Debret et al. (2007) have shown that such cycles exist but that their temporal structure and their spatial representation are not uniform. A correlation has been shown between the Bond events and glacier advances and retreats in Scandinavia (Nesje and Kvamme, 1991; Matthews et al., 2005) and the European Alps (Wanner et al., 2000; Holzhauser et al., 2005). There is also evidence that climate swings in the northeast American and/or the Atlantic-European area are correlated with similar fluctuations around the Mediterranean Sea and North Africa, and correspond with some proxy timeseries in the Middle East and Asia, (Fleitmann et al., 2003; Wang Y. et al., 2005; Jones et al., 2006; Yu et al., 2006), including the southwest monsoon and ENSO (Gupta et al., 2003, 2005; Goswami et al., 2006). Baker et al. (2001) even suggested linkages with the Caribbean area and the Altiplano in South America. Based on our analysis of the timeseries in Fig. 2 we support the idea that "Bond Cycles" are effective during selected time periods in the NH, but question their relevance for the SH until a plausible mechanism for the transmission of the signal is detected (see also Bütikofer, 2007).

Transitions between warmer and colder multi-century periods, especially the transition from the MWP (Hughes and Diaz, 1994; Crowley and Lowery, 2000) or the MCA (Graham et al., 2007) to the LIA (Grove, 2004), may provide the best opportunities to study the

Please cite this article in press as: Wanner, H., et al., Mid- to Late Holocene climate change: an overview, Quaternary Science Reviews (2008), doi:10.1016/j.quascirev.2008.06.013

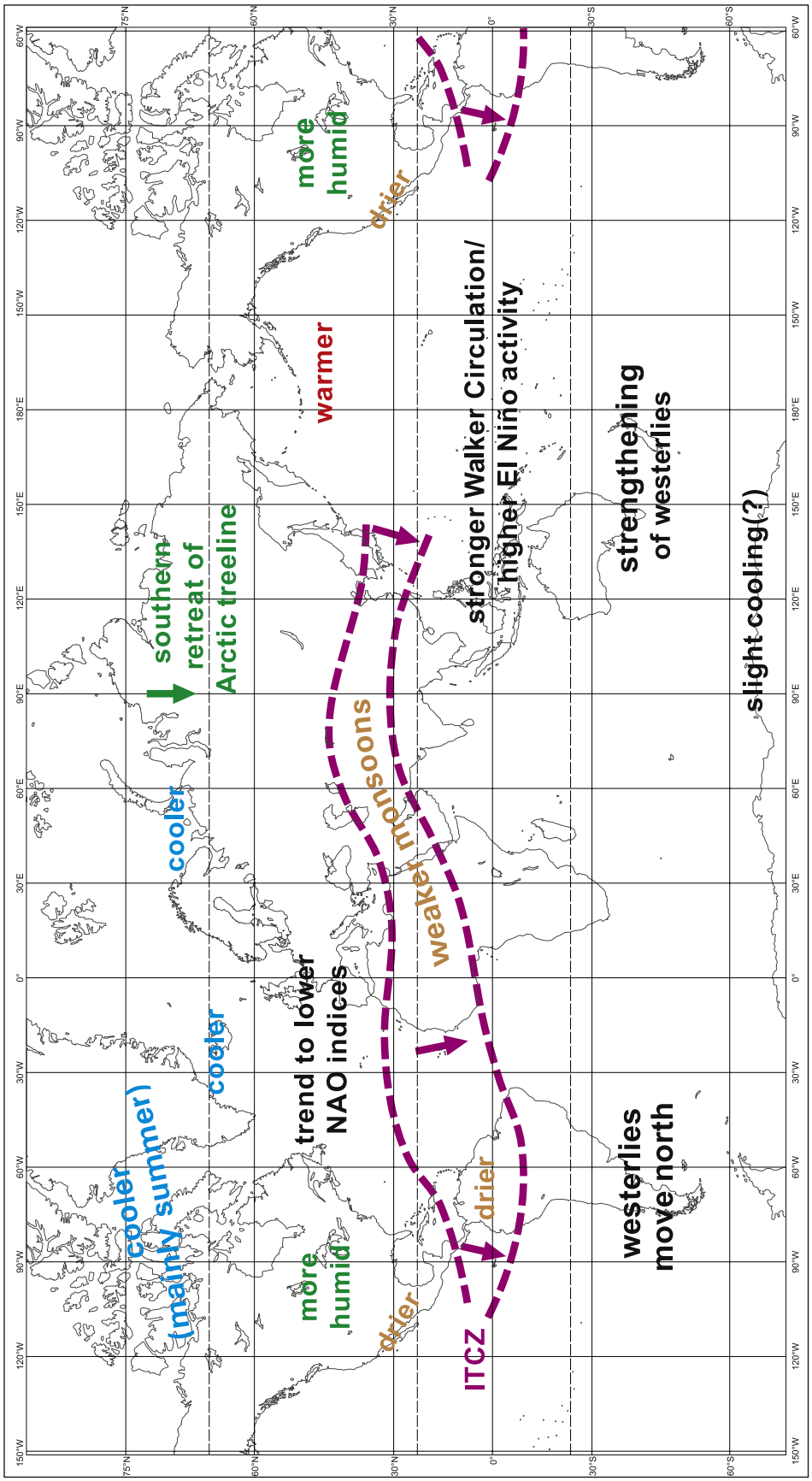

Fig. 18. Spatial synthesis: global climate change for the preindustrial period (AD ~1700) compared to the MH (~6000 cal years BP).

Please cite this article in press as: Wanner, H., et al., Mid- to Late Holocene climate change: an overview, Quaternary Science Reviews (2008), doi:10.1016/j.quascirev.2008.06.013

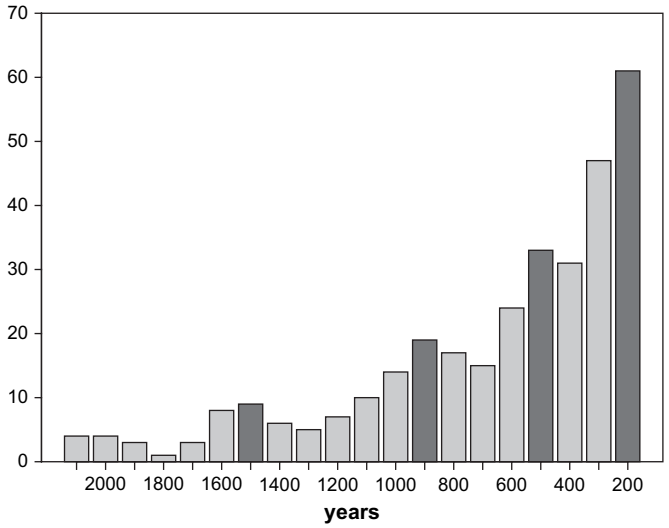

Fig. 19. Number of all significant spectral peaks found in our timeseries analysis (see refs. in Table 1), as well as in the existing literature (see refs. in the Table 2). Dark grey bars mark apparently higher frequencies.

processes of multi-centennial to millennial climate variability. It is still an open question whether the MWP–LIA transition was caused by external forcing, and its spatial extent is still not entirely clear; also Bradley et al. (2003) demonstrated that the time of the warm peak during the MWP was not simultaneous in different areas of the globe. For the LIA the glacier maxima in Fig. 4 suggest a certain synchroneity, though the temporal resolution of these data is too low to guarantee simultaneity.

6.3. Question 3: Can we identify periods with rapid large-scale climate shifts or transitions?

Several papers (e.g., Jennings et al., 2002; Mayewski et al., 2004) have shown that rapid transitions have occurred in regional climates. Mayewski et al. (2004) indicated five periods of significant rapid climate change during the last 6 kyr BP. They connected the four events 6000–5000, 4200–3800, 3500–2500 and 1200–1000 cal years BP with a "cool poles, dry tropics" pattern, and postulated that solar variability could be a plausible forcing for the two largest of these events (6000–5000 and 3500–2500 cal years BP). The fifth event, linked to a "cool poles, wet tropics" pattern, started in ~600 cal years BP and corresponds to the LIA. Mayewski et al. suggested that solar variability and possibly volcanic aerosols had a major influence on climate during this last interval.

Contrary to the conclusions of Mayewki et al. (2004), we cannot find any time period for which a rapid or dramatic climatic transition appears even in a majority of the timeseries in Figs. 2 or 4. A noteworthy shift occurred in the timeseries of the North Atlantic, Israel and E Africa around 5200 cal years BP. A second event is visible in the timeseries of North America, Mexico and the Cariaco Basin between about 3100 and 2500 cal years BP. There is no indication that explosive tropical volcanic eruptions could have influenced these transitions. Interestingly, the ^{10}Be data in Fig. 7a show positive trends during both periods.

It has to be asked whether the period between 4200 and 3800 cal years BP, mentioned by Mayewski et al. (2004) and Yu et al. (2006) is of special significance because the collapse of the Akkadian Empire (Cullen et al., 2000; deMenocal, 2001) and the severe North American drought (Booth et al., 2005) appeared at the same time. During the latter period the frequency of large El Nino events decreased strongly (Fig. 12).

6.4. Question 4: Do the climate variations correspond with known variations of natural forcing factors, such as orbital parameters, solar irradiance, explosive tropical volcanic eruptions and greenhouse gases?

At the millennial scale, orbital (Milankovitch) forcing dominates. In the NH outside the polar region insolation changes led to a strong cooling during the LH, especially in summer (Figs. 6 and 18). The redistribution of solar energy was also responsible for the southward migration of the ITCZ and the weakening of the Afro-Asian monsoon system (Haug et al., 2001; Broccoli et al., 2006). In the SH the reaction to orbital changes has been more muted and apparently more complex, probably because heat transport in the ocean played the major role (Stott et al., 2004; Renssen et al., 2005b).

There have been many largely speculative attempts to attribute decadal to multi-centennial fluctuations, as represented in the timeseries of Figs. 2 and 4, to solar variability and volcanic forcing. If we compare the spectra of solar activity (Fig. 8) with the frequency of the spectral peaks in the Holocene timeseries in Fig. 19 we recognise that there is a rough coincidence between the 208 years Suess (or de Vries) cycle and a clustering of frequencies of variation in climate proxies around the spectral band of ~200 years. The same applies to the solar cycle peak around 500 years. Unfortunately, the solar activity data do not allow us to extend the analysis to the characteristic 1500 years timescale of the "Bond Cycles". As noted by Debret et al. (2007), the origin of these cycles remains unknown. Debret et al. listed solar activity, ocean current intensity variation, tidal forcing, atmospheric processes or modifications of the geomagnetic field as possible triggers.

Turney et al. (2005) concluded that North Atlantic climate changes on centennial to millennial time scales were not driven by a linear response to solar activity. Solar forcing has been invoked as the main trigger, e.g. for glacier (Holzhauser et al., 2005) and lake level (Magny, 2004) fluctuations in central Europe, and temperature changes in Alaska (Wiles et al., 2004). We suggest that the evidence for such a linkage is very weak.

The same holds for volcanic forcing. One single tropical volcanic eruption leads to a climate signal which lasts for about 2–3 years (Robock, 2000). The structure of this spatiotemporal signal is quite complex (Gerber et al., 2003; Shindell et al., 2004; Fischer et al., 2006; Ammann et al., 2007). However, a strong eruption or a sequence of eruptions could potentially have a substantial impact. Based on a network of temperature-sensitive tree-ring density chronologies in different regions of the northern boreal forests Briffa et al. (1998) showed that strong single eruptions or groups of eruptions (e.g. around AD 1600 or shortly after AD 1800) can lower summer temperatures dramatically However it appears from Fig. 9 that more large tropical volcanic eruptions have occurred during certain intervals of the last millennium, i.e. between AD 1200 and 1350 or around AD 1700 and 1800, than at other times during the Holocene. These maxima of volcanic activity happen to coincide with both low orbitally induced insolation in the NH and an unusual concentration of solar activity minima. Therefore, it seems plausible that the cold intervals of the past millennium, including the LIA, might be attributed to a combination of orbital, volcanic and solar forcing.

Finally, it has to be emphasised that forcing signals with higher frequencies might be transformed into low frequency ones by slow reactors such as ice caps, or by internal feedbacks. Moreover, Wunsch (2000) stated that a broad band of quasiperiodic variability rather than any kind of significant spectral peak is typical for climate records.

Please cite this article in press as: Wanner, H., et al., Mid- to Late Holocene climate change: an overview, Quaternary Science Reviews (2008), doi:10.1016/j.quascirev.2008.06.013

6.5. Question 5: What was the involvement of natural variability modes, such as the El Niño Southern Oscillation (ENSO) and the North Atlantic Oscillation (NAO), in climate change during the Holocene?

Internal modes of the climate system are important sources of natural variability. Teleconnections induced by these modes can potentially be influenced by external forcing, although model studies (Stott and Tett, 1998; Goosse et al., 2005b; Bengtsson et al., 2006) have shown that, on the regional scale, the effect of the forcings may be less important and that natural variability is often underestimated as a cause of regional climate variations.

If we assume, as mentioned above, that the ENSO activity increased and the NAO moved toward negative indices until about 1800–1900 cal years BP, we can make use of the correlations between the indices of these climate modes and the SSTs (Rimbu et al., 2004). The La Niña-like conditions during the MH lead to drought, e.g. on the coast of Peru and, possibly, in the mid-continent of North America. In the North Pacific area the SSTs increased during the last six millennia (Kim et al., 2004). The Walker Circulation intensified, and a higher dryness took place in tropical Australia after 3700 cal years BP (Shulmeister, 1999). In the North Atlantic Ocean and the western Mediterranean Sea the SSTs mostly decreased (Marchal et al., 2002; Kim et al., 2004). An increasing SST trend was determined in the eastern Mediterranean Sea and the ocean areas southeast of it (Kim et al., 2004). This trend pattern is consistent with the decreasing NAO indices between the MH and the LH.

6.6. Question 6: Are models able to simulate climate variability at different timescales, and to what extent can they diagnose the underlying processes?

EMICs can reproduce the general decrease in summer temperatures at mid- and high-latitudes over the last 6000 years associated with the decline of insolation in boreal summer. They show a slight increase of winter temperatures in the northern mid-latitudes, and a cooling of the Southern Ocean during austral summer, spring and winter. Compared to modern conditions, quasi-equilibrium simulations with GCMs demonstrate a stronger (weaker) seasonal cycle in the NH (SH) compared to today and increased temperatures up to 2 K over the NH during boreal summer (Braconnot et al., 2007a, b) leading to enhanced continental lows and a stronger summer monsoon. Transient simulations, mostly performed using acceleration techniques, produce a smooth transition from the MH to the present with opposing temperature trends in the tropics and extratropics. The forcing on millennial timescales also affects high frequency variability, such as ENSO and NAO/NAM.

On decadal to multi-centennial timescales, forced variability can in principle be either a direct response to forcing on these timescales, or a result of slower forcings in combination with feedbacks and thresholds in the climate system. The most spectacular example of a simulated non-linear feedback during the past 6000 years is the (rapid or gradual?) desertification of the Saharan region between about 6000 and 4000 cal years BP. Transient simulations of boreal winter and summer temperatures with ECHO-G, forced with orbital and solar forcing, show strong centennial variability superimposed on the general NH cooling trend. Simulations of the last 500–1000 years BP have included natural (solar activity, volcanoes) and anthropogenic (land cover change, increasing GHG's and sulfate concentration) forcings. EMICs simulate relatively modest changes between AD 1000 and 1850, with a range of 0.5 °C in global mean temperature. Some AOGCMs have simulated slightly larger changes. All simulations reproduce a relatively warm global-scale climate during the early part of the millennium (albeit cooler than during the 20th century), followed by a gradual cooling until the 19th century. This general model finding is consistent with the suggestion that the contrast between the MWP and the LIA was due to the coincidence of solar activity minima with an increased number of volcanic events during the LIA.

The LIA is simulated as the period with the strongest cooling during the last 8 kyr. Simulations including a dynamical ocean show that, due to an increasing solar irradiance, the magnitude of the AMOC tends to decrease during the LIA by a few percent (e.g. Weber, 2001; Weber et al., 2004) due to warming and reduced ocean surface density in the high latitudes. This reduces the northward heat transport and provides a negative feedback due to the initial warming by the higher solar irradiance. On the other hand, the simulations described in Goosse and Renssen (2004) show, in response to a decrease in solar irradiance, a reduced oceanic heat transport toward the Norwegian Sea, increasing sea ice and a reduction of the deep mixing as well as the heat flux from the ocean. The probability of such a process increases if the mean state and not the internal variability dominates, as during the LH. The question remains whether the SH is also cooled, namely by a north-south transport of cold deepwater, or warmed because of the reduced northward heat transport.

In summary, one can say that the proxy timeseries as well as the available simulations indicate that mainly two types of climate variability occurred during the last 6000 years:

(1) The distribution of total solar irradiance substantially changed over the course of the last 6000 years due to changes in the orbital parameters. The largest changes occurred during boreal summer and autumn when the solar irradiance was progressively reduced in the NH and enhanced in the SH. Therefore, the ITCZ and the monsoon systems moved south. The weakening of the summer monsoons over time led to a dryness in Central America, northern Africa and what are now the deserts of Eurasia; this trend started after about 5500 cal years BP and was abrupt in some regions (e.g. in Mexico or the Lake Chad area between about 4200 and 3800 cal years BP). Orbital forcing also led to changes in the behaviour of the main phenomena of internal climate system variability, above all ENSO in the Pacific region and NAO in the Atlantic region. There are indications in both observations and simulations that ENSO activity increased and the NAO index shifted towards more negative values.

(2) At decadal to multi-century timescales, climate variability shows a complex picture with indications of a possible role for (i) rapid changes of the natural forcing factors such as solar activity fluctuations and/or large tropical volcanic eruptions; (ii) internal variability including ENSO and NAO; (iii) changes of the thermohaline circulation; (iv) complex feedback mechanisms between ocean, atmosphere, sea ice and vegetation. Notable swings occurred between warm and cold periods, especially the hemispheric-scale warming leading into the MWP and subsequent cooling into the LIA. However, there is scant evidence either for the cyclicity of climate variations on this time scale, or for the large-scale synchroneity of abrupt events. There is evidence for "Bond events" in some NH records although their cyclicity is doubtful (they may or may not be analogous to Dansgaard–Oeschger events), and their origins obscure. The LIA appears at least to be a hemispheric phenomenon, and model simulations support the inference that it may have been brought about by the coincidence of low NH orbital forcing during the Late Holocene with unusually low solar activity and a high number of major volcanic events.

Acknowledgements

The authors wish to thank the PAGES programme as well as the Swiss NCCR Climate for supporting various scientific meetings and workshops on Mid- to Late Holocene climate change. They also thank

very much Andreas Brodbeck for the excellent graphical support, and G. Bürger and S. Schimanke for graphical help. They are highly indebted to Louise Newman and Paul Della-Marta for their proof-reading of the English text, and to Atle Nesje and two anonymous reviewers for their valuable comments. The first author (H.W.) also expresses his thanks to the NCAR for the financial support during his stay in Boulder.

Appendix A. List of abbreviations

AGCM	Atmosphere General Circulation Model
AMO	Atlantic Multidecadal Oscillation
AMOC	Atlantic Meridional Overturning Circulation
AO	Arctic Oscillation
AOGCM	Atmosphere-Ocean General Circulation Model
BIOME 6000	Paleovegetation Mapping Project of IGBP
BP	Before Present (means before AD 1950)
CCM	Community Climate Model
CLIMAP	Climate Mapping, Analysis and Prediction Project
COHMAP	Cooperative Holocene Mapping Project
EBM	Energy Balance Model
ECHO-G	Hamburg AOGCM
EH	Early Holocene
EMIC	Earth System Model of Intermediate Complexity
ENSO	El Niño Southern Oscillation
EPICA	European Ice Core Project in Antarctica
GAIM	Global Analysis, Interpretation and Modeling Project
GCM	General Circulation Model
GENESIS	Global Environmental and Ecological Simulation of Interactive Systems
GISP	Greenland Ice Sheet Project
GLSDB	Global Lake Status Data Base
GRIP	Greenland Ice Core Project
HYDE	Anthropogenic land use dataset
IGBP	International Geosphere-Biosphere Programme
IPWP	Indo Pacific Warm Pool
IOM	Indian Ocean Monsoon
IRD	Ice Rafted Debris
ITCZ	Intertropical Convergence Zone
LGM	Last Glacial Maximum
LH	Late Holocene
LIA	Little Ice Age
LIATE	Little Ice Age Type Event
MCA	Medieval Climate Anomaly
MH	Mid-Holocene
MWE	Medieval Warm Epoch
MWP	Medieval Warm Period
NAM	Northern Annular Mode
NAO	North Atlantic Oscillation
NH	Northern Hemisphere
PAGES	Past Global Changes Programme
PDO	Pacific Decadal Oscillation
PMIP	Paleoclimate Modeling Intercomparison Project
REDFIT	Software used for spectral analysis
SH	Southern Hemisphere
SST	Sea Surface Temperature
TEMPO	Testing Earth System Models with Paleo-Observations
THC	Thermohaline circulation

References

Abbott, M.B., Binford, M.W., Brenner, M., Kelts, K., 1997. A 3500 ^{14}C yr high-resolution record of water-level changes in Lake Titicaca, Bolivia/Peru. Quaternary Research 47, 169–180.

Abbott, M.B., Wolfe, B.B., Aravena, R., Wolfe, A.P., Seltzer, G.O., 2000. Holocene hydrological reconstructions from stable isotopes and paleolimnology, Cordillera Real, Bolivia. Quaternary Science Reviews 19, 1801–1820.

Abbott, M.B., Wolfe, B.B., Wolfe, A.P., Seltzer, G.O., Aravena, R., Mark, B.G., Polissar, P.J., Rodbell, D.T., Rowe, H.D., Vuille, M., 2003. Holocene paleohydrology and glacial history of the central Andes using multiproxy lake sediment studies. Palaeogeography, Palaeoclimatology. Palaeoecology 194 (1-3), 123–138.

Abram, N.J., Gagan, M.K., Liu, Z., Hantoro, W.S., McCulloch, M.T., Suwargadi, B.W., 2007. Seasonal characteristics of the Indian Ocean Dipole during the Holocene epoch. Nature 445, 299–302.

Alyea, F.N., 1972. Numerical simulation of an ice age paleoclimate. Atmosopheric Science Paper No. 193. Colorado State University.

Ammann, C.M., Naveau, P., 2003. Statistical analysis of tropical explosive volcanism occurrences over the last 6 centuries. Geophysical Research Letters 30(5), doi:10.1029/2000GL016388.

Ammann, C.M., Joos, F., Schimel, D.S., Otto-Bliesner, B.L., Tomas, R.A., 2007. Solar influence on climate during the past millennium: results from transient simulations with the NCAR Climate System Model. Proceedings of the National Academy of Sciences USA 104, 3713–3718.

Anderson, L., Abbott, M.B., Finney, B.P., 2001. Holocene climate inferred from oxygen isotope ratios in lake sediments, Central Brooks Range, Alaska. Quaternary Research 55, 313–321.

Anderson, L., Abbott, M.B., Finney, B.P., Burns, S.J., 2005. Regional atmospheric circulation change in the North Pacific during the Holocene inferred from lacustrine carbonate oxygen isotopes, Yukon Territory, Canada. Quaternary Research 64, 21–35.

Andrews, J.T., Jennings, A.E., Moros, M., Hillaire-Marcel, C., Eberle, D., 2006. Is there a pervasive Holocene ice-rafted debris (IRD) signal in the northern North Atlantic? The answer appears to be either no, or it depends on the proxy!. PAGES News 14/2, 7–9.

Baker, P.A., Rigsby, C.A., Seltzer, G.O., Fritz, S.C., Lowenstein, T.K., Bacher, N.P., Veliz, C., 2001. Tropical climate changes at millennial and orbital timescales in the Bolivian Altiplano. Nature 409, 698–701.

Baker, P.A., Fritz, S.C., Garland, J., Ekdahl, E., 2005. Holocene hydrologic variation at Lake Titicaca, Bolivia/Peru, and its relationship to North Atlantic climate variation. Journal of Quaternary Science 20, 655–662.

Bakke, J., Dahl, S.O., Paasche, Ø., Løvlie, R., Nesje, A., 2005. Glacier fluctuations, equilibrium-line altitudes and palaeoclimate in Lyngen, northern Norway, during the Lateglacial and Holocene. The Holocene 15, 518–540.

Bakke, J., Lie, Ø., Dahl, S., Nesje, A., Bjune, A., 2008. Strength and spatial patterns of the Holocene wintertime westerlies in the NE Atlantic region. Global and Planetary Change 60, 28–41.

Bar-Matthews, M., Ayalon, A., Gilmour, M., Matthews, A., Hawkesworth, C.J., 2003. Sea-land oxygen isotopic relationships from planktonic foraminifera and speleothems in the Eastern Mediterranean region and their implication for paleorainfall during interglacial intervals. Geochimica et Cosmochimica Acta 67, 3181–3199.

Bar-Yosef, O., 1998. The Natufian culture in the Levant, threshold to the origins of agriculture. Evolutionary Anthropology 6, 159–177.

Battle, M., Bender, M., Sowers, T., Tans, P.P., Butler, J.H., Elkins, J.W., Ellis, J.T., Conway, T., Zhang, N., Lang, P., Clarke, A.D., 1996. Atmospheric gas concentrations over the past century measured in air from firn at the South Pole. Nature 383, 231–235.

Bauer, E., Claussen, M., Brovkin, V., Huenerbein, A., 2003. Assessing climate forcings of the Earth system for the past millennium. Geophysical Research Letters 30, 1276.

Behling, H., 1995. Investigations into the Late Pleistocene and Holocene history of vegetation and climate in Santa Catarina (S Brazil). Vegetation History and Archaeobotany 4, 127–152.

Behling, H., Pillar, V.D., 2007. Late Quaternary vegetation, biodiversity and fire dynamics on the southern Brazilian highland and their implication for conservation and management of modern Araucaria forest and grassland ecosystems. Philosophical Transactions of the Royal Society B Biological Sciences 362, 243–251.

Behre, K.-E., 2003. Eine neue Meeresspiegelkurve für die südliche Nordsee. Probleme der Küstenforschung im südlichen Nordseegebiet 28.

Bendle, J.A.P., Rosell-Melé, A., 2007. High-resolution alkenone sea surface temperature variability on the North Atlantic Icelandic Shelf: implications for Nordic Seas palaeoclimatic development during the Holocene. The Holocene 17, 9–24.

Bengtsson, L., Hodges, K.I., Roeckner, E., Brokopf, R., 2006. On the natural variability of the pre-industrial European climate. Climate Dynamics 27, 743–760.

Berger, A., 1978. Long-term variations of daily insolation and Quaternary climate changes. Journal of Atmospheric Sciences 35, 2362–2367.

Bertrand, C., Loutre, M.F., Crucifix, M., Berger, A., 2002. Climate of the last millennium: a sensitivity study. Tellus 54A, 221–244.

Bianchi, G.G., McCave, I.N., 1999. Holocene periodicity in North Atlantic climate and deep-ocean flow south of Iceland. Nature 397, 515–517.

Bigelow, N.H., Brubaker, L.B., Edwards, M.E., Harrison, S.P., Prentice, I.C., Anderson, P.M., Andreev, A.A., Bartlein, P.J., Christensen, T.R., Cramer, W., Kaplan, J.O., Lozhkin, A.V., Matveyeva, N.V., Murray, D.F., McGuire, A.D., Razzhivin, V.Y., Ritchie, J.C., Smith, B., Walker, D.A., Gajewski, K., Wolf, V., Holmqvist, B.H., Igarashi, Y., Kremenetskii, K., Paus, A., Pisaric, M.F.J., Volkova, V.S., 2003. Climate change and Arctic ecosystems: 1. Vegetation changes north of 55 degrees N between the last glacial maximum, mid-Holocene, and present. Journal of Geophysical Research Atmospheres 108 (D19), 8170, doi:10.1029/2002JD002558.

Please cite this article in press as: Wanner, H., et al., Mid- to Late Holocene climate change: an overview, Quaternary Science Reviews (2008), doi:10.1016/j.quascirev.2008.06.013

Bjune, A.E., Bakke, J., Nesje, A., Birks, H.J.B., 2005. Holocene mean July temperature and winter precipitation in western Norway inferred from palynological and glaciological lake-sediment proxies. The Holocene 15, 177–189.

Blunier, T., Chappellaz, J., Schwander, J., Barnola, J.-M., Desperts, T., Stauffer, B., Raynaud, D., 1993. Atmospheric methane, record from a Greenland ice core over the last 1000 years. Geophysical Research Letters 20 (20), 2219–2222.

Blunier, T., Chappellaz, J., Schwander, J., Stauffer, B., Raynaud, D., 1995. Variations in atmospheric methane concentration during the Holocene epoch. Nature 374, 46–49.

Bond, G., Lotti, R., 1995. Iceberg discharges into the North Atlantic on millennial time scales during the last glaciation. Science 267, 1005–1010.

Bond, G., Showers, W., Cheseby, M., Lotti, R., Almasi, P., deMenocal, P., Priore, P., Cullen, H., Hajdas, I., Bonani, G., 1997. A pervasive millennial-scale cycle in the North Atlantic Holocene and glacial climates. Science 294, 2130–2136.

Bond, G., Kromer, B., Beer, J., Muscheler, R., Evans, M.N., Showers, W., Hoffmann, S., Lotti-Bond, R., Hajdas, I., Bonani, G., 2001. Persistent solar influence on North Atlantic climate during the Holocene. Science 278, 1257–1266.

Bonfils, C., de Noblet-Ducoudré, N., Braconnot, P., 2001. Hot desert albedo and climate change: mid Holocene monsoon in North Africa. Journal of Climate 17, 3724–3737.

Booth, R.K., Jackson, S.T., Forman, S.L., Kutzbach, J.E., Bettis III, E.A., Kreig, J., Wright, D.K., 2005. A severe centennial-scale drought in mid-continental North America 4200 years ago and apparent global linkages. The Holocene 15, 321–328.

Booth, R.K., Notaro, M., Jackson, S.T., Kutzbach, J.E., 2006. Widespread drought episodes in the western Great Lakes region during the past 2000 years: geographic extent and potential mechanisms. Earth and Planetary Science Letters 242, 415–427.

Braconnot, P., Joussaume, S., Marti, O., de Noblet, N., 1999. Synergistic feedbacks from ocean and vegetation on the African monsoon response to mid-Holocene insolation. Geophysical Research Letters 26, 2481–2484.

Braconnot, P., Harrison, S.P., Joussaume, S., Hewitt, C.D., Kitoh, A., Kutzbach, J.E., Liu, Z., Otto Bliesner, B., Syktus, J., Weber, S.L., 2004. Evaluation of PMIP coupled ocean-atmosphere simulations of the mid-Holocene. In: Battarbee, R.W., Gasse, F., Stickley, C.E. (Eds.), Past Climate Variability through Europe and Africa. Developments in Paleoenvrionmental Research 6. Springer, Dordrecht, The Netherlands.

Braconnot, P., Otto-Bliesner, B., Harrison, S., Joussaume, S., Peterchmitt, J.-Y., Abe-Ouchi, A., Crucifix, M., Driesschaert, E., Fichefet, T., Hewitt, C.D., Kageyama, M., Kitoh, A., Laîné, A., Loutre, M.-F., Marti, O., Merkel, U., Ramstein, G., Valdes, P., Weber, S.L., Yu, Y., Zhao, Y., 2007a. Results of PMIP2 coupled simulations of the Mid-Holocene and Last Glacial Maximum – Part 1: experiments and large-scale features. Climate of the Past 3, 261–277.

Braconnot, P., Otto-Bliesner, B., Harrison, S., Joussaume, S., Peterchmitt, J.-Y., Abe-Ouchi, A., Crucifix, M., Driesschaert, E., Fichefet, T., Hewitt, C.D., Kageyama, M., Kitoh, A., Laîné, A., Loutre, M.-F., Marti, O., Merkel, U., Ramstein, G., Valdes, P., Weber, S.L., Yu, Y., Zhao, Y., 2007b. Results of PMIP2 coupled simulations of the Mid-Holocene and Last Glacial Maximum – Part 2: feedbacks with emphasis on the location of the ITCZ and mid- and high latitudes heat budget. Climate of the Past 3, 279–296.

Bradley, R.S., Jones, P.D., 1995. Climate Since A.D. 1500. Routledge, London.

Bradley, R.S., Hughes, M.K., Diaz, H.F., 2003. Climate in medieval time. Science 302, 404–405.

Bray, J.R., 1971. Solar-climate relationships in the post-Pleistocene. Science 171, 1242–1243.

Bray, J.R., 1972. Cyclic temperature oscillations from 0–20,300 yr BP. Nature 237, 277–279.

Brewer, S., Guiot, J., Torre, F., 2007. Mid-Holocene climate change in Europe: a data-model comparison. Climate of the Past 3, 499–512.

Briffa, K.R., Jones, P.D., Schweingruber, F.H., Osborn, T.J., 1998. Influence of volcanic eruptions on Northern Hemisphere summer temperature over the past 600 years. Nature 393, 450–455.

Broccoli, A.J., Dahl, K.A., Stouffer, R.J., 2006. Response of the ITCZ to Northern Hemisphere cooling. Geophysical Research Letters 33, L01702, doi:10.1029/2005GL024546.

Broecker, W.S., 2001. Was the medieval warm period global? Science 291, 1497–1499.

Broecker, W.S., Hemming, S., 2001. Climate swings come into focus. Science 294, 2308–2309.

Broecker, W.S., Lynch-Stieglitz, J., Clark, E., Hajdas, I., Bonani, G., 2001. What caused the atmosphere's CO_2 content to rise during the last 8000 years? Geochemistry Geophysics Geosystems 2 2001GC000177.

Brook, E.J., Harder, S., Severinghaus, J., Steig, E.J., Sucher, C.M., 2000. On the origin and timing of rapid changes in atmospheric methane during the last glacial period. Global Biogeochemical Cycles 14, 559–572.

Brostrom, A., Coe, M., Harrison, S.P., Gallimore, R., Kutzbach, J.E., Foley, J., Prentice, I.C., Behling, P., 1998. Land surface feedbacks and palaeomonsoons in northern Africa. Geophysical Research Letters 25, 3615–3618.

Brovkin, V., Claussen, M., Petoukhov, V., Ganopolski, A., 1998. On the stability of the atmosphere–vegetation system in the Sahara/Sahel region. Journal of Geophysical Research Atmospheres 103, 1613–1624.

Brovkin, V., Bendtsen, J., Claussen, M., Ganopolski, A., Kubatzki, C., Petoukhov, V., Andreev, A., 2002. Carbon cycle, vegetation and climate dynamics in the Holocene: Experiments with the CLIMBER-2 model. Global Biogeochemical Cycles 16 (4), 1139. doi:10.1029/2001GB001662.

Brovkin, V., Levis, S., Loutre, M.F., Crucifix, M., Claussen, M., Ganopolski, A., Kubatzki, C., Petoukhov, V., 2003. Stability analysis of the climate–vegetation system in the northern high latitudes. Climatic Change 57, 119–138.

Brovkin, V., Claussen, M., Driesschaert, E., Fichefet, T., Kicklighter, T., Loutre, M.-F., Matthews, H.D., Ramankutty, N., Schaeffer, M., Sokolov, A., 2006. Biogeophysical effects of historical land cover changes simulated by six Earth system models of intermediate complexity. Climate Dynamics 26, 587–600.

Brown, J., Collins, M., Tudhope, A., 2006. Coupled model simulations of mid-Holocene ENSO and comparisons with coral oxygen isotope records. Advances in Geosciences 6, 29–33.

Bryson, R.A., Goodman, B.M., 1980. Volcanic activity and climate change. Science 207, 1041–1044.

Burroughs, W.J., 2003. Weather Cycles. Cambridge University Press, Cambridge.

Bütikofer, J., 2007. Millennial scale climate variability during the last 6000 years – tracking down the Bond cycles. Diploma thesis. University of Bern (http://www.giub.unibe.ch/klimet/docs/diplom_jbuetikofer.pdf).

Calvo, E., Grimalt, J., Jansen, E., 2002. High resolution U^{K}_{37} sea surface temperature in the Norwegian Sea during the Holocene. Quaternary Science Reviews 21, 1385–1394.

Carrington, D.P., Gallimore, R.G., Kutzbach, J.E., 2001. Climate sensitivity to wetlands and wetland vegetation in mid-Holocene North Africa. Climate Dynamics 17, 151–157.

Castellano, E., Becagli, S., Hansson, M., Hutterli, M., Petit, J.R., Rampino, M.R., Severi, M., Steffensen, J.P., Traversi, R., Udisti, R., 2005. Holocene volcanic history as recorded in the sulphate stratigraphy of the European Project for Ice Coring in Antarctica Dome C (EDC96) ice Core. Journal of Geophysical Research 110, D06114, doi:10.1029/2004JD005259.

Chapman, M.R., Shackleton, N.J., 2000. Evidence of 550-year and 1000-year cyclicities in North Atlantic circulation patterns during the Holocene. The Holocene 10, 287–291.

Chappellaz, J., Blunier, T., Kints, S., Dällenbach, A., Barnola, J.-M., Schwander, J., Raynaud, D., Stauffer, B., 1997. Changes in the atmospheric CH_4 gradient between Greenland and Antarctica during the Holocene. Journal of Geophysical Research 102 (D13), 15987–15999.

Charney, J.G., 1975. Dynamics of deserts and drought in the Sahel. Quarterly Journal of the Royal Meteorological Society 101, 193–202.

Claussen, M., Gayler, V., 1997. The greening of the Sahara during the mid-Holocene: results of an interactive atmosphere-biome model. Global Ecology and Biogeography Letters 6, 369–377.

Claussen, M., Brovkin, V., Ganopolski, A., Hoelzmann, P., Pachur, H.-J., 1999. Simulation of an abrupt change in Saharan vegetation in the mid-Holocene. Geophysical Research Letters 26, 2037–2040.

Claussen, M., Mysak, L.A., Weaver, A.J., Crucifix, M., Fichefet, T., Loutre, M.F., Weber, S.L., Alcamo, J., Alexeev, V.A., Berger, A., Calov, R., Ganopolski, A., Goosse, H., Lohman, G., Lunkeit, F., Mohkov, I.I., Petoukhov, V., Stone, P., Wang, Z., 2002. Earth System Models of Intermediate Complexity: closing the gap in the spectrum of climate system models. Climate Dynamics 18, 579–586.

Clemens, S.C., 2005. Millennial-band climate spectrum resolved and linked to centennial-scale solar cycles. Quaternary Science Reviews 24, 521–531.

Clement, A.C., Seager, R., Cane, M.A., 1999. Orbital controls on the tropical climate. Paleoceanography 14, 441–456.

Clement, A.C., Seager, R., Cane, M.A., 2000. Suppression of El Niño during the mid-Holocene by changes in the Earth's orbit. Paleoceanography 15, 731–737.

Clement, A.C., Cane, M.A., Seager, R., 2001. An orbitally driven tropical source for abrupt climate change. Journal of Climate 14, 2369–2375.

Clement, A.C., Hall, A., Broccoli, A., 2004. The importance of precessional signals in the tropical climate. Climate Dynamics 22, 327–341.

CLIMAP Project Members, 1976. The surface of the ice-age earth. Science 191, 1138–1144.

CLIMAP Project Members, 1981. Seasonal reconstructions of the Earth's surface at the last glacial maximum. Geological Society of America Map and Chart Series MC-36.

Codron, F., 2001. Sensitivity of the tropical Pacific to a change of orbital forcing in two versions of a coupled GCM. Climate Dynamics 17, 187–203.

COHMAP Members, 1988. Climatic changes of the last 18,000 years: observations and model simulations. Science 241, 1043–1052.

Cole, J., 2001. Enhanced: A slow dance for El Niño. Science 291, 1496–1497.

Crowley, T.J., 2000. Causes of climate change over the past 1000 years. Science 289, 270–277.

Crowley, T.J., 2002. Cycles, cycles, everywhere. Science 295, 1473–1474.

Crowley, T.J., Lowery, T.S., 2000. How warm was the medieval warm period? Ambio 29, 51–54.

Crowley, T.J., Vinther, B.M., in preparation. A plausible retuned chronology for the GISP 2 ice core for the last 6000 years. (in preparation).

Crucifix, M., Loutre, M.F., Tulkens, P., Fichefet, T., Berger, A., 2002. Climate evolution during the Holocene: a study with an Earth system model of intermediate complexity. Climate Dynamics 19 (1), 43–60.

Cubasch, U., Voss, R., Hegerl, G.C., Waszkewitz, J., Crowley, T.J., 1997. Simulation of the influence of solar radiation variations on the global climate with an ocean–atmosphere general circulation model. Climate Dynamics 13, 757–767.

Cubasch, U., Voss, R., 2000. The influence of total solar irradiance on climate. Space Science Reviews 94, 185–198.

Cubasch, U., Bürger, G., Fast, I., Spangehl, T., Wagner, S., 2004. The direct solar influence on climate: modeling the lower atmosphere. Memorie della Societa Astronomica Italiana 76, 810–818.

Please cite this article in press as: Wanner, H., et al., Mid- to Late Holocene climate change: an overview, Quaternary Science Reviews (2008), doi:10.1016/j.quascirev.2008.06.013

Cubasch, U., Bürger, G., Fast, I., Spangehl, T., 2006. The past 1000 years revisited. In: Iversen, T., Lystad, M. (Eds.), RegClim General Technical Report No. 9. Norway, Norwegian Meteorological Institute, Oslo.

Cullen, H.M., deMenocal, P.B., Hemming, S., Hemming, G., Brown, F.H., Guilderson, F.H., Sirocko, F., 2000. Climate change and the collapse of the Akkadian empire: evidence from the deep sea. Geology 28, 379–382.

Dahl, S.O., Nesje, A., 1996. A new approach to calculating Holocene winter precipitation by combining glacier equilibrium-line altitudes and pine-tree limits: a case study from Hardangerjøkulen, central southern Norway. The Holocene 6, 381–398.

Dahl, S.O., Bakke, J., Lie, O., Nesje, A., 2003. Reconstruction of former glacier equilibrium-line altitudes based on proglacial sites: an evaluation of approaches and selection of sites. Quaternary Science Reviews 22, 275–287.

Dai, A., Hu, A., Meehl, G.A., Washington, W.M., Strand, W.G., 2005. Atlantic thermohaline circulation in a coupled general circulation model: unforced variations versus forced changes. Journal of Climate 18, 3270–3293.

Dalfes, N., Kukla, G., Weiss, H., 1996. Third Millennium BC Climate Change and Old World Collapse. Springer, Berlin, Heidelberg, New York.

D'Arrigo, R., Villalba, R., Wiles, G.C., 2001. Tree ring estimates of Pacific decadal climate variability. Climate Dynamics 18, 219–224.

Davis, B.A.S., Brewer, S., Stevenson, A.C., Guiot, J., 2003. The temperature of Europe during the Holocene reconstructed from pollen data. Quaternary Science Reviews 22, 1701–1716.

de Beaulieu, J.-L., Miras, Y., Andrieu-Ponel, V., Guiter, F., 2005. Vegetation dynamics in north-western Mediterranean regions: instability of the Mediterranean bioclimate. Plant Biosystems 139, 114–126.

Debret, M., Bout-Roumazeilles, V., Grousset, F., Desmet, M., McManus, J.F., Massei, N., Sebag, D., Petit, J.-R., Copard, Y., Trentesaux, A., 2007. The origin of the 1500-year climate cycles in Holocene North-Atlantic records. Climate of the Past 3, 569–575.

Delworth, T., Mannabe, S., Stouffer, R.J., 1993. Interdecadal variations of the thermohaline circulation in a coupled ocean-atmosphere model. Journal of Climate 6, 1993–2011.

Delworth, T.L., Mann, M.E., 2000. Observed and simulated multidecadal variability in the Northern Hemisphere. Climate Dynamics 16, 661–676.

deMenocal, P.B., 2001. Cultural responses to climate change during the Late Holocene. Science 292, 667–673.

deMenocal, P.B., Ortiz, J., Guilderson, T., Sarntheim, M., 2000. Coherent high- and low-latitude climate variability during the Holocene warm period. Science 288, 2198–2202.

de Noblet-Ducoudré, N., Claussen, M., Prentice, I.C., 2000. Mid-Holocene greening of the Sahara: first results of the GAIM 6000 yr BP experiment with two asynchronously coupled atmosphere/biosphere models. Climate Dynamics 16, 643–659.

Denton, G.H., Karlén, W., 1973. Holocene climatic variations – their pattern and possible cause. Quaternary Research 3, 155–205.

DeWitt, D., Schneider, E.K., 1998. The tropical ocean response to a change in orbital forcing. Technical Report 56. Center for Ocean-Land-Atmosphere Studies.

DeWitt, D., Schneider, E.K., 2000. The tropical response to a change in solar forcing. Journal of Climate 13, 1133–1149.

Diaz, H.F., Hoerling, M.P., Eischeid, J.K., 2001. ENSO variability, teleconnections and climate change. International Journal of Climatology 21, 1845–1862.

Diffenbaugh, N.S., Sloan, L.C., 2002. Global climate sensitivity to land surface change: the Mid Holocene revisited. Geophysical Research Letters 29 (10), 1476. doi:10.1029/2002GL014880.

Doherty, R., Kutzbach, J., Foley, J., Pollard, D., 2000. Fully coupled climate/dynamical vegetation model simulations over Northern Africa during the mid-Holocene. Climate Dynamics 16, 561–573.

Donnelly, J.P., Woodruff, J.D., 2007. Intense hurricane activity over the past 5000 years controlled by El Niño and the West African monsoon. Nature 447, 465–468.

Dykoski, C.A., Edwards, R.L., Cheng, H., Yuan, D., Cai, Y., Zhang, M., Lin, Y., Qing, J., An, Z., Revenaugh, J., 2005. A high-resolution, absolute-dated Holocene and deglacial Asian monsoon record from Dongge Cave, China. Earth and Planetary Science Letters 233, 71–86.

Edwards, M.E., Anderson, P.M., Brubaker, L.B., Ager, T.A., Andreev, A.A., Bigelow, N.H., Cwynar, L.C., Eisner, W.R., Harrison, S.P., Hu, F.-S., Jolly, D., Lozhkin, A.V., McDonald, G.M., Mock, C.J., Ritchie, J.C., Sher, A.V., Spear, R.W., Williams, J.W., Yu, G., 2000. Pollen-based biomes for Beringia 18,000, 6,000 and 0 ^{14}C yr BP. Journal of Biogeography 27, 521–554.

Ellis, J.M., Calkin, P.E., 1984. Chronology of Holocene glaciation, central Brooks Range, Alaska. Geological Society of America Bulletin 95, 897–912.

Enfield, D.B., Mestas-Nuñez, A.M., Trimble, P.J., 2001. The Atlantic multidecadal oscillation and its relation to rainfall and river flows in the continental US. Geophysical Research Letters 28, 2077–2080.

Esper, J., Cook, E.R., Schweingruber, F.H., 2002. Low-frequency signals in long tree-line chronologies for reconstructing past temperature variability. Science 295, 2250–2253.

Feddema, J., Oleson, K., Bonan, G., Mearns, L., Washington, W., Meehl, G., Nychka, D., 2005. A comparison of a GCM response to historical anthropogenic land cover change and model sensitivity to uncertainty in present-day land cover representations. Climate Dynamics 25, 581–609.

Fischer, E., Luterbacher, J., Zorita, E., Tett, S.F.B., Casty, C., Wanner, H., 2006. European climate response to tropical volcanic eruptions over the last half millennium. Geophysical Research Letters 34, L05707.

Fischer, H., Mieding, B., 2005. A 1,000-year ice core record of interannual to multidecadal variations in atmospheric circulation over the North Atlantic. Climate Dynamics 25, 65–74.

Fisher, D.A., Koerner, R.M., Reeh, N., 1994. Holocene climatic records from Agassiz Ice Cap, Ellesmere Island NWT, Canada. The Holocene 5, 19–24.

Fleitmann, D., Burns, S.J., Mudelsee, M., Neff, U., Kramers, J., Mangini, A., Matter, A., 2003. Holocene forcing of the Indian monsoon recorded in a stalagmite from southern Oman. Science 300, 1737–1739.

Flückiger, J., Dällenbach, A., Blunier, T., Stauffer, B., Stocker, T.F., Raynaud, D., Barnola, J.-M., 1999. Variations in atmospheric N_2O concentration during abrupt climatic changes. Science 285, 227–230.

Flückiger, J., Monnin, E., Stauffer, B., Schwander, J., Stocker, T.F., Chappellaz, J., Raynaud, D., Barnola, J.-M., 2002. High resolution Holocene N_2O ice core record and its relationship with CH_4 and CO_2. Global Biogeochemical Cycles 16 (1), 1010. doi:10.1029/2001GB001417.

Foley, J.A., Kutzbach, J.E., Coe, M.T., Levis, S., 1994. Feedbacks between climate and boreal forests during the Holocene epoch. Nature 371, 52–54.

Friedlingstein, P., Cox, P., Betts, R., Bopp, L., Von Bloh, W., Brovkin, V., Cadule, P., Doney, S., Eby, M., Fung, I., Bala, G., John, J., Jones, C., Joos, F., Kato, T., Kawamiya, M., Knorr, W., Lindsay, K., Matthews, H.D., Raddatz, T., Rayner, P., Reick, C., Roeckner, E., Schnitzler, K.G., Schnur, R., Strassmann, K., Weaver, A.J., Yoshikawa, C., Zeng, N., 2006. Climate-carbon cycle feedback analysis: results from the (CMIP)-M-4 model intercomparison. Journal of Climate 19 3337–3335.

Fritz, S.L., Metcalfe, S.E., Dean, W., 2001. Holocene climate patterns in the Americas inferred from paleolimnological records. In: Markgraf, V. (Ed.), Interhemispheric Climate Linkage. Academic Press, San Diego, CA.

Fröhlich, C., Lean, J., 2004. Solar radiative output and its variability: evidence and mechanisms. Astronomy and Astrophysics Review 12 (4), 273–320.

Gagan, M.K., Ayliffe, L.K., Hopley, D., Cali, J.A., Mortimer, G.E., Chappell, J., McCulloch, M.T., Head, M.J., 1998. Temperature and surface-ocean water balance of the mid-Holocene tropical western Pacific. Science 279, 1014–1018.

Gagan, M.K., Hendy, E.J., Haberle, S.G., Hantoro, W.S., 2004. Post-glacial evolution of the Indo-Pacific warm pool and El Niño-Southern Oscillation. Quaternary International 118-119, 127–143.

Gajewski, K., Viau, A., Sawada, M., Atkinson, D., Wilson, S., 2001. Sphagnum peatland distribution in North America and Eurasia during the past 21,000 years. Global Biogeochemical Cycles 15, 297–310.

Gallimore, R., Jacob, R., Kutzbach, J., 2005. Coupled atmosphere–ocean–vegetation simulations for modern and mid-Holocene climates: role of extratropical vegetation cover feedbacks. Climate Dynamics 25, 755–776.

Ganopolski, A., Kubatzki, C., Claussen, M., Brovkin, V., Petoukhov, V., 1998. The influence of vegetation–atmosphere–ocean interaction on climate during the mid-Holocene. Science 280, 1916–1919.

Gao, C., Robock, A., submitted. Volcanic forcing of climate over the past 1500 years: an improved ice-core-based index for climate models. Journal of Geophysical Research (submitted).

Gasse, F., 2000. Hydrological changes in the African tropics since the Last Glacial Maximum. Quaternary Science Reviews 19, 189–211.

Gasse, F., van Campo, E., 1994. Abrupt post-glacial climate events in West Asia and North Africa monsoon domains. Earth and Planetary Science Letters 126, 435–456.

Gedalof, Z., Smith, D.J., 2001. Interdecadal climate variability and regime-scale shifts in Pacific North America. Geophysical Research Letters 28, 1515–1518.

Gedalof, Z., Mantua, N.J., Peterson, D.L., 2002. A multi-century perspective of variability in the Pacific Decadal Oscillation: new insight from tree rings and coral. Geophysical Research Letters 29, 2204–2207.

Geirsdottir, A., Hardardottir, J., Andrews, J.T., 2000. Late-Holocene terrestrial glacial history of Miki and I.C. Jacobsen Fjords, East Greenland. The Holocene 10, 123–134.

Gellatly, A.F., Chinn, T.J.H., Roethlisberger, F., 1988. Holocene glacier variations in New Zealand. Quaternary Sciences Reviews 7, 227–242.

Gerber, S., Joos, F., Brugger, P., Stocker, T.F., Mann, M.E., Sitch, S., Scholze, M., 2003. Constraining temperature variations over the last millennium by comparing simulated and observed atmospheric CO_2. Climate Dynamics 20, 281–299.

Gladstone, R.M., Ross, I., Valdes, P.J., Abe-Ouchi, A., Braconnot, P., Brewer, S., Kageyama, M., Kitoh, A., Legrande, A., Marti, O., Ohgaito, R., Otto-Bliesner, B., Peltier, W.R., Vettoretti, G., 2005. Mid-Holocene NAO: A PMIP2 model intercomparison. Geophysical Research Letters 32, L16707. doi:10.1029/2005GL.023596.

Glasser, N.F., Harrison, S., Winchester, V., Masamu, A., 2004. Late Pleistocene and Holocene palaeoclimate and glacier fluctuations in Patagonia. Global and Planetary Change 431, 79–101.

Goldenberg, S.B., Landsea, C.W., Mestas-Nuñez, A.M., Gray, S.T., 2001. The recent increase in Atlantic hurricane activity: causes and implications. Science 293, 474–479.

González-Rouco, F., von Storch, H., Zorita, E., 2003. Deep soil temperature as proxy for surface air-temperature in a coupled model simulation of the last thousand years. Geophysical Research Letters 30, 2116.

Goosse, H., Renssen, H., 2004. Exciting natural modes of variability by solar and volcanic forcing: idealized and realistic experiments. Climate Dynamics 23, 153–163.

Goosse, H., Masson-Delmotte, V., Renssen, H., Delmotte, M., Fichefet, T., Morgan, V., van Ommen, T., Khim, B.K., Stenni, B., 2004. A late medieval warm period in the Southern Ocean as a delayed response to external forcing? Geophysical Research Letters 31, 6203–6206.

Goosse, H., Crowley, T., Zorita, E., Ammann, C., Renssen, H., Driesschaert, E., 2005a. Modelling the climate of the last millennium: what causes the differences between simulations? Geophysical Research Letters 32, L06710. doi:10.1029/2005GL22368.

Please cite this article in press as: Wanner, H., et al., Mid- to Late Holocene climate change: an overview, Quaternary Science Reviews (2008), doi:10.1016/j.quascirev.2008.06.013

Goosse, H., Renssen, H., Timmermann, A., Bradley, R.S., 2005b. Internal and forced climate variability during the last millennium: a model-data comparison using ensemble simulations. Quaternary Science Reviews 24, 1345–1360.

Goosse, H., Arzel, O., Luterbacher, J., Mann, M.E., Renssen, H., Riedwyl, N., Timmermann, A., Xoplaki, E., Wanner, H., 2006. The origin of the European "Medieval Warm Period". Climate of the Past 2, 99–113.

Goswami, B.N., Madhsoodanan, M.S., Neema, C.P., Sengupta, D., 2006. A physical mechanism for North Atlantic SST influence on the Indian summer monsoon. Geophysical Research Letters 33, L02706. doi:10.1029/2005GL 024803.

Graf, H.-F., Kirchner, I., Robock, A., Schult, I., 1993. Pinatubo eruption winter climate effects: model versus observations. Climate Dynamics 9, 81–93.

Graf, H.-F., Feichter, J., Langmann, J., 1997. Volcanic sulphur emission: Estimates of source strength and its contribution to the global distribution. Journal of Geophysical Research 102, 10727–10738.

Graham, N.E., Hughes, M.K., Ammann, C.M., Cobb, K.M., Hoerling, M.P., Kennett, D.J., Rein, B., Stott, L., Wigand, P.E., Xu, T., 2007. Tropical Pacific – mid-latitude teleconnections in medieval times. Climatic Change 83, 241–285.

Gray, S.T., Graumlich, L.J., Betancourt, J.L., Pederson, G.T., 2004. A tree-ring based reconstruction of the Atlantic Multidecadal oscillation since 1567 AD. Geophysical Research Letters 31, L12205.

Groll, N., Widmann, M., 2006. Sensitivity of temperature teleconnections to orbital changes in AO-GCM simulations. Geophysical Research Letters 33, L12705.

Groll, N., Widmann, M., Jones, J.M., Kaspar, F., Lorenz, S.J., 2005. Simulated relationships between regional temperatures and large-scale circulation: 125 kyr BP (Eemian) and the preindustrial period. Journal of Climate 18, 4032–4045.

Grosjean, M., Messerli, B., Veit, H., Geyh, M.A., Schreier, H., 1998. A late-Holocene (2600 BP) glacial advance in the south- central Andes (298S), northern Chile. The Holocene 8, 473–479.

Grosjean, M., Cartajena, I., Geyh, M.A., Nuñez, L.A., 2003. From proxy-data to paleoclimate interpretation: the mid-Holocene paradox of the Atacama Desert, northern Chile. Palaeogeography, Palaeoclimatology. Palaeoecology 1941, 247–258.

Grosjean, M., Suter, P., Trachsel, M., Wanner, H., 2007. Ice-borne prehistoric finds in the Swiss Alps reflect Holocene glacier fluctuations. Journal of Quaternary Science 22 (3), 203–207.

Grove, J.M., 2004. Little Ice Ages: Ancient and Modern. Routledge, New York.

Grove, J.M., Switsur, R., 1994. Glacial geological evidence for the Medieval Warm Period. Climatic Change 26, 143–169.

Gupta, A.K., Anderson, D.M., Overpeck, J.T., 2003. Abrupt changes in the Asian southwest monsoon during the Holocene and their links to the North Atlantic Ocean. Nature 421, 354–357.

Gupta, A.K., Das, M., Anderson, D.M., 2005. Solar influence on the Indian summer monsoon during the Holocene. Geophysical Research Letters 32, L17703. doi:10.1029/2005GL022685.

Haigh, J.D., 1996. The impact of solar variability on climate. Science 272, 981–984.

Hall, I.R., Bianchi, G.G., Evans, J.R., 2004. Centennial to millennial scale Holocene climate-deep water linkage in the North Atlantic. Quaternary Science Reviews 23, 1529–1536.

Hall, A., Clement, A., Thompson, D.W., Broccoli, A., Jackson, C., 2005. The importance of atmospheric dynamics in the northern hemisphere wintertime climate response to changes in the Earth's orbit. Journal of Climate 18, 1315–1325.

Hall, N.M.J., Valdes, P.J., 1997. A GCM simulation 6000 years ago. Journal of Climate 10, 3–17.

Hare, S.R., Mantua, N.J., Francis, R.C., 1999. Inverse production regimes: Alaskan and West Coast Salmon. Fisheries 24, 6–14.

Harder, S.L., Shindell, D.T., Schmidt, G.A., Brook, E.J., 2007. A global climate model study of CH_4 emissions during the Holocene and glacial–interglacial transitions constrained by ice core data. Global Biogeochemical Cycles 21 (1), GB1011. doi:10.1029/2005GB002680.

Harrison, S.P., Dodson, J., 1993. Climates of Australia and New Guinea since 18,000 yr BP. In: Wright Jr., H.E., Kutzbach, J.E., Webb III, T., Ruddiman, W.F., Street-Perrott, F.A., Bartlein, P.J. (Eds.), Global Climates since the Last Glacial Maximum. University of Minnesota Press, Minneapolis, MN, pp. 265–293.

Harrison, S.P., Kutzbach, J.E., Prentice, I.C., Behling, P.J., Sykes, M.T., 1995. The response of northern hemisphere extratropical climate and vegetation to orbitally induced changes in insolation during the last interglaciation. Quaternary Research 43, 174–184.

Harrison, S.P., Jolly, D., Laarif, F., Abe-Ouchi, A., Dong, B., Herterich, K., Hewitt, C., Joussaume, S., Kutzbach, J.E., Mitchell, J., de Noblet, N., Valdes, P., 1998. Intercomparison of simulated global vegetation distributions in response to 6 kyr BP orbital forcing. Journal of Climate 11, 2721–2742.

Harrison, S.P., Yu, G., Takahara, H., Prentice, I.C., 2001. Paleovegetation - Diversity of temperate plants in east Asia. Nature 213, 129–130.

Harrison, S.P., Kutzbach, J.E., Liu, Z., Bartlein, P.J., Otto-Bliesner, B., Muhs, D., Prentice, I.C., Thompson, R.S., 2003. Mid-Holocene climates of the Americas: a dynamic response to changed seasonality. Climate Dynamics 20, 663–688.

Haug, G.H., Hughen, K.A., Sigman, D.M., Peterson, L.C., Röhl, U., 2001. Southward migration of the Intertropical Convergence Zone through the Holocene. Science 293, 1304–1308.

Haug, G.H., Günther, D., Peterson, L.C., Sigman, D.M., Hughen, K.A., Aeschlimann, B., 2003. Climate and the collapse of Maya civilization. Science 299, 1731–1735.

Hegerl, G.C., Hasselmann, K., Cubasch, U., Mitchell, J.F.B., Roeckner, E., Voss, R., Waszkewitz, J., 1997. Multi-fingerprint detection and attribution analysis of greenhouse gas, greenhouse gas-plus-aerosol and solar forced climate change. Climate Dynamics 13, 613–634.

Hegerl, G.C., Crowley, T.J., Baum, S.K., Kim, K.-Y., Hyde, W.T., 2003. Detection of volcanic, solar and greenhouse gas signals in paleo-reconstructions of Northern Hemispheric temperature. Geophysical Research Letters 30 (5), 1242. doi:10.1029/2002GL016635.

Hegerl, G.C., Zwiers, F.W., Braconnot, P., Nicholls, N., Penner, J.E., Stott, P.A., 2007. Understanding and attributing climate change. In: Solomon, S., Qin, D., Manning, M., Chen, Z., Marquis, M., Averyt, K.B., Tignor, M., Miller, H.L. (Eds.), Climate Change 2007: The Physical Science BasisContribution of Working Group I to the Fourth Assesement Report of the Intergovernmental Panel on Climate Change. Cambridge University Press, Cambridge and New York.

Heikkilä, M., Seppä, H., 2003. A 11,000 yr paleotemperature reconstruction from the southern boreal zone in Finland. Quaternary Science Reviews 22, 541–554.

Hodell, D.A., Curtis, J.H., Brenner, M., 1995. Possible role of climate in the collapse of classic Maya civilization. Nature 375, 391–394.

Hodell, D.A., Kanfoush, S.L., Shemesh, A., Crosta, X., Charles, C.D., Guilderson, T.P., 2001. Abrupt cooling of Antarctic surface waters and sea ice expansion in the South Atlantic sector of the Southern Ocean at 5000 cal years BP. Quaternary Research 56, 191–198.

Hoelzmann, P., Jolly, D., Harrison, S.P., Laarif, F., Bonnefille, R., Pachur, H.J., 1998. Mid-Holocene land surface conditions in northern Africa and the Arabian Peninsula: a data set for the analysis of biogeophysical feedbacks in the climate system. Global Biogeochemical Cycles 12, 35–51.

Holmgren, K., Lee-Thorp, J.A., Cooper, G.R.J., Lundblad, K., Partridge, T.C., Scott, L., SithaldeenTalma, R.A.S., Tyson, P.D., 2003. Persistent millennial-scale climatic variability over the past 25,000 years in Southern Africa. Quaternary Science Reviews 22 (21-22), 2311–2326.

Holzhauser, H., Magny, M., Zumbühl, H.J., 2005. Glacier and lake-level variations in west-central Europe over the last 3500 years. The Holocene 15, 789–801.

Hormes, A., Müller, B.U., Schlüchter, C., 2001. The Alps with little ice: evidence for eight Holocene phases of reduced glacier extent in the Central Swiss Alps. The Holocene 11, 255–265.

Hu, F.S., Kaufman, D., Yoneji, S., Nelson, D., Shemesh, A., Huang, Y., Tian, J., Bond, G., Clegg, B., Brown, T., 2003. Cyclic variation and solar forcing of Holocene climate in the Alaskan subarctic. Science 301, 1890–1893.

Huebener, H., Cubasch, U., Langematz, U., Spangehl, T., Niehörster, F., Fast, I., Kunze, M., 2007. Ensemble climate simulations using a fully coupled ocean–troposphere–stratosphere general circulation model. Philosophical Transactions of the Royal Society 365, 2089–2101.

Hughes, M.K., Diaz, H.F., 1994. Was there a "Medieval Warm Period", and if so, where and when? Climatic Change 26, 109–142.

Humlum, O., Elberling, B., Hormes, A., Fjordheim, K., Hansen, O.H., Heinemeier, J., 2005. Late-Holocene glacier growth in Svalbard, documented by subglacial relict vegetation and living soil microbes. The Holocene 15, 396–407.

Hunt, B.G., 1998. Natural climatic variability as an explanation for historical climatic fluctuations. Climatic Change 38, 133–157.

Hurrell, J.W., Kushnir, Y., Ottersen, G., Visbeck, M. (Eds.), 2003. The North Atlantic Oscillation. Climatic Significance and Environmental Impact. Geophysical Monograph 134. American Geophysical Union, Washington, DC.

Indermühle, A., Stocker, T.F., Joos, F., Fischer, H., Smith, H.J., Wahlen, M., Deck, B., Mastroianni, D., Tschumi, J., Blunier, T., Stauffer, B., 1999. Holocene carbon-cycle dynamics based on CO_2 trapped in ice at Taylor Dome, Antarctica. Nature 398, 121–126.

IPCC, 2007. Climate Change 2007: The Physical Science Basis. In: Solomon, S., Qin, D., Manning, M., Chen, Z., Marquis, M., Averyt, K.B., Tignor, M., Miller, H.L. (Eds.), Contribution of Working Group I to the Fourth Assessment Report of the Intergovernmental Panel on Climate Change. Cambridge University Press, Cambridge and New York.

Irizarry-Ortiz, M.M., Wang, G.L., Eltahir, E.A.B., 2003. Role of the biosphere in the mid-Holocene climate of West Africa. Journal of Geophysical Research Atmospheres 108 (D2), 4042. doi:10.1029/2001JD000989.

Jansen, E., Overpeck, J., Briffa, K.R., Duplessy, J.-C., Joos, F., Masson-Delmotte, V., Olago, D., Otto Bliesner, B., Peltier, W.R., Rahmstorf, S., Ramesh, D., Raynaud, D., Rind, D., Solomina, O., Villalba, R., Zhang, D., 2007. Palaeoclimate. In: Solomon, S., Qin, D., Manning, M., Chen, Z., Marquis, M., Averyt, K.B., Tignor, M., Miller, H.L. (Eds.), Climate Change 2007: The Physical Science BasisContribution of Working Group I to the Fourth Assesement Report of the Intergovernmental Panel on Climate Change. Cambridge University Press, Cambridge and New York.

Jennings, A.E., Knudsen, K.L., Hald, M., Hansen, C.V., Andrews, J.T., 2002. A mid-Holocene shift in Arctic sea-ice variability on the East Greenland Shelf. The Holocene 12, 49–58.

Jenny, B., Wilhelm, D., Valero-Garces, B., 2003. The southern westerlies in Central Chile: holocene precipitation estimates based on a water balance model for Laguna Aculeo (33°50′ S). Climate Dynamics 20, 269–280.

Jolly, D., Prentice, I.C., Bonnefille, R., Ballouche, A., Bengo, M., Brenac, P., Buchet, G., Burney, D., Cazet, J.P., Cheddadi, R., Edorh, T., Elenga, H., Elmoutaki, S., Guiot, J., Laarif, F., Lamb, H., Lezine, A.M., Maley, J., Mbenza, M., Peyron, O., Reille, M., Reynaud-Farrera, I., Riollet, G., Ritchie, J.C., Roche, E., Scott, L., Semmanda, I., Straka, H., Umer, M., Van Campo, E., Vilimumbalo, S., Vincens, A., Waller, M., 1998a. Biome reconstruction from pollen and plant macrofossil data for Africa and the Arabian peninsula at 0 and 6000 years. Journal of Biogeography 25, 1007–1027.

Jolly, D., Harrison, S.P., Damnati, B., Bonnefille, R., 1998b. Simulated climate and biomes of Africa during the late quaternary: comparison with pollen and lake status data. Quaternary Science Reviews 17, 629–657.

Jones, M.D., Roberts, N., Leng, M.J., Türkeş, M., 2006. A high-resolution late Holocene lake isotope record from Turkey and links to North Atlantic and monsoon climate. Geology 34, 361–364.

Please cite this article in press as: Wanner, H., et al., Mid- to Late Holocene climate change: an overview, Quaternary Science Reviews (2008), doi:10.1016/j.quascirev.2008.06.013

Jones, P.D., Mann, M.E., 2004. Climate over past millennia. Reviews of Geophysics 42, 1–42.

Joos, F., Gerber, S., Prentice, I.C., Otto-Bliesner, B.L., Valdes, P.J., 2004. Transient simulations of Holocene atmospheric carbon dioxide and terrestrial carbon since the Last Glacial Maximum. Global Biogeochemical Cycles 18, GB2002. doi:10.1029/2003GB002156.

Joos, F., Spahni, R., 2008. Rates of change in natural and anthropogenic radiative forcing over the past 20,000 years. Proceedings of the National Academy of Sciences of the USA 105, 1425–1430.

Jörin, U.E., Stocker, T.F., Schlüchter, C., 2006. Multi-century glacier fluctuations in the Swiss Alps during the Holocene. The Holocene 16, 697–704.

Joussaume, S., Taylor, K.E., 1995. Status of the Paleoclimate Modeling Intercomparison Project, in: Proceedings of the First International AMIP Scientific Conference, WCRP-92, Monterey, USA, pp. 425-430.

Joussaume, S., Taylor, K.E., Braconnot, P., Mitchell, J.F.B., Kutzbach, J.E., Harrison, S.P., Prentice, I.C., Broccoli, A.J., Abe-Ouchi, A., Bartlein, P.J., Bonfils, C., Dong, B., Guiot, J., Herterich, K., Hewitt, C.D., Jolly, D., Kim, J.W., Kislov, A., Kitoh, A., Loutre, M.F., Masson, V., McAvaney, B., McFarlane, N., de Noblet, N., Peltier, W.R., Peterschmitt, J.Y., Pollard, D., Rind, D., Royer, J.F., Schlesinger, M.E., Syktus, J., Thompson, S., Valdes, P., Vettoretti, G., Webb, R.S., Wyputta, U., 1999. Monsoon changes for 6000 years ago: results of 18 simulations from the Paleoclimate Modeling Intercomparison Project (PMIP). Geophysical Research Letters 26, 859–862.

Jouzel, J., Masson, V., Cattani, O., Falourd, S., Stievenard, M., Stenni, B., Longinell, A., Johnsen, S.J., Steffensen, J.P., Petit, J.R., Schwander, J., Souchez, J.R., Barkov, N.I., 2001. A new 27 ky high resolution East Antarctic climate record. Geophysical Research Letters 28 (16), 3199–3202.

Kaplan, J.O., 2001. Geophysical applications of vegetation modeling. Unpublished PhD thesis. Lund University.

Kaplan, J.O., Prentice, I.C., Knorr, W., Valdes, P.J., 2002. Modeling the dynamics of terrestrial carbon storage since the Last Glacial Maximum. Geophysical Research Letters 29 (22), 2074. doi:10.1029/2002GL015230.

Kaplan, J.O., Bigelow, N.H., Prentice, I.C., Harrison, S.P., Bartlein, P.J., Christensen, T.R., Cramer, W., Matveyeva, N.V., McGuire, A.D., Murray, D.F., Razzhivin, V.Y., Smith, B., Walker, D.A., Anderson, P.M., Andreev, A.A., Brubaker, L.B., Edwards, M.E., Lozhkin, A.V., 2003. Climate change and Arctic ecosystems: 2. Modeling, paleodata-model comparisons, and future projections. Journal of Geophysical Research Atmospheres 108 (D19), 8171. doi:10.1029/2002JD002559.

Kaplan, J.O., Folberth, G., Hauglustaine, D.A., 2006. Role of methane and biogenic volatile organic compound sources in late glacial and Holocene fluctuations of atmospheric methane concentrations. Global Biogeochemical Cycles 20, GB2016. doi:10.1029/2005GB002590.

Kaser, G., Osmaston, H., 2002. Tropical Glaciers. Cambridge University Press, Cambridge.

Kaspar, F., Kuhl, N., Cubasch, U., Litt, T., 2005. A model-data comparison of European temperatures in the Eemian interglacial. Geophysical Research Letters 32, L11703.

Kaufman, D.-S., Ager, T.A., Anderson, N.J., Anderson, P.M., Andrews, J.T., Bartlein, P.J., Brubaker, L.B., Coats, L.L., Cwynar, L.C., Duvall, M.L., Dyke, A.S., Edwards, M.E., Eisner, W.R., Gajewski, K., Geirsdóttir, A., Hu, F.S., Jennings, A.E., Kaplan, M.R., Kerwin, M.W., Lozhkin, A.V., MacDonald, G.M., Miller, G.H., Mock, C.J., Oswald, W.W., Otto-Bliesner, B.L., Porinchu, D.F., Rühland, K., Smol, J.P., Steig, E.J., Wolfe, B.B., 2004. Holocene thermal maximum in the western Arctic (0–180°W). Quaternary Science Reviews 23, 529–560.

Keefer, D.K., de France, S.D., Moseley, M.E., Richardson III, J.B., Satterlee, D.R., Day-Lewis, A., 1998. Early maritime economy and El Niño events at Quebrada Tacahuay, Peru. Science 281, 1833–1835.

Keigwin, L.D., Pickart, R.S., 1999. Slope water current over the Laurentian fan on interannual to millennial time scales. Science 286, 520–523.

Kerr, R.A., 2000. A North Atlantic climate pacemaker for the centuries. Science 288, 1984–1986.

Kilian, R., Schneider, C., Koch, J., Fesq-Martin, M., Biester, H., Casassa, G., Arévalo, M., Wendt, G., Baeza, O.J., Behrmann, J., 2007. Palaeoecological constraints on late Glacial and Holocene ice retreat in the Southern Andes (53°S). Global and Planetary Change. doi:10.1016/j.gloplacha.2006.11 034.

Kim, J.-H., Rimbu, N., Lorenz, S.J., Lohmann, G., Nam, S.-I., Schouten, S., Rühlemann, C., Schneider, R.R., 2004. North Pacific and North Atlantic sea-surface temperature variability during the Holocene. Quaternary Science Reviews 23, 2141–2154.

Kirch, P.V., 2005. Archaeology and global change: the Holocene record. Annual Review of Environment and Resources 30, 409–440.

Klein Goldewijk, K., Ramankutty, N., 2004. Land cover change over the last three centuries due to human activities: the availability of new global data sets. Geojournal 61, 335–344.

Knorr, W., Schnitzler, K.-G., 2006. Enhanced albedo feedback in North Africa from possible combined vegetation and soil-formation processes. Climate Dynamics 26, 55–63.

Knight, J.R., Allan, J.R., Folland, C., Vellinga, M., Mann, M., 2005. A signature of persistent natural thermohaline circulation cycles in observed climate. Geophysical Research Letters 32, L20708.

Koç, N., Jansen, E., Hald, M., Labeyrie, L., 1996. Late glacial-Holocene sea surface temperatures and gradients between the North Atlantic and the Norwegian Sea: Implications for the Nordic heat pump. In: Andrews, J.T. (Ed.), The Late Glacial Paleooceanography of the North Atlantic Margins. Geological Society Special Publication, pp. 177–185.

Koch, J., Menounos, B., Clague, G., Osborn, G.D., 2004. Environmental change in Garibaldi Provincial Park, Southern Coast Mountains, British Columbia. Geoscience Canada 31 (3), 127–135.

Koch, J., Clague, J.J., 2006. Are insolation and sunspot activity the primary drivers of Holocene glacier fluctuations? PAGES News 14 (3), 20–21.

Koch, J., Clague, J.J., submitted. Holocene glacier history of the Canadian Cordillera in a global context. Journal of Quaternary Science (submitted).

Kodera, K., 2005. Possible solar modulation of the ENSO cycle. Papers in Meteorology and Geophysics 55, 21–33.

Kodera, K., Kuroda, Y., 2002. Dynamical response to the solar cycle. Journal of Geophysical Research 107. doi:10.1029/2002JD002224.

Kohfeld, K.E., Harrison, S., 2000. How well can we simulate past climates? Evaluating the models using global palaeoenvironmental data sets. Quaternary Science Reviews 19, 321–346.

Kutzbach, J.E., 1981. Monsoon climate of the early Holocene: climate experiment with the Earth's orbital parameters for 9000 years ago. Science 214, 59–61.

Kutzbach, J.E., Otto-Bliesner, B.L., 1982. The sensitivity of the African-Asian monsoonal climate to orbital parameter changes for 9000 years BP in a low-resolution general circulation model. Journal of the Atmospheric Sciences 39, 1177–1188.

Kutzbach, J.E., Street-Perrott, F.A., 1985. Milankovitch forcing of fluctuations in the level of tropical lakes from 18 to 0 kyr BP. Nature 317, 130–134.

Kutzbach, J.E., Guetter, P.J., 1986. The influence of changing orbital parameters and surface boundary conditions on climate simulations for the past 18 000 years. Journal of the Atmospheric Sciences 43 (16), 1726–1759.

Kutzbach, J., Bonan, G., Foley, J., Harrison, S.P., 1996. Vegetation and soil feedbacks on the response of the African monsoon to orbital forcing in the early to middle Holocene. Nature 384, 623–626.

Lamb, H.H., 1965. The early medieval warm epoch and its sequel. Palaeogeography, Palaeoclimatology. Palaeoecology 1, 13–37.

Lamb, H.H., 1969. The new look of climatology. Nature 223, 1209–1215.

Lamy, F., Hebbeln, D., Röhl, U., Wefer, G., 2001. Holocene rainfall variability in southern Chile: a marine record of latitudinal shifts of the Southern Westerlies. Earth and Planetary Science Letters 185, 369–382.

Lamy, F., Arz, H.W., Bond, G.C., Bahr, A., Pätzold, J., 2006. Multicentennial-scale hydrological changes in the Black Sea and northern Red Sea during the Holocene and the Arctic/North Atlantic Oscillation. Paleoceanography 21, PA1008.

Langdon, P.G., Barber, K.E., Hughes, P.D.M., 2003. A 7500-year peat-based palaeoclimatic reconstruction and evidence for an 1100-year cyclicity in bog surface wetness from Temple Hill Moss, Pentland Hills, southeast Scotland. Quaternary Science Reviews 22, 259–274.

Laskar, J., Robutel, P., Joutel, F., Gastineau, M., Correia, A.C.M., Levrard, B., 2004. A long-term numerical solution for the insolation quantities of the earth. Astronomy & Astrophysics 428 (1), 261–285.

Latif, M., Roeckner, E., Botzet, M., Esch, M., Haak, H., Hagemann, S., Jungclaus, J., Legutke, S., Marsland, S., Mikolajewicz, U., Mitchell, J., 2004. Reconstructing, monitoring, and predicting multidecadal-scale changes in the North Atlantic thermohaline circulation with sea surface temperature. Journal of Climate 17, 1605–1614.

Lean, J., Beer, J., Bradley, R.S., 1995. Reconstruction of solar irradiance since 1610: implications for climate change. Geophysical Research Letters 22, 3195–3198.

Levis, S., Bonan, G.B., Bonfils, C., 2004. Soil feedback drives the mid-Holocene North African monsoon northward in fully coupled CCSM2 simulations with a dynamic vegetation model. Climate Dynamics 23, 791–802.

Lie, O., Dahl, S.O., Nesje, A., Matthews, J.A., Sandvold, S., 2004. Holocene fluctuations of a polythermal glacier in high-alpine eastern Jotunheimen, central-southern Norway. Quaternary Science Reviews 23 (18-19), 1925–1945.

Liu, Z., Kutzbach, J., Wu, L., 2000. Modeling climate shift of El Nino variability in the Holocene. Geophysical Research Letters 27, 2265–2268.

Liu, Z., Harrison, S.P., Kutzbach, J., Otto-Bliesner, B., 2004. Global monsoons in the Mid-Holocene and oceanic feedback. Climate Dynamics 22, 157–182.

Liu, Z., Wang, Y., Gallimore, R., Notaro, M., Prentice, I.C., 2006. On the cause of abrupt vegetation collapse in North Africa during the Holocene: climate variability vs. vegetation feedback. Geophysical Research Letters 33, L22709. doi:10.1029/2006GL028062.

Liu, Z., Wang, Y., Gallimore, R., Gasse, F., Johnson, T., deMenocal, P., Adkins, J., Notaro, M., Prentice, I.C., Kutzbach, J., Jacob, R., Behling, P., Wang, L., Ong, E., 2007. Simulating the transient evolution and abrupt change of Northern Africa atmosphere–ocean–terrestrial ecosystem in the Holocene. Quaternary Science Reviews 26, 1818–1837.

Lorenz, S.J., Lohmann, G., 2004. Acceleration technique for Milankovitch type forcing in a coupled atmosphere-ocean climate circulation model: method and application for the Holocene. Climate Dynamics 23, 727–747.

Lorenz, S., Grieger, B., Helbig, P., Herterich, K., 1996. Investigating the sensitivity of the Atmospheric General Circulation Model ECHAM3 to paleoclimatic conditions. Geol. Rundsch 85, 513–524.

Lubinsky, D.J., Forman, S.L., Miller, G.H., 1999. Holocene glacier and climate fluctuations on Franz Josef Land, Arctic Russia, 80°N. Quaternary Science Reviews 18 (1), 85–108.

Luckman, B.H., 2000. The Little Ice Age in the Canadian Rockies. Geomorphology 32 (3), 357–384.

Luckman, B.H., Villalba, R., 2001. Assessing the synchroneity of glacier fluctuations in the Western Cordillera of the Americas during the last millennium. In: Markgraf, V. (Ed.), Interhemispheric Climate Linkages. Academic Press, San Diego, CA, pp. 119–140.

Please cite this article in press as: Wanner, H., et al., Mid- to Late Holocene climate change: an overview, Quaternary Science Reviews (2008), doi:10.1016/j.quascirev.2008.06.013

Luckman, B., Wilson, R., 2005. Summer temperature in the Canadian Rockies during the last millennium – a revised record. Climate Dynamics 24, 131–144.
Luterbacher, J., Xoplaki, E., Dietrich, D., Jones, P.D., Davies, T.D., Portis, D., González-Rouco, J.F., von Storch, H., Gyalistras, D., Casty, C., Wanner, H., 2001. Extending NAO reconstructions back to 1500. Atmospheric Science Letters 2, 114–124.
MacDonald, G.M., Case, R.A., 2005. Variations in the Pacific Decadal Oscillation over the past millennium. Geophysical Research Letters 32, L08703.
MacDonald, G.M., Velichko, A.A., Kremenetski, C.V., Borisova, O.K., Goleva, A.A., Andreev, A.A., Cwynar, L.C., Riding, R.T., Forman, S.L., Edwards, T.W.D., Aravena, R., Hammarlund, D., Szeicz, J.M., Gattaulin, V.N., 2000. Holocene treeline history and climate change across northern Eurasia. Quaternary Research 53, 302–311.
MacDonald, G.M., Beilman, D.W., Kremenetski, C.V., Sheng, Y., Smith, L.C., Velichko, A.A., 2006. Rapid early development of circumarctic peatlands and atmospheric CH_4 and CO_2 variations. Science 314, 285–288.
MacFarling Meure, C., Etheridge, D., Trudinger, C., Steele, P., Langenfelds, R., van Ommen, T., Smith, A., Elkins, J., 2006. Law Dome CO_2, CH_4 and N_2O ice core records extended to 2000 years BP. Geophysical Research Letters 33, L14810. doi:10.1029/2006GL026152.
Magny, M., 2004. Holocene climate variability as reflected by mid-European lake-level fluctuations and its probable impact on prehistoric human settlements. Quaternary International 113, 65–79.
Manabe, S., Hahn, D.G., 1977. Simulation of the tropical climate of an ice age. Journal of Geophysical Research 82, 3889–3911.
Mann, M.E., Bradley, R.S., Hughes, M.K., 1998. Global-scale temperature patterns and climate forcing over the past six centuries. Nature 392, 779–787.
Mann, M.E., Bradley, R.S., Hughes, M.K., 1999. Northern Hemisphere temperatures during the past millennium: inferences, uncertainties and limitations. Geophysical Research Letters 26, 759–762.
Mantua, N.J., Hare, S.R., 2002. The Pacific Decadal Oscillation. Journal of Oceanography 58, 35–44.
Mantua, N.J., Hare, S.R., Zhang, Y., Wallace, J.M., Francis, R.C., 1997. A Pacific interdecadal climate oscillation with impacts on salmon production. Bulletin of the American Meteorological Society 78, 1069–1079.
Marchal, O., Cacho, I., Stocker, T.F., Grimalt, J.O., Calvo, E., Martrat, B., Shackleton, N., Vautravers, M., Cortijo, E., van Kreveld, S., Andersson, C., Koç, N., Chapman, M., Sbaffi, L., Duplessy, J.-C., Sarnthein, M., Turon, J.-L., Duprat, J., Jansen, E., 2002. Apparent long-term cooling of the sea surface in the northeast Atlantic and Mediterranean during the Holocene. Quaternary Science Reviews 21, 455–483.
Marchant, R., Hooghiemstra, H., 2004. Rapid environmental change in African and South American tropics around 4000 years before present: a review. Earth-Science Reviews 66, 217–260.
Marchant, R.A., Behling, H., Berrio, J.C., Cleef, A., Duivenvoorden, J., van Geel, B., van der Hammen, T., Hooghiemstra, H., Kuhry, P., Melief, B.M., van Reenen, G., Wille, M., 2001. Late Holocene Colombian vegetation dynamics. Quaternary Science Reviews 20, 1289–1308.
Marchant, R., Behling, H., Berrio, J.C., Cleef, A., Duivenvoorden, J., Hooghiemstra, H., Kuhry, P., Melief, B., Schreve-Brinkman, E., van Geel, B., van der Hammen, T., van Reenen, G., Wille, M., 2002. Pollen-based biome reconstructions for Colombia at 3000, 6000, 9000, 12000, 15000 and 18000 ^{14}C yr ago: late Quaternary tropical vegetation dynamics. Journal of Quaternary Science 17, 113–129.
Markgraf, V., 1993. Paleoenvironments and paleoclimates in Tierra del Fuego and southernmost Patagonia, South America. Palaeogeography, Palaeoclimatology, Palaeoecology 102 (1-2), 53–68.
Markgraf, V., Dodson, J.R., Kershaw, A.P., McGlone, M.S., Nicholls, N., 1992. Evolution of late Pleistocene and Holocene climates in the circum-South Pacific land areas. Climate Dynamics 6, 193–211.
Masson, V., Cheddadi, R., Braconnot, P., Joussaume, S., Texier, D., participants, P.M.I.P., 1999. Mid-Holocene climate in Europe: what can we infer from PMIP model-data comparisons? Climate Dynamics 15, 163–182.
Masson, V., Vimeux, F., Jouzel, J., Morgan, V., Delmotte, M., Ciais, P., Hammer, C., Johnsen, S., Lipenkov, V.Y., Mosley-Thompson, E., Petit, J.-R., Steig, E.J., Stievenard, M., Vaikmar, R., 2000. Holocene climate variability in Antarctica based on 11 ice-core isotopic records. Quaternary Research 54, 348–358.
Masson-Delmotte, V., Kageyama, M., Braconnot, P., Charbit, S., Krinner, G., Ritz, C., Guilyardi, E., Jouzel, J., Abe-Ouchi, A., Crucifix, M., Gladstone, R.M., Hewitt, C.D., Kitoh, A., LeGrande, A.N., Marti, O., Merkel, U., Motoi, T., Ohgaito, R., Otto-Bliesner, B., Peltier, W.R., Ross, I., Valdes, P.J., Vettoretti, G., Weber, S.L., Wolk, F., Yu, Y., 2006. Past and future polar amplification of climate change: climate model intercomparison and ice-core constraints. Climate Dynamics 26, 513–529.
Matthews, H.D., Weaver, A.J., Eby, M., Meissner, K.J., 2003. Radiative forcing of climate by historical land cover change. Geophysical Research Letters 30 (2), 1055. doi:10.1029/2002GL016098.
Matthews, H.D., Weaver, A.J., Meissner, K.J., Gillet, N.P., Eby, M., 2004. Natural and anthropogenic climate change: incorporating historical land cover change, vegetation dynamics and the global carbon cycle. Climate Dynamics 22, 461–479.
Matthews, J.A., Dahl, S.O., Nesje, A., Berrisford, M.S., Andersson, C., 2000. Holocene glacier variations in central Jotunheimen, southern Norway based on distal glaciolacustrine sediment cores. Quaternary Science Reviews 19, 1625–1647.
Matthews, J.A., Berrisford, M.S., Dressera, P.Q., Nesje, A., Dahl, S.O., Bjune, A.E., Bakke, J.H., Birks, J.B., Lie, Ø., Dumayne-Peaty, L., Barnetth, E., 2005. Holocene glacier history of Bjørnbreen and climatic reconstruction in central Jotunheimen, Norway, based on proximal glaciofluvial stream-bank mires. Quaternary Science Reviews 24, 67–90.
Matthews, J.A., Briffa, K.R., 2005. The 'Little Ice Age': re-evaluation of an evolving concept. Geografiska Annaler 87 A, 17–36.
Mayewski, P.A., Rohling, E.E., Stager, J.C., Karlen, W., Maasch, K.A., Meeker, L.D., Meyerson, E.A., Gasse, F., van Kreveld, S., Holmgren, K., Lee-Thorp, J., Rosqvist, G., Rack, F., Staubwasser, M., Schneider, R.R., Steig, E.J., 2004. Holocene climate variability. Quaternary Research 62, 243–255.
McCormack, F.G., Hogg, A.G., Blackwell, P.G., Buck, C.E., Higham, P.J., Reimer, P.J., 2004. SHCAL04 Southern Hemisphere calibration, 0–11.0 cal kyr BP. Radiocarbon 48, 1087–1092.
McGhee, R., 1981. Archaeological evidence for climatic change during the last 5000 years. In: Wigley, T.M.L., Ingram, M.J., Farmer, G. (Eds.), Climate and History. Cambridge University Press, Cambridge.
McGregor, H.V., Gagan, M.K., 2004. Western Pacific coral $\delta^{18}O$ records of anomalous Holocene variability in the El Niño-Southern Oscillation. Geophysical Research Letters 31, L11204. doi:10.1029/2004GL019972.
Mercer, J.T., 1982. Holocene glacier variations in southern South America. Striae 18, 35–40.
Mikolajewicz, U., Scholze, M., Voss, R., 2003. Simulating near-equilibrium climate and vegetation for 6000 cal. years BP. Holocene 13, 319–326.
Minobe, S., 1997. A 50-70 year climatic oscillation over the North Pacific and North America. Geophysical Research Letters 24, 683–686.
Mitchell, J.F.B., 1977. The effect on climate of changing the Earth's orbital parameters: two summer integrations with fixed sea surface temperatures. Meteorological Office Technical Note II/100, 18 pp.
Moberg, A., Sonechkin, D.M., Holmgren, K., Datsenko, N.M., Wibjörn, K., 2005. Highly variable Northern Hemisphere temperatures reconstructed from low- and high-resolution proxy data. Nature 433, 613–617.
Monnin, E., Steig, E.J., Siegenthaler, U., Kawamura, K., Schwander, J., Stauffer, B., Stocker, T.F., Morse, D.L., Barnola, J.-M., Bellier, B., 2004. Evidence for substantial accumulation rate variability in Antarctica during the Holocene, through synchronization of CO_2 in the Taylor Dome, Dome C and DML ice cores. Earth and Planetary Science Letters 224 (1-2), 45–54.
Moros, M., Andrews, J.T., Eberl, D.D., Jansen, E., 2006. Holocene history of drift ice in the northern North Atlantic: evidence for different spatial and temporal modes. Paleoceanography 21, PA2017. doi:10.1029/2005PA001214.
Moy, C.M., Seltzer, G.O., Rodbell, D.T., Anderson, D.M., 2002. Variability of El Niño/Southern Oscillation activity at millennial timescales during the Holocene epoch. Nature 420, 162–165.
Müller, S.A., Joos, F., Edwards, N.R., Stocker, T.F., 2006. Water mass distribution and ventilation time scales in a cost-efficient, three-dimensional ocean model. Journal of Climate 19, 5479–5499.
Müller, S.A., Joos, F., Plattner, G.-K., Edwards, N.R., Stocker, T.F., 2008. Modelled natural and excess radiocarbon – Sensitivities to the gas exchange formulation and ocean transport strength. Global Biogeochemical Cycles 22, GB3011. doi:10.1029/2007GB003065.
Muscheler, R., Joos, F., Müller, S.A., Snowball, I., 2005. Climate – how unusual is today's solar activity? Nature 436, E3–E4.
Muscheler, R., Joos, F., Edwards, N.R., Stocker, T.F., 2007. Solar activity during the last 1000 yr inferred from radionuclide records. Quaternary Science Reviews 26, 82–97.
Nederbragt, A.J., Thurow, J., 2005. Geographic coherence of millennial-scale climate cycles during the Holocene. Palaeogeography, Palaeoclimatology, Palaeoecology 221, 313–324.
Neff, U., Burns, S.J., Mangini, A., Mudelsee, M., Fleitmann, D., Matter, A., 2001. Strong coherence between solar variability and the monsoon in Oman between 9 and 6 kyr ago. Nature 411, 290–293.
Nesje, A., Dahl, S.O., 1993. Lateglacial and Holocene glacier fluctuations and climate variations in western Norway: a review. Quaternary Science Reviews 12, 255–261.
Nesje, A., Dahl, S.O., 2003. The 'Little Ice Age' – only temperature? Holocene 13 (1), 139–145.
Nesje, A., Kvamme, M., 1991. Holocene glacier and climate variations in western Norway: evidence for early Holocene glacier demise and multiple Neoglacial events. Geology 19, 610–612.
Nesje, A., Matthews, J.A., Dahl, S.O., Berrisford, M.S., Andersson, C., 2001. Holocene glacier fluctuations of Flatebreen and winter-precipitation changes in the Jostedalsbreen region, western Norway, based on glaciolacustrine sediment records. Holocene 11, 267–280.
Nesje, A., Jansen, E., Birks, J.B., Bjune, A.E., Bakke, J., Andersson, C., Dahl, S.O., Kristensen, K., Lauritzen, S.E., Lie, O., Risebrobakken, B., Svendsen, J.-I., 2005. Holocene climate variability in the northern North Atlantic region: a review of terrestrial and marine evidence. In: Drange, H., Dokken, T., Furevik, T., Gerdes, R., Berger, W. (Eds.), The Nordic Seas: An Integrated Perspective. Geophysical Monograph Series 158. American Geophysical Union, Washington, DC, pp. 289–322.
Nesje, A., Bakke, J., Dahl, S.O., Lie, Ø., Matthews, J.A., 2008. Norwegian mountain glacier in the past, present and future. Global and Planetary Change 60, 10–27.
Niggemann, S., Mangini, A., Mudelsee, M., Richter, D.K., Wurth, G., 2003. Sub-Milankovitch climatic cycles in Holocene stalagmites from Sauerland, Germany. Earth and Planetary Science Letters 216, 539–547.
Noren, A.J., Bierman, P.R., Steig, E.J., Lini, A., Southon, J., 2002. Millennial-scale storminess variability in the northeastern United States during the Holocene epoch. Nature 419, 821–824.
Nuñez, L., Grosjean, M., Cartajena, I., 2002. Human occupations and climate change in the Puna de Atacama. Chile. Science 298, 821–824.
O'Brien, S.R., Mayewski, P.A., Meeker, L.D., Meese, D.A., Twickler, M.S., Whitlow, S.I., 1995. Complexity of Holocene climate as reconstructed from a Greenland ice core. Science 270, 1962–1964.

Please cite this article in press as: Wanner, H., et al., Mid- to Late Holocene climate change: an overview, Quaternary Science Reviews (2008), doi:10.1016/j.quascirev.2008.06.013

Oerlemans, J., 2005. Extracting a climate signal from 169 glacier records. Science 308, 675–677.
Oerlemans, J., Anderson, B., Hubbard, A., Huybrechts, P., Johannesson, T., Knap, W.H., Schmeits, M., Stroeven, A.P., van de Wal, R.S.W., Wallinga, J., Zuo, Z., 1998. Modelling the response of glaciers to climate warming. Climate Dynamics 14, 267–274.
Ohgaito, R., Abe-Ouchi, A., 2007. The role of ocean thermodynamics and dynamics in Asian summer monsoon changes during the mid-Holocene. Climate Dynamics 29, 39–50.
Oppo, D., 1997. Millennial climate oscillations. Science 278, 1244–1246.
Osborn, T.J., Briffa, K.R., 2006. The spatial extent of 20th-century warmth in the context of the past 1200 years. Science 311, 841–844.
Osborn, T.J., Raper, S.C.B., Briffa, K.R., 2006. Simulated climate change during the last 1,000 years: comparing the ECHO-G general circulation model with the MAG-ICC simple climate model. Climate Dynamics 27, 185–197.
Otto-Bliesner, B., 1999. El Nino/La Nina and Sahel precipitation during the middle Holocene. Geophysical Research Letters 26, 87–90.
Otto-Bliesner, B., Brady, E., Shin, S.-I., Liu, Z., Shields, C., 2003. Modeling El Nino and its tropical teleconnections during the last glacial cycle. Geophysical Research Letters 30. doi:10.1029/2003GL018553.
Otto-Bliesner, B.L., Brady, E.C., Tomas, R., Levis, S., Kothavala, Z., 2006. Last Glacial Maximum and Holocene climate in CCSM3. Journal of Climate 19, 2526–2544.
Patricola, C.M., Cook, K.H., 2007. Dynamics of the west African Monsoon under mid-Holocene precessional forcing: regional climate model simulations. Journal of Climate 20, 694–716.
Peristykh, A.N., Damon, P.E., 2003. Persistence of the Gleissberg 88-year solar cycle over the last ~12,000 years: evidence from cosmogenic isotopes. Journal of Geophysical Research 108 (A1), 1003.
Petit, J.R., Jouzel, J., Raynaud, D., Barkov, N.I., Barnola, J.M., Basile, I., Bender, M., Chappellaz, J., Davis, M., Delaygue, G., Delmotte, M., Kotlyakov, V.M., Legrand, M., Lipenkov, V.Y., Lorius, C., Pepin, L., Ritz, C., Saltzman, E., Stievenard, M., 1999. Climate and atmospheric history of the past 420,000 years from the Vostok ice core, Antarctica. Nature 399, 429–436.
Pickett, E.J., Harrison, S.P., Hope, G., Harle, K., Dodson, J.R., Kershaw, A.P., Prentice, I.C., Backhouse, J., Colhoun, E.A., D'Costa, D., Flenley, J., Grindrod, J., Haberle, S., Hassell, C., Kenyon, C., Macphail, M., Martin, H., Martin, A.H., McKenzie, M., Newsome, J.C., Penny, D., Powell, J., Raine, J.I., Southern, W., Stevenson, J., Sutra, J.P., Thomas, I., van der Kaars, S., Ward, J., 2004. Pollen-based reconstructions of biome distributions for Australia, Southeast Asia and the Pacific (SEAPAC region) at 0, 6000 and 18,000 C-14 yr BP. Journal of Biogeography 31, 1381–1444.
Pierrehumbert, R.T., 1999. Huascarán δ^{18}Oas an indicator of tropical climate during the Last Glacial Maximum. Geophysical Research Letters 26, 1345–1348.
PMIP, 2000. Paleoclimate Modeling Intercomparison Project (PMIP). Proceedings of the Third PMIP Workshop, WCRP-111, WMO/TD-No. 10007.
Poore, R.Z., Dowsett, H.J., Verardo, S., Quinn, T.M., 2003. Millennial- to century-scale variability in Gulf of Mexico Holocene climate records. Paleoceanography 18 (2), 1048.
Porter, S., 2000. Onset of neoglaciation in the Southern Hemisphere. Journal of Quaternary Science 15 (4), 395–408.
Porter, S.C., Denton, G.H., 1967. Chronology of neoglaciation in the North American Cordillera. American Journal of Science 265, 177–210.
Porter, S., Weijian, Z., 2006. Synchronism of Holocene East Asian monsoon variations and North Atlantic drift-ice tracers. Quaternary Research 65, 443–449.
Prentice, I.C., Webb III, T., 1998. BIOME 6000. Reconstructing global mid-Holocene vegetation patterns from paleoecological records. Journal of Biogeography 25, 997–1005.
Prentice, I.C., Bartlein, P.J., Webb, T., 1991. Vegetation and climate change in eastern North America since the last glacial maximum. Ecology 72, 2038–2056.
Prentice, I.C., Guiot, J., Huntley, B., Jolly, D., Cheddadi, R., 1996. Reconstructing biomes from palaeoecological data: a general method and its application to European pollen data at 0 and 6 ka. Climate Dynamics 12, 185–194.
Prentice, I.C., Jolly, D., Biome 6000 participants, 2000. Mid-Holocene and glacial-maximum vegetation geography of the northern continents and Africa. Journal of Biogeography 27, 507–519.
Prinn, R.G., Weiss, R.F., Fraser, P.J., Simmonds, P.G., Cunnold, D.M., Alyea, F.N., O'Doherty, S., Salameh, P., Miller, B.R., Huang, J., Wang, R.H.J., Hartley, D.E., Harth, C., Steele, L.P., Sturrock, G., Midgley, P.M., McCulloch, A., 2000. A history of chemically and radiatively important gases in air deduced from ALE/GAGE/AGAGE. Journal of Geophysical Research 105 (D14), 17751–17792.
Reimer, P.J., Baillie, M.G.L., Bard, E., Bayliss, A., Beck, J.W., Bertrand, C.J.H., Blackwell, P.G., Buck, C.E., Burr, G.S., Cutler, K.B., Damon, P.E., Edwards, R.L., Fairbanks, R.G., Friedrich, M., Guilderson, T.P., Hogg, A.G., Hughen, K.A., Kromer, B., McCormac, G., Manning, S., Ramsey, C.B., Reimer, R.W., Remmele, S., Southon, J.R., Stuiver, M., Talamo, S., Taylor, F.W., van der Plicht, J., Weyhenmeye, C.E., 2004. INTCAL04 terrestrial radiocarbon age calibration, 0–26 cal kyr BP. Radiocarbon 48, 1029–1058.
Rein, B., Lückge, A., Sirocko, F., 2004. A major ENSO anomaly during the Medieval period. Geophysical Research Letters 31, L17211. doi:10.1029/2004GL. 20161.
Rein, B., Lückge, A., Reinhardt, L., Sirocko, F., Wolf, A., Dullo, W.-C., 2005. El Niño variability off Peru during the last 20,000 years. Paleoceanography 20, PA4003. doi:10.1029/2004PA001099.
Renssen, H., Osborn, T., 2003. Holocene climate variability investigated using data-model comparisons. CLIVAR Exchanges 26, 1–3.
Renssen, H., Brovkin, V., Fichefet, T., Goosse, H., 2003. Holocene climatic instability during the termination of the African Humid Period. Geophysical Research Letters 30 (4), 1184. doi:1029/2002GL016636.
Renssen, H., Goosse, H., Fichefet, T., Brovkin, V., Driesschaert, E., Wolk, F., 2005a. Simulating the Holocene climate evolution at northern high latitudes using a coupled atmosphere–sea ice–ocean–vegetation mode. Climate Dynamics 24, 23–43.
Renssen, H., Goosse, H., Fichefet, T., Masson-Delmotte, V., Koç, N., 2005b. The Holocene climate evolution in the high-latitude Southern Hemisphere simulated by a coupled atmosphere–sea ice–ocean–vegetation model. The Holocene 15, 951–964.
Renssen, H., Goosse, H., Muscheler, R., 2006a. Coupled climate model simulation of Holocene cooling events: solar forcing triggers oceanic feedback. Climate of the Past 2, 79–90.
Renssen, H., Brovkin, V., Fichefet, T., Goosse, H., 2006b. Simulation of the Holocene climate evolution in Northern Africa: the termination of the African Humid Period. Quaternary International 150, 95–102.
Reyes, A.V., Clague, J.J., 2004. Stratigraphic evidence for multiple Holocene advances of Lilloet Glacier, southern Coast Mountains, British Columbia. Canadian Journal of Earth Sciences 41 (8), 903–918.
Ridgwell, A.J., Watson, A.J., Maslin, M.A., Kaplan, J.O., 2003. Implications of coral reef buildup for the controls on atmospheric CO_2 since the last glacial maximum. Paleoceanography 18 (4), 1083. doi: 1010.1029/2003PA000893.
Rimbu, N., Lohmann, G., Kim, J.-H., Arz, H.W., Schneider, R., 2003. Arctic/North Atlantic Oscillation signature in Holocene sea surface temperature trends as obtained from alkenone data. Geophysical Research Letters 30 (6), 1280. doi:10.1029/2002GL016570.
Rimbu, N., Lohmann, G., Lorenz, S.J., Kim, J.H., Schneider, R.R., 2004. Holocene climate variability as derived from alkenone sea surface temperature and coupled ocean-atmosphere model experiments. Climate Dynamics 23, 215–227.
Rind, D., Overpeck, J., 1993. Hypothesized causes of decade-to century-scale climate variability: climate model results. Quaternary Science Reviews 12, 357–374.
Risebrobakken, B., Jansen, E., Andersson, C., Mjelde, E., Hevrøy, K., 2003. A high-resolution study of Holocene paleoclimatic and paleoceanographic changes in the Nordic Seas. Paleoceanography 18, 1017.
Robock, A., 2000. Volcanic eruptions and climate. Reviews of Geophysics 38, 191–219.
Rodbell, D.T., Seltzer, G.O., Anderson, D.M., Abbott, M.B., Enfield, D.B., Newman, J.H., 1999. An ~15,000-year record of El Niño-driven alleviation in southwestern Ecuador. Science 283, 516–520.
Roethlisberger, F., 1986. 10,000 Jahre Gletschergeschichte der Erde. Verlag Sauerländer, Aarau.
Rossignol-Strick, M., 1983. African monsoons, an immediate climate response to orbital insolation. Nature 304, 46–49.
Rousse, S., Kissel, C., Laj, C., Eríksson, J., Knudsen, K.-L., 2006. Holocene centennial to millennial-scale climatic variability: evidence from high-resolution magnetic analyses of the last 10 cal kyr off North Iceland (core MD99-2275). Earth and Planetary Science Letters 242, 390–405.
Ruddiman, W.F., 2003. The anthropogenic greenhouse era began thousands of years ago. Climatic Change 61, 261–293.
Ruddiman, W.F., Thomson, J.S., 2001. The case for human causes of increased atmospheric CH_4 over the last 5000 years. Quaternary Science Reviews 20, 1769–1777.
Sarnthein, M., van Kreveld, S., Erlenkeuser, H., Grootes, P.M., Kucera, M., Pflaumann, U., Schulz, M., 2003. Centennial-to-millennial-scale periodicities of Holocene climate and sediment injections off the western Barents shelf, 75 degrees N. Boreas 32 (3), 447–461.
Schmidt, G.A., Shindell, D.T., Miller, R.L., Mann, M.E., Rind, D., 2004. General circulation modelling of Holocene climate variability. Quaternary Science Reviews 23, 2167–2181.
Schubert, S.D., Suarez, M.J., Pegion, P.J., Koster, R.D., Bacmeister, J.T., 2004. On the cause of the 1930s Dust Bowl. Science 303, 1855–1859.
Schulz, M., Mudelsee, M., 2002. REDFIT: estimating red-noise spectra directly from unevenly spaced paleoclimatic time series. Computers & Geosciences 28, 421–426.
Schulz, M., Paul, A., 2002. Holocene climate variability on centennial-to-millennial time scales: 1. Climate records from the North-Atlantic realm. In: Wefer, G., Berger, W.H., Behre, K.E., Jansen, E. (Eds.), Climate Development and History of the North Atlantic Realm. Springer, Berlin, Heidelberg.
Schurgers, G., Mikolajewicz, U., Gröger, M., Maier-Reimer, E., Vizcaíno, M., Winguth, A., 2006. Changes in terrestrial carbon storage during interglacials: a comparison between Eemian and Holocene. Climate of the Past 2, 449–483.
Seppä, H., Birks, H.J.B., 2001. July mean temperature and annual precipitation trends during the Holocene in the Fennoscandian tree-line area: pollen-based climate reconstructions. The Holocene 11, 527–537.
Shen, C., Wang, W.-C., Gong, W., Hao, Z., 2006. A Pacific Decadal Oscillation record since 1470 AD reconstructed from proxy data of summer rainfall over eastern China. Geophysical Research Letters 33, L03702.
Shindell, D.T., Schmidt, G.A., Mann, M.E., Rind, D., Waple, A., 2001. Solar forcing of regional climate change during the Maunder Minimum. Science 294, 2149–2152.
Shindell, D.T., Schmidt, G.A., Mann, M.E., Faluvegi, G., 2004. Dynamic winter climate response to large tropical volcanic eruptions since 1600. Journal of Geophysical Research 109, D05104. doi:10.1029/2003JD004151.
Shulmeister, J., 1999. Australasian evidence for mid-Holocene climate change implies precessional control of Walker Circulation in the Pacific. Quaternary International 57/58, 81–91.
Shulmeister, J., Lees, B.G., 1995. Pollen evidence from tropical Australia for the onset of an ENSO dominated climate at c. 4000 BP. The Holocene 5, 10–18.
Shulmeister, J., Goodwin, I., Renwick, J., Harle, K., Armand, L., McGlone, M.S., Cook, E., Dodson, J., Hesse, P., Mayewski, P., Curran, M., 2004. The Southern

Hemisphere westerlies in the Australasian sector over the last glacial cycle: a synthesis. Quaternary International 118-119, 23–53.
Shulmeister, J., Rodbell, D.T., Gagan, M.K., Seltzer, G.O., 2006. Inter-hemispheric linkages in climate change: paleo-perspectives for future climate change. Climate of the Past 2, 167–185.
Shuman, B., Bartlein, P.J., Webb, T., 2005. The magnitudes of millennial- and orbital-scale climate change in eastern North America during the late Quaternary. Quaternary Science Reviews 24, 20–21.
Siegenthaler, U., Oeschger, H., 1987. Biospheric CO_2 emissions during the past 200 years reconstructed by deconvolution of ice core data. Tellus B 39/1–2, 140-154.
Siegenthaler, U., Monnin, E., Kawamura, K., Spahni, R., Schwander, J., Stauffer, B., Stocker, T.F., Barnola, J.-M., Fischer, H., 2005. Supporting evidence from the EPICA Dronning Maud Land ice core for atmospheric CO_2 changes during the past millennium. Tellus 57 B, 51–57.
Simpson, J.J., Hufford, G.L., Daly, C., Berg, J.S., Fleming, M.D., 2005. Comparing maps of mean monthly surface temperature and precipitation for Alaska and adjacent areas of Canada produced by two different methods. Arctic 56, 137–161.
Skilbeck, C.G., Rolph, T.C., Hill, N., Woods, J., Wilkens, R.H., 2005. Holocene millennial/centennial scale multiproxy cyclicity in temperate eastern Australian estuary sediments. Journal of Quaternary Science 20, 327–347.
Smith, L.C., MacDonald, G.M., Velichko, A.A., Beilman, D.W., Borisova, O.K., Frey, K.E., Kremenetski, K.V., Sheng, Y., 2004. Siberian peatlands a net carbon sink and global methane source since the early Holocene. Science 303, 353–356.
Solanki, S.K., Krivova, N.S., 2003. Can solar variability explain global warming since 1970? Journal of Geophysical Research Space Physics 108 (Art. No. 1200).
Solanki, S.K., Usoskin, I.G., Kromer, B., Schüssler, M., Beer, J., 2004. Unusual activity of the Sun during recent decades compared to the previous 11,000 years. Nature 431, 1084–1087.
Solomina, O., Haeberli, W., Kull, C., Wiles, G., 2008. Historical and Holocene glacier-climate variations: general concepts and overview. Global and Planetary Change 60, 1–9.
Solomon, S., 1999. Stratospheric ozone depletion: a review of concepts and history. Reviews of Geophysics 37, 275–316.
Spahni, R., Chappellaz, J., Stocker, T.F., Loulergue, L., Hausammann, G., Kawamura, K., Flückiger, J., Schwander, J., Raynaud, D., Masson-Delmotte, V., Jouzel, J., 2005. Atmospheric methane and nitrous oxide of the late Pleistocene from Antarctic ice cores. Science 310, 1317–1321.
Stauffer, B., Flückiger, J., Monnin, E., Schwander, J., Barnola, J.-M., Chappellaz, J., 2002. Atmospheric CO_2, CH_4 and N_2O records over the past 60,000 years based on the comparison of different polar ice cores. Annals of Glaciology 35, 202–208.
Steig, E.J., Brook, E.J., White, J.W.C., Sucher, C.M., Bender, M.L., Lehman, S.J., Morse, D.L., Waddington, E.D., Clow, G.D., 1998. Synchronous climate changes in Antarctica and the North Atlantic. Science 282, 92–95.
Steiner, D., Pauling, A., Nussbaumer, S.U., Nesje, A., Luterbacher, J., Wanner, H., Zumbühl, H.J., 2008. Sensitivity of European glaciers to precipitation and temperature – two case studies. Climatic Change. doi: 10.1007/s10584-008-9393-1.
Stocker, T.F., 1996. An overview of century time-scale variability in the climate system: observations and models. In: Anderson, D.L.T., Willebrand, J. (Eds.), Decadal Climate Variability: Dynamics and Predictability. Springer Verlag, pp. 379–406.
Stocker, T.F., Mysak, L.A., 1992. Climatic fluctuations on the century time scale: a review of high resolution proxy-data. Climatic Change 20, 227–250.
Stott, L.K., Cannariato, K., Thunell, R., Haug, G.H., Koutavas, A., Lund, S., 2004. Decline in surface temperature and salinity in the western tropical Pacific ocean in the Holocene epoch. Nature 431, 56–59.
Stott, P.A., Tett, S.F.B., 1998. Scale-dependent detection of climate change. Journal of Climate 11, 3282–3294.
Stott, P.A., Jones, G.S., Lowe, J.A., Thorne, P., Durman, C., Johns, T.C., Thelen, J.C., 2006. Transient climate simulations with the HadGEM1 climate model: causes of past warming and future climate change. Journal of Climate 19, 2763–2782.
Strassmann, K.M., Joos, F., Fischer, G., 2008. Simulating effects of land use changes on carbon fluxes: past contributions to atmospheric CO_2 increases and future commitments due to losses of terrestrial sink capacity. Tellus B 60 (4), 583–603.
Street-Perrott, F.A., Harrison, S.A., 1984. Temporal variations in lake levels since 30,000 yr BP – An index of the global hydrological cycle. In: Hansen, J.E., Takahashi, T. (Eds.), Climate Processes and Climate Sensitivity. American Geophysical Union, Washington, DC, pp. 118–129.
Street-Perrott, F.A., Harrison, S.P., 1985. Lake levels and climate reconstruction. In: Hecht, A.D. (Ed.), Palaeoclimatic Analysis and Modelling. John Wiley, New York, pp. 291–340.
Stuiver, M., Grootes, P.M., Braziunas, T.F., 1995. The GISP2 delta ^{18}O climate record of the past 16,500 years and the role of the sun, ocean, and volcanoes. Quaternary Research 44 (3), 341–354.
Sutton, R.T., Hodson, D.L.R., 2003. Influence of the ocean on North Atlantic climate variability 1871–1999. Journal of Climate 16, 3296–3313.
Sutton, R.T., Hodson, D.L.R., 2005. Atlantic ocean forcing of North American and European summer climate. Science 309, 115–118.
Svendsen, J.I., Mangerud, J., 1997. Holocene glacial and climatic variations on Spitsbergen, Svalbard. The Holocene 7, 45–57.
Takahara, H., Sugita, S., Harrison, S.P., Miyoshi, N., Morita, Y., Uchiyama, T., 2000. Pollen-based reconstructions of Japanese biomes at 0, 6000 and 18,000 ^{14}C BP. Journal of Biogeography 27, 665–683.
Tarasov, P.E., Webb III, T., Andreev, A.A., Afanas'eva, N.B., Berezina, N.A., Bezusko, L.G., Blyakharchuk, T.A., Bolikhovskaya, N.S., Cheddadi, R., Chernavskaya, M.M., Chernova, G.M., Dorofeyuk, N.I., Dirksen, V.G., Elina, G.A., Filimonova, L.V., Glebov, F.Z., Guiot, J., Gunova, V.S., Harrison, S.P., Jolly, D., Khomutova, V.I., Kvavadze, E.V., Osipova, I.M., Panova, N.K., Prentice, I.C., Saarse, L., Sevastyanov, D.V., Volkova, V.S., Zernitskaya, V.P., 1998. Present-day and mid-Holocene biomes reconstructed from pollen and plant macrofossil data from the former Soviet Union and Mongolia. Journal of Biogeography 25, 1029–1053.
TEMPO Members, 1996. Potential role of vegetation feedback in the climate sensitivity of high-latitude regions: a case study at 6000 years BP. Global Biogeochemical Cycles 10/4, 727–736.
Tett, S., Betts, R., Crowley, T., Gregory, J., Johns, T., Jones, A., Osborn, T.J., Öström, E., Robert, D.L., Woodage, M.J., 2007. The impact of natural and anthropogenic forcings on climate and hydrology since 1550. Climate Dynamics. Climate Dynamics 28, 3–34.
Texier, D., de Noblet, N., Harrison, S.P., Haxeltine, A., Jolly, D., Joussaume, S., Laarif, F., Prentice, I.C., Tarasov, P., 1997. Quantifying the role of biosphere-atmosphere feedbacks in climate change: coupled model simulations for 6000 years BP and comparison with palaeodata for northern Eurasia and northern Africa. Climate Dynamics 13, 865–882.
Texier, D., de Noblet, N., Braconnot, P., 2000. Sensitivity of the African and Asian monsoons to mid-Holocene insolation and data-inferred surface changes. Journal of Climate 13, 164–181.
Thompson, D.W.J., Wallace, J.M., 2001. Regional climate impacts of the Northern Hemisphere annular mode. Science 293, 85–89.
Thompson, L.G., Mosley-Thompson, E., Davis, M.E., Lin, P.N., Henderson, K.A., Coledai, J., Bolzan, J.J.F., Liu, K.B., 1995. Late-Glacial stage and Holocene tropical ice core records from Huascaran, Peru. Science 269, 46–50.
Thompson, L.G., Mosley-Thompson, E., Davis, M.E., Henderson, K.A., Brecher, H.H., Zagorodnov, V.S., Mashiotta, T.A., Lin, P.N., Mikhalenko, V.N., Hardy, D.R., Beer, J., 2002. Kilimanjaro ice core records: evidence of Holocene climate change in tropical Africa. Science 298, 589–593.
Thompson, L.G., Mosley-Thompson, E., Davis, M.E., Lin, P.-N., Henderson, K., Mashiotta, T.A., 2003. Tropical glacier and ice core evidence of climate change on annual to millennial scales. Climatic Change 59, 137–155.
Thompson, L.G., Mosley-Thompson, E., Brecher, H., Davis, M., Leon, B., Les, D., Lin, P.N., Mashiotta, T., Mountain, K., 2006. Abrupt tropical climate change: past and present. Proceedings of the National Academy of Sciences USA 103, 10536–10543.
Thompson, R.S., Anderson, K.H., 2000. Biomes of western North America at 18,000, 6000 and 0 C-14 yr BP reconstructed from pollen and packrat midden data. Journal of Biogeography 27, 555–584.
Timmermann, A., Latif, M., Voss, R., Grotzner, R.A., 1998. Northern hemispheric interdecadal variability: a coupled air-sea mode. Journal of Climate 11, 1906–1931.
Timmermann, A., Lorenz, S.J., An, S.-I., Clement, A., Xia, S.P., 2007. The effect of orbital forcing on the mean climate and variability of the tropical Pacific. Journal of Climate 20, 4147–4159.
Torrence, C., Compo, G.P., 1998. A practical guide to wavelet analysis. Bulletin of the American Meteorological Society 79, 61–78.
Tudhope, A.W., Chilcott, C.P., McCulloch, M.T., Cook, E.R., Chappell, J., Ellam, R.M., Lea, D.W., Lough, J.M., Shimmield, G.B., 2001. Variability in the El Niño-Southern Oscillation through a glacial–interglacial cycle. Science 291, 1511–1517.
Turney, C., Baillie, M., Clemens, S., Brown, D., Palmer, J., Pilcher, J., Reimer, P., Leuschner, H.H., 2005. Testing solar forcing of pervasive Holocene climate cycles. Journal of Quaternary Science 20 (6), 511–518.
van Geel, B., Heusser, C., Renssen, H., Schuurmans, C., 2000. Climatic change in Chile at around 2700 BP and global evidence for solar forcing: a hypothesis. The Holocene 10, 659–664.
van Loon, H., Meehl, G.A., Arblaster, J.M., 2004. A decadal solar effect in the tropics in July–August. Journal of Atmospheric and Solar-Terrestrial Physics 66, 1767–1778.
van Loon, H., Meehl, G.A., Shea, D.J., 2007. Coupled air-sea response to solar forcing in the Pacific region during Northern winter. Journal of Geophysical Research 112, D02108. doi:10.1029/2006JD007378.
Vellinga, M., Wu, P., 2004. Low-latitude freshwater influence on centennial variability of the Atlantic thermohaline circulation. Journal of Climate 17, 4498–4511.
Venegas, S., Mysak, L.A., 2000. Is there a dominant timescale of natural climate variability in the Arctic? Journal of Climate 13, 3412–3434.
Vettoretti, G., Peltier, W.R., McFarlane, N.A., 1998. Simulations of mid-Holocene climate using an atmospheric general circulation model. Journal of Climate 11, 2607–2627.
Viau, A.E., Gajewski, K., Sawada, M.C., Fines, P., 2006. Millennial-scale temperature variations in North America during the Holocene. Journal of Geophysical Research 111 (D9), D09102.
Vinther, B.M., Clausen, H.B., Johnsen, S.J., Rasmussen, S.O., Andersen, K.K., Buchardt, S.L., Dahl Jensen, D., Seierstad, I.K., Siggaard-Andersen, M.L., Steffensen, J.P., Svensson, A., Olsen, J., Heinemeier, J., 2006. A synchronized dating of three Greenland ice cores throughout the Holocene. Journal of Geophysical Research 111, D13102.
Vonmoos, M., Beer, J., Muscheler, R., 2006. Large variations in Holocene solar activity - constraints from ^{10}Be in the GRIP ice core. Journal of Geophysical Research 111, A10105. doi:10.1029/2005JA011500.
von Storch, H., Zorita, E., Jones, J.M., Dmitriev, Y., Tett, S.F.B., 2004. Reconstructing past climate from noisy data. Science 306, 679–682.
Wagner, S., Widmann, M., Jones, J.M., Mayer, C., Ohlendorf, C., Schäbitz, F., 2007. Transient simulations, empirical reconstructions and forcing mechanisms for

Please cite this article in press as: Wanner, H., et al., Mid- to Late Holocene climate change: an overview, Quaternary Science Reviews (2008), doi:10.1016/j.quascirev.2008.06.013

the Mid-Holocene hydrological climate in Southern Patagonia. Climate Dynamics 29, 333–355.
Wagner, S., Jones, J.M., Widmann, M., Kaspar, F., 2008. Transient simulation with a coupled atmosphere-ocean GCM for the period 7000 BP–4500 BP. (submitted).
Wang, Y., Cheng, H., Edwards, R.L., He, Y., Kong, X., An, Z., Wu, J., Kelly, M.J., Dykoski, C.A., Li, X., 2005. The Holocene Asian monsoon: links to solar changes and North Atlantic climate. Science 308, 854–857.
Wang, Y.M., Mysak, L., Wang, Z., Brovkin, V., 2005a. The greening of the McGill Paleoclimate model. Part II: simulation of Holocene millennial-scale climate changes. Climate Dynamics 24, 481–496.
Wang, Y.M., Lean, J.L., Sheeley, N.R., 2005b. Modeling the sun's magnetic field and irradiance since 1713. Astrophysical Journal 625, 522–538.
Wanner, H., Holzhauser, H., Pfister, C., Zumbühl, H., 2000. Interannual to century scale climate variability in the European Alps. Erdkunde (Earth Science) 54, 62–69.
Wanner, H., Brönnimann, S., Casty, C., Gyalistras, D., Luterbacher, J., Schmutz, C., Stephenson, D.B., Xoplaki, E., 2001. North Atlantic Oscillation – concepts and studies. Surveys in Geophysics 22, 321–382.
Weber, S.L., 2001. The impact of orbital forcing on the climate of an intermediate-complexity coupled model. Global and Planetary Change 30, 7–12.
Weber, S.L., Crowley, T.J., van der Schrier, G., 2004. Solar irradiance forcing of centennial climate variability during the Holocene. Climate Dynamics 22, 539–553.
Weiss, H., Bradley, R.S., 2001. What drives societal collapse? Science 291, 609–610.
Weiss, H., Courtney, M.-A., Wetterstrom, W., Guichard, F., Senior, L., Meadow, R., Curnow, A., 1993. The genesis and collapse of third millennium north Mesopotamian civilization. Science 261, 995–1004.
White, W.B., 2006. Response of tropical global ocean temperature to the sun's quasi-decadal UV radiative forcing of the stratosphere. Journal of Geophysical Research 111, C09020. doi:10.1029/2004JC002552.
White, W.B., Tourre, Y.M., Barlow, M., Dettinger, M., 2003. A delayed action oscillator shared by biennial, interannual, and decadal signals in the Pacific Basin. Journal of Geophysical Research 108, doi:10.1029/2002JC001490.
Wiles, G.C., Calkin, P.E., Post, A., 1995. Glacier fluctuations in the Kenai Fjords, Alaska, USA – an evaluation of controls on iceberg-calving glaciers. Arctic and Alpine Research 27, 234–245.
Wiles, G., D'Arrigo, R., Villalba, R., Calkin, P., Barclay, D.J., 2004. Century-scale solar variability and Alaskan temperature change over the past millennium. Geophysical Research Letters 31, L15203.
Willard, D.A., Bernhardt, C.E., Korejwo, D.A., Meyers, S.R., 2005. Impact of millennial-scale Holocene climate variability on eastern North American terrestrial ecosystems: pollen-based climatic reconstruction. Global and Planetary Change 47, 17–35.
Williams, J., Barry, R.G., Washington, W.W., 1974. Simulation of the atmospheric circulation using the NCAR global circulation model with ice age boundary conditions. Journal of Applied Meteorology 13, 305–317.
Williams, M., Eugster, W., Rastetter, E.B., McFadden, J.P., Chapin III, F., 2000. The controls on net ecosystem productivity along an arctic transect: a model comparison with flux measurements. Global Change Biology 6 (Suppl. 1), 116–126.
Wohlfahrt, J., Harrison, S.P., Braconnot, P., 2004. Synergistic feedbacks between ocean and vegetation on mid- and high-latitude climates during the mid-Holocene. Climate Dynamics 22, 223–238.
Wright, H.E., Kutzbach, J.E., Webb III, T., Ruddiman, W.F., Street-Perrot, E.A., Bartlein, P.J. (Eds.), 1993. Global Climates Since the Last Glacial Maximum. University of Minnesota Press, Minneapolis, MN.
Wunsch, C., 2000. On sharp spectral lines in the climate record and the millennial peak. Paleoceanography 15 (4), 417–424.
Wunsch, C., 2006. Abrupt climate change: an alternative view. Quaternary Research 65, 191–203.
Yang, B., Bräuning, A., Dong, Z., Zhang, Z., Keqing, J., 2008. Late Holocene monsoonal temperate glacier fluctuations on the Tibetan Plateau. Global and Planetary Change 60, 126–140.
Yiou, P., Fuhrer, K., Meeker, L.D., Jouzel, J., Johnsen, S.J., Mayewski, P.A., 1997. Paleoclimatic variability inferred from spectral analysis of Greenland and Antarctic ice core data. Journal of Geophysical Research 102, 26441–26454.
Yu, G., Prentice, I.C., Harrison, S.P., Sun, X.J., 1998. Pollen-based biome reconstructions for China at 0 and 6000 years. Journal of Biogeography 25, 1055–1069.
Yu, G., Chen, X., Ni, J., Cheddadi, R., Guiot, J., Han, H., Harrison, S.P., Huang, C., Ke, M., Kong, Z., Li, S., Li, W., Liew, P., Liu, G., Liu, J., Liu, Q., Liu, K.B., Prentice, I.C., Qui, W., Ren, G., Song, C., Sugita, S., Sun, X., Tang, L., Van Campo, E., Xia, Y., Xu, Q., Yan, S., Yang, X., Zhao, J., 2000. Palaeovegetation of China: a pollen data-based synthesis for the mid-Holocene and last glacial maximum. Journal of Biogeography 27, 635–664.
Yu, Y.T., Yang, T., Li, J., Liu, J., An, C., Liu, X., Fan, Z., Lu, Z., Li, Y., Su, X., 2006. Millennial-scale Holocene climate variability in the NW China drylands and links to the tropical Pacific and the North Atlantic. Palaeogeography, Palaeoclimatology. Palaeoecology 233, 149–162.
Yu, Z.C., Campbell, I.D., Campbell, C., Vitt, D.H., Bond, G.C., Apps, M.J., 2003. Carbon sequestration in western Canadian peat highly sensitive to Holocene wet-dry climate cycles at millennial timescales. Holocene 13, 801–808.
Zhao, Y., Braconnot, P., Marti, O.Y., Harrison, S.P., Hewitt, C., Kitoh, A., Liu, Z., Mikolajewicz, U., Otto-Bliesner, B., Weber, S.L., 2005. A multi-model analysis of the role of the ocean on the African and Indian Monsoon during the Mid-Holocene. Climate Dynamics 25, 777–800.
Zheng, B., Shiyie, L., Wang, S., 1994. Evolution of glacier on the Surrounding Mountains of the Zoige Basin. Study of Formation and Evolution, Environmental Change and Ecological Systems of the Tibetan Plateau. Beijing Print, Beijing.
Zhou, S., Chen, F., Pan, B., Cao, J., Li, J., Derbyshire, E., 1991. Environmental change during the Holocene in western China on a millennial timescale. The Holocene 1, 151–156.
Zielinski, G.A., 2000. Use of paleo-records in determining variability within the volcanism-climate system. Quaternary Science Reviews 19, 417–438.
Zielinski, G.A., Fiacco, R.J., Mayewski, P.A., Meeker, L.D., Whitlow, S.I., Twickler, M.S., Germani, M.S., Endo, K., Yasui, M., 1994. Climatic impact of the A.D. 1783 Asama (Japan) eruption was minimal: evidence from the GISP2 ice core. Geophysical Research Letters 21, 2365–2368.
Zielinski, G.A., Mayewski, P.A., Meeker, L.D., Whitlow, S., Twickler, M.S., 1996. A 110,000-yr record of explosive volcanism from the GISP2 (Greenland) ice core. Quaternary Research 45, 109–118.
Zorita, E., von Storch, H., González-Rouco, J.F., Cubasch, U., Luterbacher, J., Legutke, S., Fischer-Bruns, I., Schlese, U., 2004. Transient simulation of the climate of the last five centuries with an atmosphere–ocean coupled model: late Maunder Minimum and the Little Ice Age. Meteorologische Zeitschrift 13, 271–289.

Please cite this article in press as: Wanner, H., et al., Mid- to Late Holocene climate change: an overview, Quaternary Science Reviews (2008), doi:10.1016/j.quascirev.2008.06.013